CHEMICAL CHARACTERIZATION AND TWO-STEP CURE KINETICS OF A HIGH PERFORMANCE EPOXY ADHESIVE SYSTEM

A thesis by

Joel D. Flores
BS, University of San Carlos (Cebu, Philippines), 2000

Submitted to the Department of Chemistry
and the Faculty of the Graduate School of
Wichita State University
in partial fulfillment of
the requirements for the degree of

Master of Science

July 2006

CHEMICAL CHARACTERIZATION AND TWO-STEP CURE KINETICS OF A HIGH PERFORMANCE EPOXY ADHESIVE SYSTEM

I have examined the final copy of this thesis to form and content and recommend that it be accepted in partial fulfillment of the requirements for the degree of Master of Science with a major in Chemistry.

_____
Dr. William T. K. Stevenson, Committee Chair

We have read this thesis and recommend its acceptance:

_____
Dr. Dennis H. Burns, Committee Member

_____
Dr. David M. Eichhorn, Committee Member

_____
Dr. Michael J. Van Stipdonk, Committee Member

_____
Dr. Chihdar C. Yang, Committee Member

ACKNOWLEDGMENTS

A number of individuals have helped me in completing this work. Dr William T. Stevenson, my research advisor, has been tremendously generous in his support during my short stay at WSU. My committee members are also gratefully acknowledged for their critical comments and suggestions. I am also thankful to the WSU Chemistry Department for financial support. I am indebted to Dr. Vincent Storhaug for his assistance in the analytical work, Amanda Alliband for generating some of the NMR spectra and to Rama Gandikota for helping me in the DSC experiments.

My appreciation goes also to my family and friends. Without them, this would have been a meaningless endeavor.

ABSTRACT

The cure kinetics of a high performance epoxy adhesive system based on TGDDM/DGEBA/DDS/DICY and toughened with carboxy terminated poly(acrylonitrile-*co*-butadiene) rubber with aluminum filler was investigated using differential scanning calorimetry. Three different sets of experiments were performed to follow the cure kinetics of the adhesive in a multi-step cure cycle. Three-dimensional plots of data entered into a surface-fitting software allowed for the interpolation of the degree and rate of cure as functions of heating rate and temperature, time and temperature, or time and initial degree of cure. Isothermal cure was modeled successfully using the kinetic model of Kamal. The gel point of the adhesive was measured using dynamic shear rheometry under isothermal conditions. Methods were developed to combine ramp and soak segments so that both the conversion (a) and rate of cure (da/dt) can be followed through a two-step cure cycle of the type used to cure composite pre-preg and adhesive in an industrial setting.

TABLE OF CONTENTS

CHAPTER Page

1. INTRODUCTION……..…… 1

1.1. Introduction……..…… 1

1.2. Curing of Epoxy with Amines…… 1

1.3. Kinetics of Epoxy-Amine Polymerization……..… 5

1.3.1. Differential Scanning Calorimetry (DSC)……... 7

1.3.2. Kinetic Models of Epoxy-Amine Cure……..….. 9

1.4. Epoxy-Based Adhesives……..… 13

1.5. Overview of this Study…….….. 18

2. CHEMICAL CHARACTERIZATION OF THE FILM ADHESIVE…… 20

2.1. Introduction…….……. 20

2.2. Experimental…….……... 20

2.2.1. Materials…….……..… 20

2.2.2. FT-IR Spectroscopy……..……... 21

2.2.3. Nuclear Magnetic Resonance Spectroscopy…….…..……..… 21

2.2.4. Elemental Analysis…….....…... 22

2.2.5. Thin-Layer Chromatography……... 22

2.3. Results and Discussion……...… 22

2.3.1. FT-IR spectroscopy……...….. 24

2.3.2. NMR Spectroscopy……..….…... 24

2.3.3. Elemental Analysis…….. 33

2.3.4. Thin-Layer Chromatography……... 34

2.3.5. Composition of the Film Adhesive…….…. 34

3. CURE KINETICS OF THE FILM ADHESIVE…….. 38

3.1. Introduction…… 38

3.2. Experimental…….. 41

3.2.1. Thermal Analysis……..… 41

3.2.2. Dynamic Shear Rheometry…….…. 42

3.3. Results and Discussions…….…. 43

3.3.1. Dynamic Temperature Scanning…….…. 43

3.3.2. Isothermal Scanning……..… 57

3.3.3. Combined Ramp and Soak Experiments….…….……... 77

3.3.4. Dynamic Shear Rheometry…….. 87

4. CONCLUSIONS…… 92

REFERENCES …… 95

APPENDICES……. 100

A Calculation of the apparent energy of activation of cure…….……. 101

B 2D plots of the degree of cure (α) versus time for the film adhesive cured under isothermal conditions (140°C to 180°C) after a slow ramp to the cure temperature……. 108

C 3D plot of the degree of cure (α) versus time and initial degree of cure for the film adhesive cured under isothermal conditions (140°C to 180°C) after a slow ramp to that temperature……..……..…. 116

D 2D plot of the rate of cure versus time for the film adhesive cured under isothermal conditions (140 °C to 180°C) after a slow ramp to the cure temperature……..….. 120

E 3D plot of the rate of cure versus time and initial degree of cure for the film adhesive cured under isothermal conditions (140°C and 180°C) after a slow ramp to that temperature …… 128

F 2D plots of the degree of cure (α) as a function of time for the combined ramp and soak experiments over a range of heating rates up to soak temperatures of 170 °C, 175 °C, and 180 °C, followed by isothermal scan at that temperature. ……... 132

G 2D plots of the rate of cure as a function of time for the combined ramp and soak experiments over a range of heating rates up to soak temperatures of 170 °C, 175 °C, and 180 °C, followed by isothermal scanning at that temperature…….. 134

H Plots of the development of storage modulus (G'), loss modulus (G") and complex modulus (G*) for the film adhesive as a function of time during isothermal cure at 130 °C, 135 °C, 140 °C, and 150 °C…….. 136

LIST OF TABLES

TABLE PAGE

2.1 Approximate composition of the film adhesive……. 36

3.1 Kinetic parameters for the isothermal data fitted into equation (15)……. 75

LIST OF FIGURES

FIGURE PAGE

1.1. Major reactions occurring in the polymerization of epoxy with amines…….. 3

1.2. Epoxy ring opening catalyzed by proton donors (HX) ……. 6

1.3. A typical DSC output in dynamic temperature scanning mode. The shaded area represents the amount of heat associated with the reaction or transition…… 8

1.4. Some commonly used aromatic epoxy resin systems……..... 14

1.5. Some common less reactive amine compounds used to cure epoxy resin……. 16

2.1. FT-IR spectrum of the uncured film adhesive as a KBr disc…….……... 23

2.2. ^{1}H NMR spectrum of the uncured film adhesive dissolved in CD_3COCD_3 (*a*) and in $CDCl_3$ (*b*). Insoluble components were removed prior to obtaining the spectra ..…….. 25

2.3. Comparison of ^{1}H NMR spectrum of *(a)* carboxy-terminated poly(acrylonitrile-*co*-butadiene) to that of the film adhesive (*b*) in $CDCl_3$….. 27

2.4. Comparison of ^{1}H NMR spectrum of *(a)* *N,N,N'N'*-tetraglycidyl-4,4'-diamino diphenylmethane (TGDDM) epoxy resin to that of the film adhesive (*b*) in $CDCl_3$…….… 28

2.5. Comparison of ^{1}H NMR spectrum of *(a)* diglycidyl ether of bisphenol A (DGEBA) epoxy resin to that of the film adhesive (*b*) in $CDCl_3$…….. 29

2.6. Comparison of ^{1}H NMR spectrum of the curing agent 4,4'-diaminodiphenylsulfone (DDS) (*a*) to that of the film adhesive (*b*) in CD_3COCD_3…… 30

2.7. Determination of the average oligomer length of the DGEBA component of the film adhesive. ^{1}H NMR spectra of the film adhesive without (*a*) and with (*b*) added Eu(FOD) shift reagent in $CDCl_3$. The base number refers to the carbon atom; the superscript refers to the protons attached to the carbon atom. Hence, 2^1 refers to proton #1 on carbon #2…… 32

2.8. Sketch of a developed thin-layer chromatography (TLC) plate using the solvent system cyclohexane:ethyl acetate:isopropyl alcohol (6:3:1)…….. 35

2.9. Structures of the major components of the film adhesive.
(a) CTBN rubber (*b*) TGDDM epoxy resin (*c*) DGEBA epoxy resin (*d*) DDS curing agent (*e*) DICY curing agent…….… 37

3.1. An example of a cure cycle for epoxy-based thermosets……. 39

3.2. An exotherm generated from dynamic temperature scanning of the film adhesive at 3°C/min from 30°C to 300°C…….. 44

3.3. DSC trace from the rescan of the film adhesive previously cured from 30°C to 300°C at 3 ^{o}C/min. Note the absence of residual exotherm. Rescanning was done at 10°C/min from 30°C to 300°C…….. 44

3.4. Degree of cure (α) of the film adhesive versus temperature over a range of heating rates……. 46

3.5. Rate of cure ($d\alpha/dt$) of the film adhesive versus temperature over a range of heating rates……. 47

3.6. Plot of degree of cure (α) of the adhesive as a function of heating rate and temperature……. 48

3.7. Plot of rate of cure ($d\alpha/dt$) of the adhesive as a function of temperature and heating rate……. 48

3.8. Apparent exothermic heat of reaction of the adhesive as determined by dynamic temperature scanning over a range of heating rates…….. 50

3.9. The gel point temperature for the adhesive, (or the temperature at which the degree of cure is 0.36) as a function of programmed heating rate…….. 51

3.10. Ultimate glass transition temperatures (Tg) of adhesive measured at a heating rate of 10°C/min from 30°C to 300°C, after curing over a range of heating rates…… 53

3.11. A plot of $\ln(d\alpha/dt)$ versus 1/T for the adhesive at $\alpha = 0.05$. Plots for other values of *a* are reproduced in Appendix A…….. 56

3.12. Plot of the apparent activation energy (*Ea*) of the adhesive cure reaction as a function of the degree of cure (α) as determined from dynamic temperature scanning data…… 56

3.13. An exotherm produced from isothermal scanning of the adhesive at 165 ^{o}C for 8 hours after a rapid jump to that temperature from 30°C……. 58

3.14. Intermediate Tg and residual exotherm produced from the rescan of the adhesive partially cured at 165°C for 8 hours. This rescan was done from 30°C to 300°C at 3°C/min……..….. 58

3.15. Ultimate Tg of the adhesive isothermally cured at 165°C for 8 hrs followed by dynamic temperatures scanning at 3°C/min from 30°C to 300°C to complete the cure. This DSC trace showing the ultimate Tg was generated from the dynamic temperature scanning at a heating rate of 10°C/min from 30°C to 300°C of the fully cured sample…….……. 59

3.16. 2D plot of the degree of cure (α) as a function of time for the film adhesive isothermally cured over a range of temperatures…… 61

3.17. Maximum degree of cure (α_{max}) attained after isothermal scanning……. 62

3.18. 2D plot of the rate of cure ($d\alpha/dt$) as a function of time for the film adhesive isothermally cured over a range of temperatures…… 64

3.19. Maximum degree of cure (α_{max}) of the adhesive attained after prolonged isothermal scanning after a rapid jump to that temperature (upper curve). Maximum reaction rate attained at the cure temperature normalized to that attained at 180°C (lower curve)……..... 65

3.20. 3D plot of the degree of cure (α) as a function of time and isothermal cure temperature……... 66

3.21. 3D plot of the rate of cure ($d\alpha/dt$) as a function of time and isothermal cure temperature…… 66

3.22. Intermediate Tg of the adhesive attained after prolonged isothermal heating, determined as 3°C/min post ramp from 30-300°C to complete the cure reaction…….. 68

3.23. Apparent heat of reaction (J/g) released during isothermal cure of the adhesive over a range of temperatures…… 69

3.24. Ultimate Tg of the adhesive after prolonged isothermal cure over a range of temperatures followed by a post cure scan at 3°C/min from 30°C to 300°C to complete the cure reaction. Ultimate Tg was determined by a second scan at 10 ^{o} C/min from 30°C to 300°C…….. 71

3.25. Maximum degree of cure (α_{max}) of the adhesive partly cured after an extensive isothermal soak as a function of the Tg attained during that isothermal scanning. This was measured from a 3°C/min post scanning from 30°C to 300°C…… 72

3.26. Time to reach the gel point (α_{gel} = 0.36) for the adhesive cured under isothermal conditions…… 73

3.27. Rate of cure versus degree of cure. Model prediction compared to isothermal data at 110 to 180°C…….. 76

3.28. Extent of cure (α) as a function of temperature up to 150°C at various heating rates (step 1)…… 78

3.29. Degree of cure as a function of time for the isothermal portion (step 2) at 150 ^{o}C after ramping to that temperature over a range of linear heating rates…… 78

3.30. Degree of cure as a function of time and initial degree of cure (from step 1 for various heating rates) for isothermal scanning at 150°C (step 2)…… 81

3.31. Rate of reaction ($d\alpha/dt$) of as a function of temperature for dynamic temperature scanning up to 150°C for a range of linear heating rates (step 1)……. 81

3.32. Reaction rate ($d\alpha/dt$) as a function of time during isothermal scanning at 150°C (step 2) after ramping to that temperature over a range of linear heating rates…….…….. 82

3.33. Reaction rate ($d\alpha/dt$) versus time and initial degree of cure for the isothermal scanning (step 2) at 150°C after ramping to that temperature over a range of linear heating rates…….……. 82

3.34. Development of the degree of cure for steps 1 and 2 of the combined dynamic and isothermal scanning experiment at 175°C. Times to the left of the y-axis correspond to ramp segment (step 1) while those to the right correspond to the soak segment (step 2)…… 85

3.35. Rates of cure ($d\alpha/dt$) for steps 1 and 2 of the combined dynamic and isothermal scanning experiment at 175°C. Times to the left of the y-axis correspond to the dynamic temperature scanning (step 1) while those to the right correspond to the isothermal scanning (step 2)…….. 86

3.36. Plot of elastic modulus (G'), loss modulus (G") and complex viscosity (G*) for the initially uncured adhesive as a function of time during isothermal cure at 130°C. The gel point (arrowed) is reached at 4433 sec…… 88

3.37. Development of tan delta with time for the adhesive cured under isothermal conditions at 130°C, 135°C, 140°C, and 150°C. Arrows mark the gel point at each temperature…… 90

3.38. Apparent degree of cure at the gel point as a function of isothermal cure temperature. Average degree of cure at the gel point for the curing at 130, 135 and 140°C was 0.36……. 91

CHAPTER 1

INTRODUCTION

1.1 Introduction

Epoxy resins have been commercially available for more than half a century. They have been used in a variety of applications including coatings, electronics, adhesives and composite materials. Although somewhat more costly than other types of resins, their ease of processing and handling, and excellent physical and chemical properties make epoxy resin systems preferable, especially in demanding applications [1, 2]. The formation of an epoxy resin system involves a curing process wherein monomeric or oligomeric polyfunctional epoxide-containing molecules are cross-linked to form a rigid macromolecular structure. Epoxy resin is composed of two precursors: (1) a polyfunctional epoxide-containing reactant or reactants and (2) a curing agent or hardener which is usually an amine compound. The physical and chemical properties of a cured epoxy resin depend on the type of precursors and the cure cycle employed to polymerize the epoxy. Epoxy systems are thermosets. Depending on the reactivity of the hardener, epoxy polymerization may require elevated temperatures. Understanding the behavior of epoxy systems during cure is vital in making materials with consistent properties [3].

1.2 Curing of Epoxy with Amines

Different types of hardeners have been used in curing epoxy. In this study, amine-based hardeners were used. For this reason, the chemistry of the polymerization of epoxy with amines is discussed briefly.

The mechanism for the polymerization of epoxy with amines has been studied extensively [3-10]. Basically, three steps are involved: (1) attack of the amine group on the least hindered methylene of the epoxide to open the ring and form a hydroxyl and a secondary amine product, (2) further reaction of the so formed secondary amine with another epoxy group to form a second hydroxyl and a tertiary amine group, and lastly, (3) an etherification reaction between the hydroxyl groups formed in steps (1) and (2), and any excess epoxy groups. This is illustrated in Figure 1.1.

The relative reaction rate of the primary and secondary amines has been studied extensively [6, 8, 11, 12]. However, complete agreement has not been reached because of differences in analytical methods and kinetic models. For example, Mijovic and Wijaya[12] reported that the reactivity of primary and secondary amines towards epoxy is dependent on the amine type. Electron-donating groups (methoxy substituent on *p*-anisidine) showed a relative reactivity ratio (R_s/R_p) of secondary amine/epoxide and primary amine/epoxide as 0.549 while the electron-withdrawing nitro group on *p*-nitroaniline gave a reactivity ratio of 0.089. Diaminodiphenylsulfone (DDS) gave an intermediate reactivity ratio of 0.223. A monufunctional phenylglycidyl ether (PGE) was used as the epoxide reactant.

Girard-Reydet, *et al* [11] studied the reactivity of different aromatic amine hardeners with diglycidyl ether of bisphenol A (DGEBA) epoxy resin. The ratio of the reactivity of the secondary amine to the primary amine is 0.45 for DDS and 0.65 for 4,4'-methylenedianiline (MDA), 4,4'-methylenebis(2,6-diethylaniline) (MDEA), and 4,4'-methylenebis(3-chloro-2,6-diethylaniline) (MCDEA). These four amines have varying degree of reactivity. Therefore, R_s/R_p increases with the basicity of the amine.

(a) Epoxy – Primary Amine

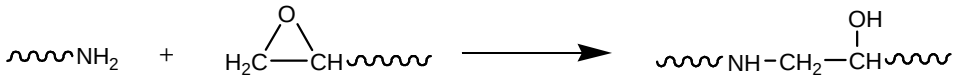

(b) Epoxy – Secondary Amine

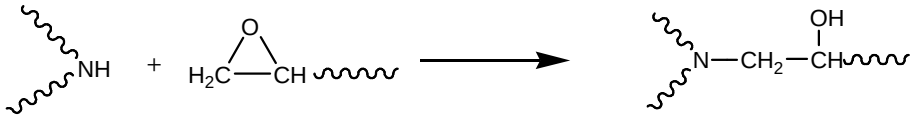

(c) Etherification

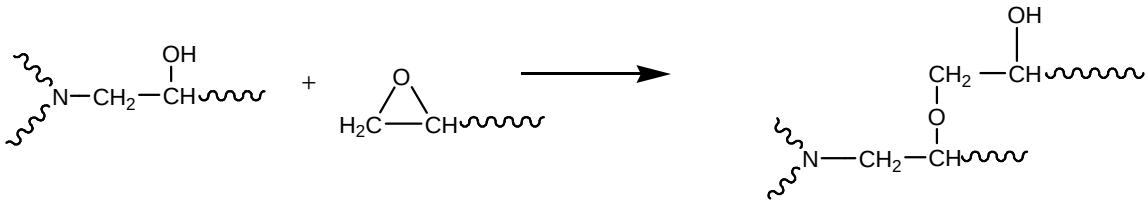

Figure 1.1. Major reactions occurring in the polymerization of epoxy with amines.

Liu, *et al* [6] investigated the influence of substituents on the aromatic amines used for curing epoxy. They reported that the relative reactivities of the secondary and primary amines can be explained in terms of structural differences and substitution effects. Electron-donating substituents to the benzene ring were found to increase reactivity of both the primary and secondary amines. Electron-withdrawing groups showed the opposite trend. In agreement with Girard-Reydet [11], deconjugation of the benzene ring pi electrons from the lone pair on the nitrogen atom enhanced the reactivity of the secondary amine compared to that of the corresponding primary amine in certain aromatic amine–epoxy combinations. Of specific relevance to our work, DGEBA and *N,N,N',N'*-tetraglycidyl-4,4'-diaminodiphenylmethane (TGDDM) resins cured with DDS produce an R_s/R_p ratio of about 0.2. In other words, there is a significant difference in the reactivity of the primary and secondary amines in DDS with these epoxy resins.

The etherification reaction is known to occur at higher temperatures and advanced degrees of cure [12]. It may be considered insignificant at the early stages of the reaction and overall, if the resin is formulated from either a stoichiometrically balanced mixture or with an excess of amines. Most of the models proposed for the cure kinetics of epoxy resins disregard the etherification reaction and it seems to work well in most instances. Cole [13, 14] developed a rigorous mathematical model that takes into account these three major reactions occurring during the polymerization of epoxy with amines. The etherification reaction is shown to be significant when curing is done at higher temperatures in the presence of excess epoxy and especially at later stages of the curing process when most of the amines have reacted.

Proton donors, such as hydroxyl groups produced from the reaction of primary or secondary amines and epoxide, the primary and secondary amines themselves, or any impurities present in the mixture are found to catalyze the curing process [7]. Tertiary amines also catalyze the ring opening of epoxide with amines. Shechter, *et al* [9] proposed the concerted reaction of amine, epoxide and proton donor to form a termolecular activated complex. Smith [7, 9] suggested a modification to this mechanism in which the same termolecular activated complex is formed from the bimolecular reaction between an adduct of the epoxide and the proton donor, and the amine (refer to Figure 1.2). The disintegration of the complex is believed to be the rate determining step. Tanaka and Mika [15] suggested that the higher basicity of an amine relative to an epoxide makes the formation of an amine-proton donor adduct more likely. King and Bell [16] provided some evidence in favor of Tanaka's suggestions.

1.3 Kinetics of Epoxy-Amine Polymerization

Predicting the properties of materials using mathematical models is tremendously useful in cutting down cost and time, especially during the design stage. With an excellent model, it is possible to predict how the system will cure [13]. The degree of cure (designated as α) which denotes the conversion of the epoxide into polymeric network is normally used to follow the progress of cure.

$$a_t = \frac{[epoxy]_0 - [epoxy]_t}{[epoxy]_0} \qquad (1)$$

Several analytical methods [6, 17-25] have been used to monitor the curing of different types of polymers. Of these, the most commonly used for epoxy resin systems is differential scanning calorimetry (DSC).

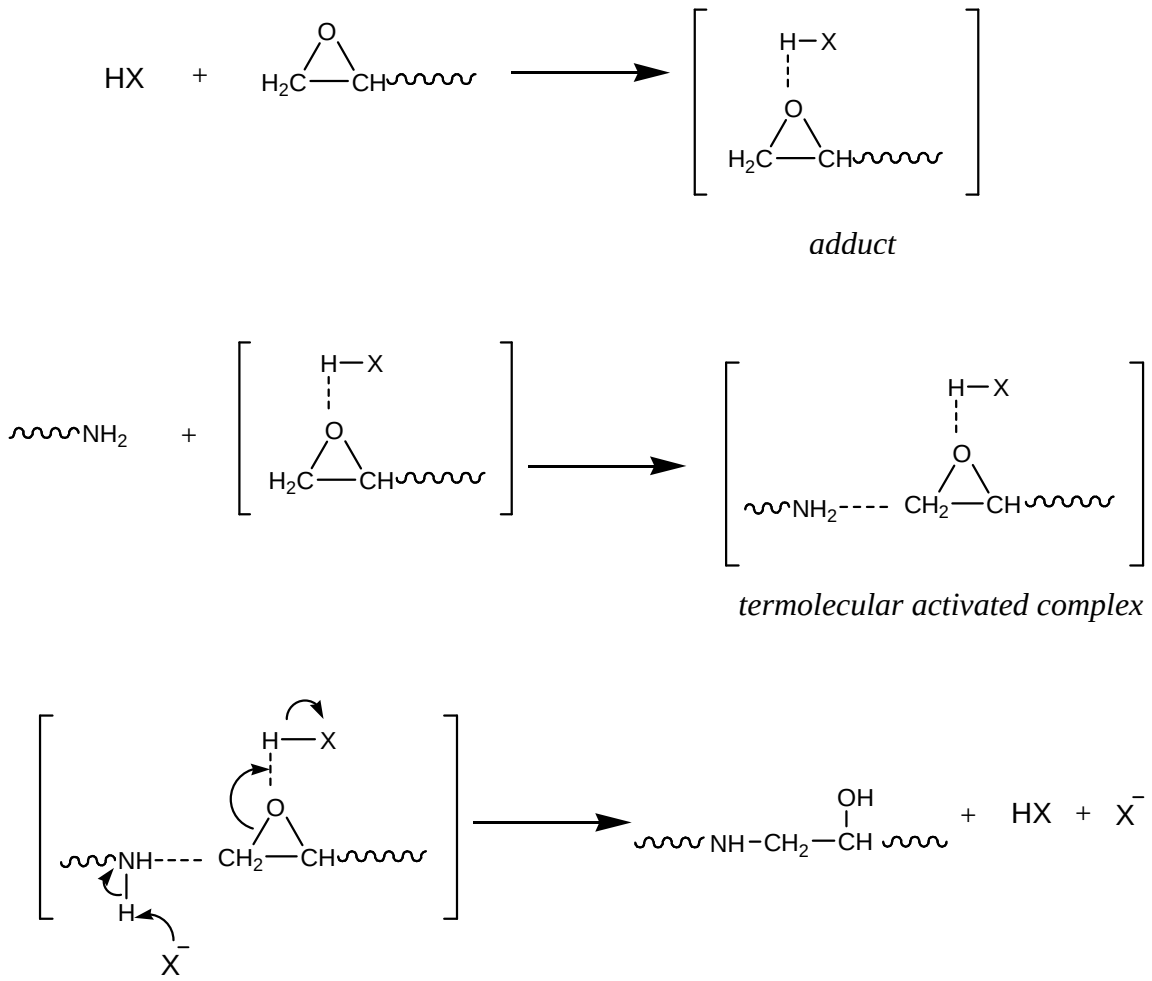

Figure 1.2. Epoxy ring opening catalyzed by proton donors (HX) [7, 9].

1.3.1 Differential Scanning Calorimetry (DSC)

DSC is used to monitor heat changes associated with chemical reactions. The cure of epoxy groups with amines is an exothermic process that can be monitored by DSC. Small sample size and ease of data gathering are the major advantages of DSC in kinetic investigations. Moreover, it can also provide information about thermal transitions such as the glass transition temperature (Tg) which can be correlated to the state of cure of a resin [3]. A differential scanning calorimeter measures the heat flow required to keep the sample and the reference material at the same temperature. DSC can be operated in two basic modes (1) dynamic temperature scanning and (2) isothermal scanning. Barton [3] gave a more detailed discussion on the principle and use of DSC.

A basic assumption in using DSC is that the heat flow relative to the baseline signal is proportional to the rate of reaction occurring in the sample compartment [3]. A typical output from a DSC run in dynamic temperature scanning mode is shown in Figure 1.3. By integrating the area between the curve and the baseline, the amount of heat associated with the reaction or transition (absorbed or released) can be determined. The total heat, Q_{total}, associated with the reaction or transition is equal to the area in the DSC trace as shown in equation (2)

$$Q_{total} = \int_{t_0}^{t_f} \left(\frac{dq}{dt} \right) dt \qquad (2)$$

where (dq/dt) is the heat flow and t_f is the time at which the DSC signal goes back to the baseline. Getting partial areas by integrating the heat flow with respect to time up to an intermediate time t would then allow the calculation of the degree of cure (a) at that point of the reaction.

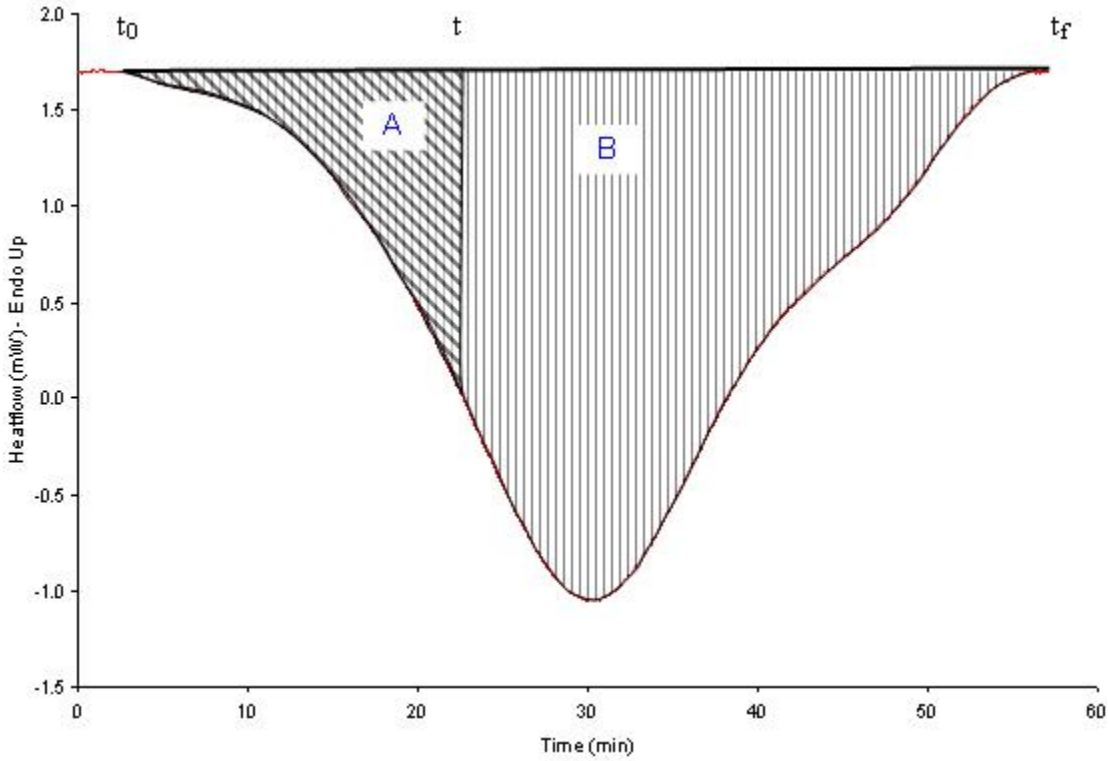

Figure 1.3. A typical DSC output in dynamic temperature scanning mode. The shaded area represents the amount of heat associated with the reaction or transition.

$$degree\ of\ cure,\ a_t = \frac{\int_{t_0}^{t}\left(\frac{dq}{dt}\right)dt}{Q_{total}} = \frac{area\ A}{area\ A + area\ B} \qquad (3)$$

A single DSC run, therefore, can generate a set of data that describes the extent of conversion of reactants to products in the course of the curing process as function of *t*. Furthermore, these data can easily be converted to rate of reaction (da/dt) by differentiating the degree of cure with respect to time. Mathematical models can then be fitted into experimental data to get kinetic parameters.

1.3.2 Kinetic Models of Epoxy-Amine Cure

There have been a number of models proposed to describe the cure kinetics of various types of epoxy resin systems. These models can be phenomenological / empirical models [26-33] or mechanistic models [4, 6, 7, 11, 13, 14, 34]. Phenomenological models are mathematical expressions made to fit the experimental data with minimal effort to describe how the reacting particles are converted to products. On the other hand, mechanistic models are based on detailed analysis of the chemical reactions that are involved in the conversion process. Such models are expected to be more accurate in predicting the kinetics of the chemical reaction [35]. However, mechanistic models are not always favored due to the complexity of resin cure [36]. Furthermore, the composition of the reacting mixture at any point during cure is not easily obtained despite technological advances in chemical analysis that are available now. With better sensitivity and design, DSC has been the preferred method for majority of the kinetic studies of epoxy resin published thus far.

An empirical model for epoxy resin cure has a general expression for the rate of reaction as [35]

$$rate\ of\ reaction,\ \frac{da}{dt} = K\,f(a) \qquad (4)$$

where a is the degree of cure, t is the reaction time, K is the time-dependent reaction rate constant, and $f(a)$ is some function of the degree of cure. The rate constant is usually considered to have an Arrhenius type temperature dependence

$$K = Ae^{\left(\frac{-E_a}{RT}\right)} \qquad (5)$$

where A is the pre-exponential factor, E_a is the energy of activation, R is the universal gas constant (8.314 J/mol-K) and T is temperature in Kelvin. Substituting the expression for K to equation (4) gives

$$\frac{da}{dt} = Af(a)e^{\left(\frac{-E_a}{RT}\right)} \qquad (6)$$

The rate of reaction usually decreases and eventually approaches zero, as the reaction comes to a completion or if it becomes impossible for the reacting groups to find each other (vitrification). In some cases, an autocatalysis may be observed wherein the rate of reaction may increase at the early stages of the reaction. Polymerization of epoxy with amine exhibits autocatalysis at the beginning of the reaction as hydroxyl groups so formed catalyze succeeding reactions.

In the absence of vitrification, the value of a at the completion of the reaction will be equal to unity. The function $f(a)$ can then be expressed as [35]

$$f(a) = g(a)(1-a)^n \qquad (7)$$

where n is the kinetic exponent and $g(a)$ is an experimentally derived function. Assuming $g(a)$ to be equal to 1, equation (7) becomes the simplest kinetic model (*an nth order kinetic model*). This has been used to model the cure of thermoset resins [35, 36].

Combining equations (4) and (7) would result in an expression of rate where the maximum rate of reaction should be observed at the start of the reaction (a = 0). Such *nth* order kinetic model fails to take into account autocatalysis which is a very significant phenomenon in the case of epoxy-amine cure. This means that the maximum rate of reaction occurs later in the reaction. If the resin vitrifies before the completion of the reaction, the maximum achievable degree of cure (a_f) will be less than unity. Equation (7) thus becomes

$$f(a) = g(a)(a_f - a)^n \qquad (8)$$

Various groups have used different expressions to describe the cure kinetics of epoxy-amine systems. Horie, *et al* [18] proposed the following model

$$\frac{da}{dt} = (K_1 + K_2 a)(1 - a)(B - a) \qquad (9)$$

where K_1 is the rate constant for the reaction catalyzed by groups initially present in the resin, K_2 is the rate constant for the reaction catalyzed by newly formed groups and represents the influence of the reaction products on the rate of reaction, and B is the initial ratio of the number of amine N-H bonds to number of epoxide groups. Loos, *et al* [26] showed that the cure kinetics of Hercules 3501-6 epoxy resin can be described with equation (9).

Many high performance materials use aromatic amine curing agents which require high temperatures. For such types of resin, etherification reactions become prominent,

and therefore, it cannot be well modeled using equation (9). Kamal, *et al* [30] developed a semi-empirical model

$$\frac{da}{dt} = Ka^{m}\left(a_{f} - a\right)^{n} \qquad (10)$$

where a_f is the maximum achievable degree of cure and the exponents *m* and *n* are fitting parameters. This model describes the observation that the maximum rate of cure does not occur at the beginning of the reaction (autocatalysis). This has been applied to the cure kinetics of an unsaturated polyester resin [30] and to the cure of graphite/epoxy Hercules AS4/3502 pre-preg [37].

According to this model, equation (10), the rate of reaction is zero at the start of the reaction, increases up to maximum value and then decreases as the reaction comes to a completion or vitrification. Realistically, the initial rate of reaction may not be zero as the reactants can also be converted into products through alternate routes. Kamal, *et al* [30] developed the following more general model

$$\frac{da}{dt} = \left(K_1 + K_2 a^{m}\right)\left(a_{f} - a\right)^{n} \qquad (11)$$

where K_1 and K_2 are Arrhenius rate constants and a_f is considered to be unity. This has been found to successfully describe the cure kinetics of both epoxy and polyester resin systems. Dusi, *et al* [31] were able to describe the cure kinetics of Cytec Fiberite 976 epoxy resin system with this model. The kinetics of cure of Araldite LY-556 was developed by Seifi and Hojjati [38] using this model as well. Stone, *et al* [39] and Han, *et al* [40] also used this model to describe the cure kinetics of unsaturated polyester resins.

1.4 Epoxy-Based Adhesives

Epoxy resins offer outstanding properties that cheaper resins cannot meet. Although a sizable proportion of epoxy resin applications are in coatings, there is a significant use of epoxy resins in high performance structural applications such as adhesives for aircraft building. Epoxy resins cure with no evolution of volatile byproducts, undergo low shrinkage during cure and adhere to many different types of surfaces such as metal, wood, glass, plastics, ceramics, concrete, asphalt and rock [41]. Epoxy adhesives represent only a small fraction of the adhesives industry but they have found unequalled performance in applications where strength and stability are critical [2].

Another advantage of epoxy systems is that there are a variety of agents (type of resin and curing agent, fillers, diluents, flexibilizers, toughening agents, etc) that can be manipulated to achieve optimum properties. However, the majority of commercially available epoxy adhesives are formulated using a relatively small number of basic components. Such formulations can range from very simple, low molecular weight, primarily aliphatic resins to multifunctional aromatic types [1].

The most widely used epoxy resins are based on the adduct of bisphenol A and the epichlorohydrin. Diglycidyl ether of bisphenol A (DGEBA) resin is a difunctional molecule with two terminal epoxide groups. Its chain length can vary to produce a product that is a moderately viscous liquid to a solid at room temperature. Longer chains are frequently used in film adhesives where a degree of structural integrity must be maintained. With the increasing demands for high performance epoxy resins, multi-functional aromatic epoxy systems which have higher epoxide content per gram of resin have been developed by Dow, Ciba-Geigy and Shell (see Figure 1.4 for resin structures).

(a) Diglycidyl ether of bisphenol A (DGEBA)

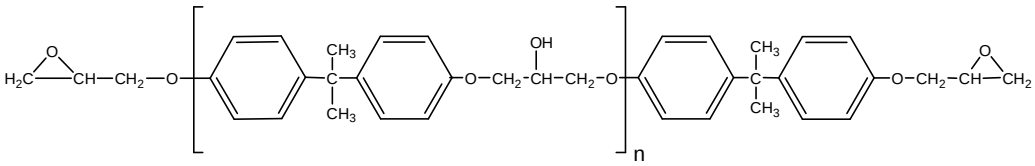

(b) *N,N,N',N'*-tetraglycidyl-4,4'-diaminodiphenyl methane (TGDDM):
Araldite MY720 (Ciba-Geigy)

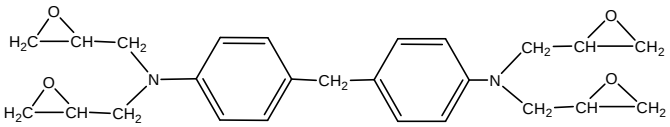

(c) *EPON 1031 (Shell)*

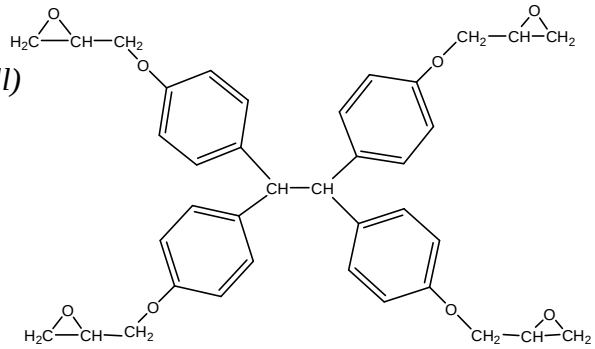

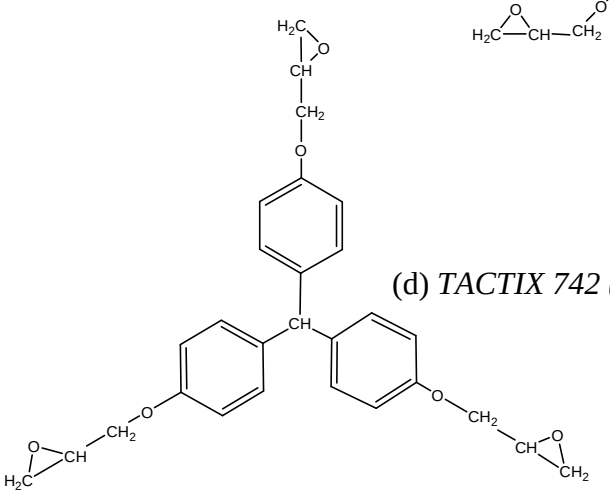

(d) *TACTIX 742 (Dow)*

Figure 1.4. Some commonly used aromatic epoxy resin systems.

Incorporation of aromatic and heterocyclic structures into the network is found to improve the thermal stability of the cured resin [42]. Thus, these epoxy resins can be employed in higher temperature applications. They are also widely used as the matrix in composite materials [43-45].

The selection of an appropriate curing agent or hardener is as important as selecting the proper epoxy resin. The type of curing agent will determine reactivity, degree of conversion, viscosity, gel time and heat requirements for cure. Furthermore, shelf life, method of application and desired properties must also be considered in the selection of the curing agent [2]. The curing agent, in part, would also determine the structure of the cured polymeric network, and hence, significantly affect its properties.

Different types of compounds have been used to cure epoxy resins. The most commonly used are aliphatic, cycloaliphatic and aromatic amines [1, 46, 47]. The functionality of the amine as curing agent for epoxy resin is determined by the number of N-H bonds in a molecule. Tertiary amines do not react readily with the epoxide but they can act as a catalyst in the ring opening reactions. Aliphatic amines react with epoxy at ambient conditions. This type of system has a very short shelf life and may produce localized charring when large volumes of resin are cured or if thermal conductivity is low [2, 41].

Cycloaliphatic amines give better thermal resistance and toughness than aliphatic amines. Being less reactive than aliphatic amines, they have a longer shelf life and can be used in larger amounts [2]. Epoxy prepared using aromatic amines (Figure 1.5), on the other hand, have both better chemical and thermal resistance than epoxy cured with

(a) meta-phenylenediamine (MPDA)

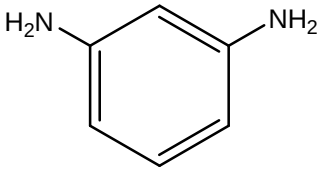

(b) 4,4’-diaminodiphenylmethane (DDM)

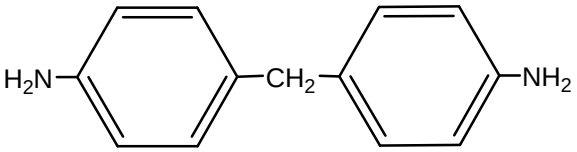

(c) 4,4’-diaminodiphenylsulfone (DDS)

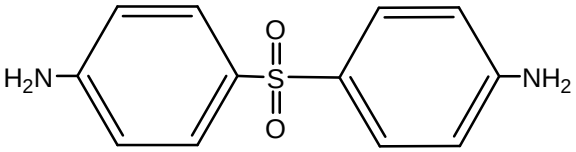

(d) Dicyandiamide (DICY)

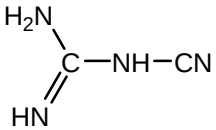

Figure 1.5. Some common less reactive amine compounds used to cure epoxy resin.

aliphatic amines. Their pot life is longer and they are cured at higher temperatures. The pot or shelf life refers to the length of time throughout which the epoxy resin is still useful.

A latent curing agent, dicyandiamide, has also been used for curing epoxy systems [2, 45]. Dicyandiamide (DICY) is a solid curing agent which can have a shelf life of six months with solid or liquid epoxy resins. When heated with or without catalysts, rapid polymerization ensues only after the DICY melts to form a highly cross-linked resin exhibiting excellent strength, moderate heat resistance, high solvent resistance and good electrical insulating properties [1]. Being a latent curing agent, dicyandiamide requires higher temperatures to cure and it is normally used with co-curing accelerators or catalysts such as tertiary amines. Dicyandiamide is a preferred curing agent for one-component epoxy adhesives.

Fillers are added to adhesive formulations to improve properties like shrinkage, thermal expansion, curing characteristics, viscosity, heat and electrical conductivity and lower cost. Fillers such as silica, aluminum and alumina powders are the most common additives in epoxy structural adhesives. The amount of filler can range from 20 to about 800 parts per 100 parts resin [2]. Other additives include diluents, flexibilizers and toughening agents. Carboxyl or amine terminated butadiene acrylonitrile (CTBN) rubbers have been found to toughen epoxy adhesives. These additives have minimal effect on modulus and glass transition temperature (Tg) because they phase separate on cure [1, 2]. These elastomeric modifiers are used at low levels, 3-30 parts per 100 parts resin.

1.5 Overview of this Study

This study is focused on the chemical characterization and cure kinetics of a high performance, high shear film adhesive that is used in load-bearing applications in the aerospace industry. Currently, this adhesive is cured using a “standard” cure cycle for epoxy thermosets. Different epoxy-based materials (composite pre-pregs, adhesives, coatings, etc) may not cure properly if cured together using a “standard” cure cycle. Each can have different cure profiles and combinations may require unique conditions to obtain best properties. It is therefore imperative to investigate separately the cure characteristics of these classes of materials before proposing an optimized cure cycle for their assembly.

Substandard materials made of this adhesive are occasionally produced. Hot spots have been found to occur that can lead to resin degradation and poor bonding. It is the main purpose of this study to generate data that can lead to an optimal cure profile for this adhesive. In particular, this is aimed at creating a kinetic model that will allow for the prediction of the degree and rate of cure at any point in a two-step cure cycle. Of specific significance is the identification of points at which a maximum rate of reaction (spike) occurs. To lessen the possibility of hot spots, this spike in the exotherm must be minimized and made to occur at lower temperatures. Moreover, the extent of cure at the gel point which influences the flow properties of the resin during cure must be known. For example, if resin flows excessively due to a slow build up of viscosity, a resin poor material with poor physical properties can be produced.

Chemical characterizations were performed using chromatographic and spectroscopic techniques. Peak-to-peak comparison with reference materials was found to

be a quick yet reliable way to identify and semi-quantify the major components of the adhesive.

The cure profile of the adhesive was investigated using differential scanning calorimetry (DSC). A series of dynamic temperature (ramp), isothermal (soak), and combined ramp and soak experiments were performed. A range of heating rates (0.5 to 20°C/min) was used in the ramp experiments. Isothermal scanning was performed between 110° C to 180°C for extended times. Combined ramp and soak runs were performed to model industrial ramp and soak cure profiles. Plots that would allow the prediction of the degree and rate of cure as functions of easily obtained variables were generated. Gel points were determined from rheometric experiments.

CHAPTER 2

CHEMICAL CHARACTERIZATION OF THE FILM ADHESIVE

2.1 Introduction

To better understand the cure reaction of the film adhesive, its chemical composition was first determined. A survey of related studies [43-45, 48-55] showed that the majority of commercially available high performance epoxy-based adhesives and pre-impregnated composite materials usually contain *N,N,N',N'*-tetraglycidyl-4,4'-diaminodiphenylmethane (TGDDM) and / or diglycidyl ether of bisphenol A (DGEBA) as the epoxy resin precursors and 4,4'-diaminodiphenylsulfone (DDS) as the curing agent. Our approach in identifying the components was by direct comparison of the adhesive with reference materials. Attempts to separate the components proved to be quite challenging but characteristic peaks in ^{1}H NMR spectrum of the unseparated, uncured adhesive were successfully identified. This was used as the basis to quantify the major components of the film adhesive.

2.2 Experimental

2.2.1 Materials

A sample of commercially available epoxy-based high performance, high shear film adhesive was obtained. The adhesive was kept refrigerated at -20° C until use. 4,4'-Diaminodiphenylsulfone (DDS), Europium tris(6,6,7,7,8,8,8-heptafluoro-2,2-dimethyl-3,5-octanedionate) (Eu(FOD)) shift reagent, potassium bromide (KBr), dicyandiamide (DICY) and solvents were obtained from Aldrich Chemical Company. Diglycidyl ether

of bisphenol A (DGEBA) epoxy resins (EPON™ Resin 825, 834, 1001F, 1004F and 1009F) were obtained as research samples from Resolution Performance Products. *N*,*N*,*N'*,*N'*-tetraglycidyl-4,4'-diaminodiphenylmethane (TGDDM) epoxy resin (Araldite MY 720) was purchased from Huntsman Advanced Materials. Hycar X21, a liquid acrylonitrile-butadiene liquid elastomer, was obtained as a research sample from BF Goodrich. All materials were used without further purification.

2.2.2 FT-IR Spectroscopy

A ThermoNicolet Avatar FT-IR spectrometer was used to obtain FT-IR spectra of the adhesive and reference materials as KBr disks. About 2 mg of the material was mixed with about 300 mg KBr in a dentist's "wiggle bug" mixer, then pressed at about 20000 lb pressure to produce semi-transparent disks. Alternately, components of the adhesive that are soluble in organic solvents were dissolved and then deposited on a NaCl salt plate for analysis after evaporation of the solvent. Spectra for some of the reference materials were also taken as films deposited on NaCl salt plates.

2.2.3 Nuclear Magnetic Resonance Spectroscopy

Strips of the film adhesive were dissolved in deuterated solvent, centrifuged and filtered to remove the filler. The supernatant liquid was then analyzed by ^{1}H NMR spectroscopy. ^{1}H NMR spectra of the reference materials were taken from solutions prepared by dissolving the samples in appropriate deuterated solvents. Spectra were obtained using a Varian Inova 400 MHz or a Varian Mercury 300 MHz FT-NMR spectrometer.

2.2.4 Elemental Analysis

Elemental analysis of the film adhesive was performed by Galbraith Laboratories. Carbon, hydrogen and nitrogen were determined by combustion analysis. Oxygen, sulfur and aluminum were determined by standard methods of analysis. Inductively Coupled Plasma – Mass Spectrometry (ICP-MS) was used to analyze other elements.

2.2.5 Thin-Layer Chromatography

Components of the adhesive were separated using thin layer chromatography on silica gel with fluorescent indicator. Samples (100-200mg) of the adhesive were dissolved in chloroform, centrifuged, and the supernatant liquid was painted across a preparative TLC plate. The plate was developed using a mixture of cychlohexane, ethyl acetate and isopropyl alcohol in a 6:3:1 ratio. The plate was turned 90°, and re-developed using the same solvent system to concentrate the material that was subsequently removed from the plate using THF. The four fractions so isolated were analyzed by FT-IR and ^{1}H NMR spectroscopy.

2.3 Results and Discussions

A combination of spectroscopic and separation techniques were employed to gain insights into the chemical composition of the high performance high shear film adhesive. Integrated results obtained from NMR and FT-IR spectroscopy combined with separations by thin layer chromatography (TLC), gave semi-quantitative compositional information on the adhesive. FT-IR and NMR spectra of the film adhesive and various reference materials believed to compose the film adhesive were compared and analyzed.

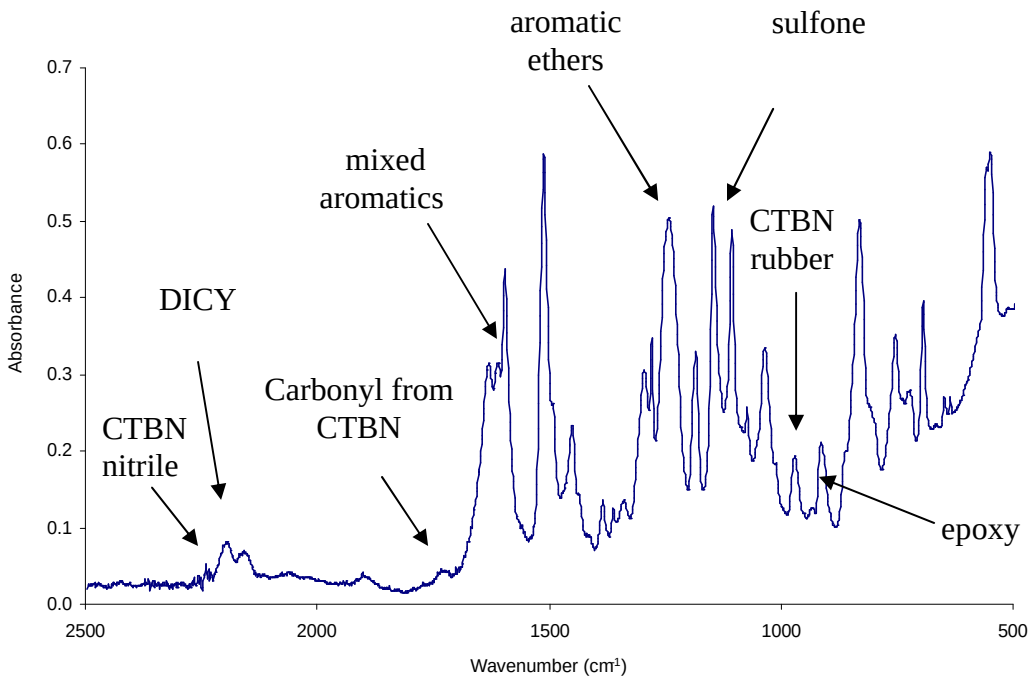

Figure 2.1. FT-IR spectrum of the uncured film adhesive as a KBr disc.

2.3.1 FT-IR spectroscopy

Figure 2.1 shows the FT-IR spectrum of the adhesive as a KBr disc. The spectrum indicated the presence of saturated and unsaturated/aromatic compounds. Carboxy terminated poly(acrylonitrile-*co*-butadiene) rubber (CTBN) was identified by its distinctive nitrile stretch at 2236 cm^{-1}, weak carbonyl stretch at about 1720 cm^{-1} due to terminal carboxylic acid groups, substituted olefinic stretches at 1630-40 cm^{-1} and out of plane bending modes at 967 and 911 cm^{-1}. Dicyandiamide (DICY) gave its very distinctive nitrile peaks at 2206 cm^{-1} and 2161 cm^{-1} and a weak out of plane bending absorption at 925 cm^{-1}. Absorbances at 1143 cm^{-1} and 1104 cm^{-1} were attributed to the sulfone group of DDS. Finally, epoxy oxirane ring gave an absorbance at 915 cm^{-1}.

2.3.2 NMR Spectroscopy

The ^{1}H NMR spectrum of an organic mixture is especially useful in compositional analysis if it contains distinct non-overlapping resonances that allow us to quantify the structural units in the mixture. ^{1}H NMR spectra of the uncured adhesive in deuterated acetone and chloroform are shown in Figure 2.2. As a number of non-overlapping signals in the spectrum were identified, this technique has been found to yield more information, more rapidly, than any other method of structural investigation.

The DDS component is not completely soluble in chloroform but is soluble in acetone. Therefore, although peaks for the aromatic protons of DDS were detected using $CDCl_3$ as the solvent, the ^{1}H NMR spectrum of the adhesive in CD_3COCD_3 was used to quantify the relative amounts of TGDDM, DDS and DGEBA. All the major components

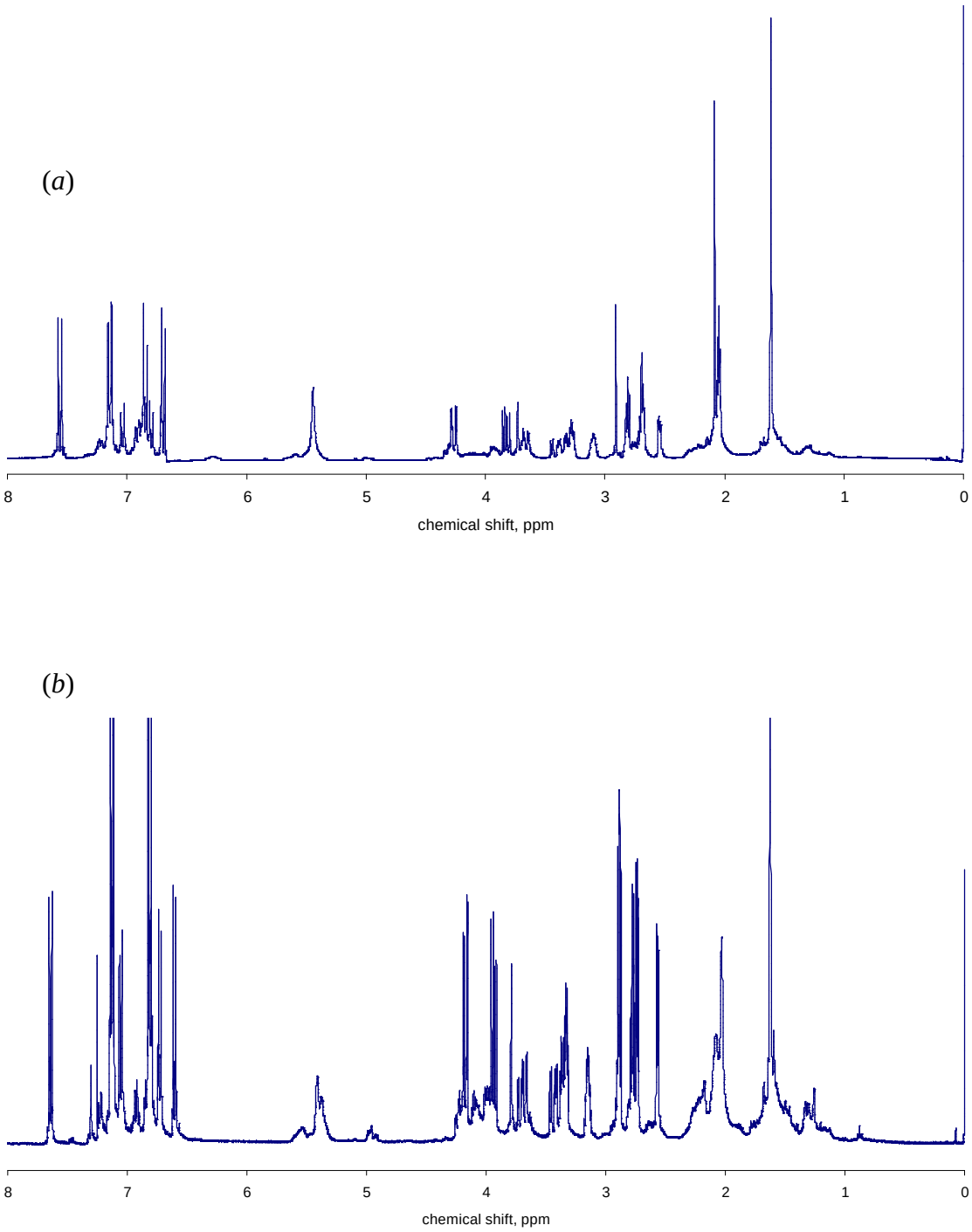

Figure 2.2. ^{1}H NMR spectrum of the uncured film adhesive dissolved in CD_3COCD_3 (*a*) and in $CDCl_3$ (*b*). Insoluble components were removed prior to obtaining the spectra.

of the adhesive, except the aluminum and dicyandiamide, were soluble in acetone. Dicyandiamide was partly soluble in acetone but very soluble in DMSO. Low molecular weight carboxy terminated poly(acrylonitrile-*co*-butadiene) rubber (CTBN) is often added to epoxy resin systems to increase fracture toughness. An approximately 10 % rubber additive was reported to enhance toughness in epoxy cresol novolac resin systems [56] and epoxy adhesives [57-59]. The rubber is miscible with the uncured resin and phase separates during cure to form a microdroplet suspension in the resin that prevents crack propagation. The CTBN rubber component was identified in the FT-IR spectrum of the uncured adhesive. Olefinic proton signals at 5-6 ppm, the α-olefin proton signals at about 2.1 ppm and other saturated protons signals at about 1.0 to 1.5 ppm were assigned to the CTBN rubber component. A comparison of the ^{1}H NMR spectra of CTBN and the film adhesive in $CDCl_3$ is shown in Figure 2.3.

Similarly, TGDDM (Figure 2.4) and DGEBA (Figure 2.5) epoxy resins, and the curing agent DDS (Figure 2.6) were found to be the other components of the film adhesive. TGDDM and DGEBA are usually used in high performance epoxy-based materials in the aerospace industry. TGDDM with a functionality of 4 gives a highly cross-linked material upon cure. In contrast, DGEBA is a bifunctional linear molecule. The balance of TGDDM and DGEBA in the mix is critical in controlling the build up of cross-link density, and hence, viscosity of the material during the curing process. For example, if the viscosity of the resin is too low, it will flow out of the assembly during cure resulting to a substandard material. Epoxy-based adhesives and fiber reinforced pre-impregnated composite materials are normally cured at elevated temperature inside a pressurized auto-clave. An overly quick increase in viscosity is also not desired as this

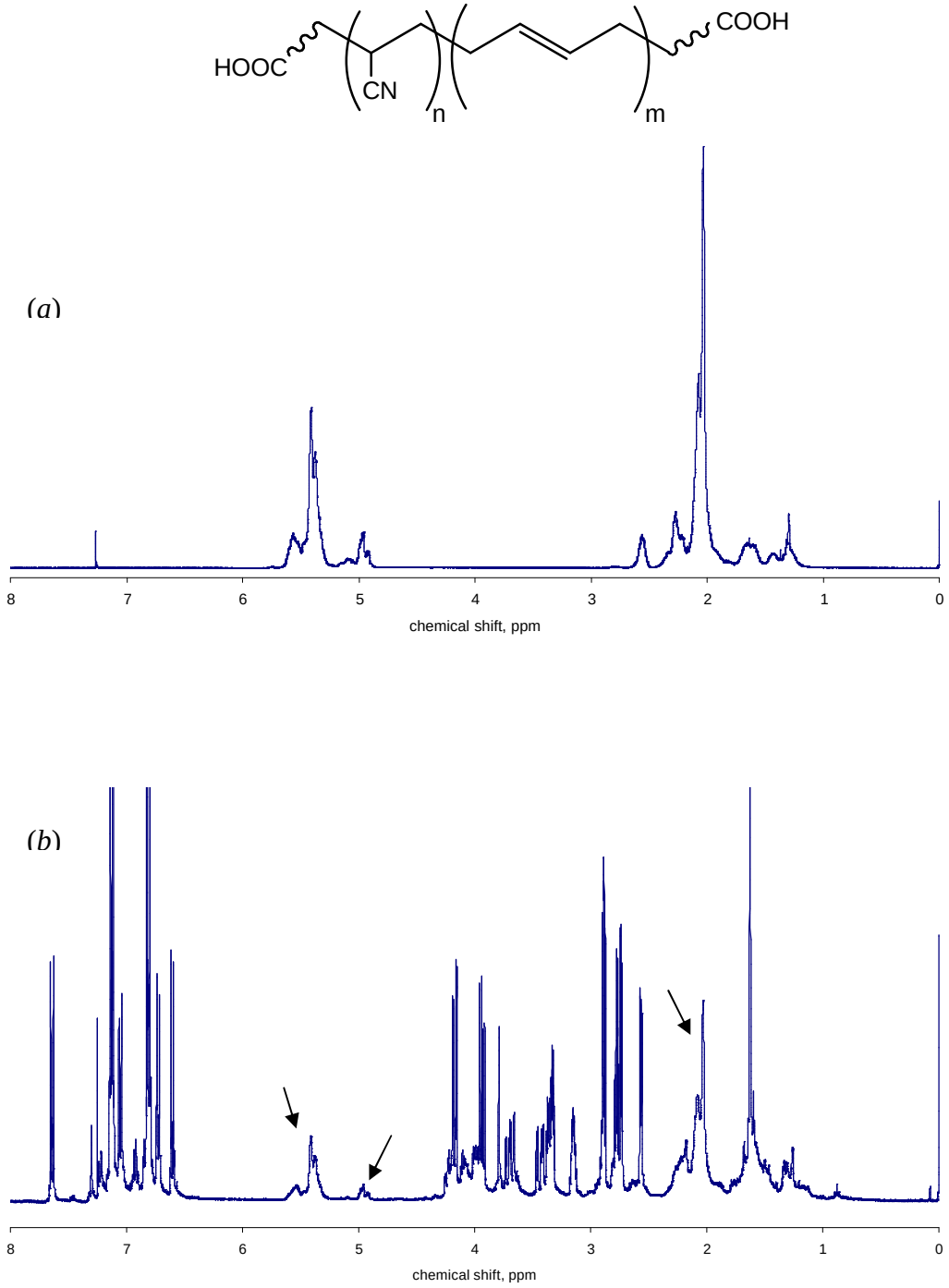

Figure 2.3. Comparison of ^{1}H NMR spectrum of *(a)* carboxy-terminated poly(acrylonitrile-*co*-butadiene) to that of the film adhesive (*b*) in $CDCl_3$.

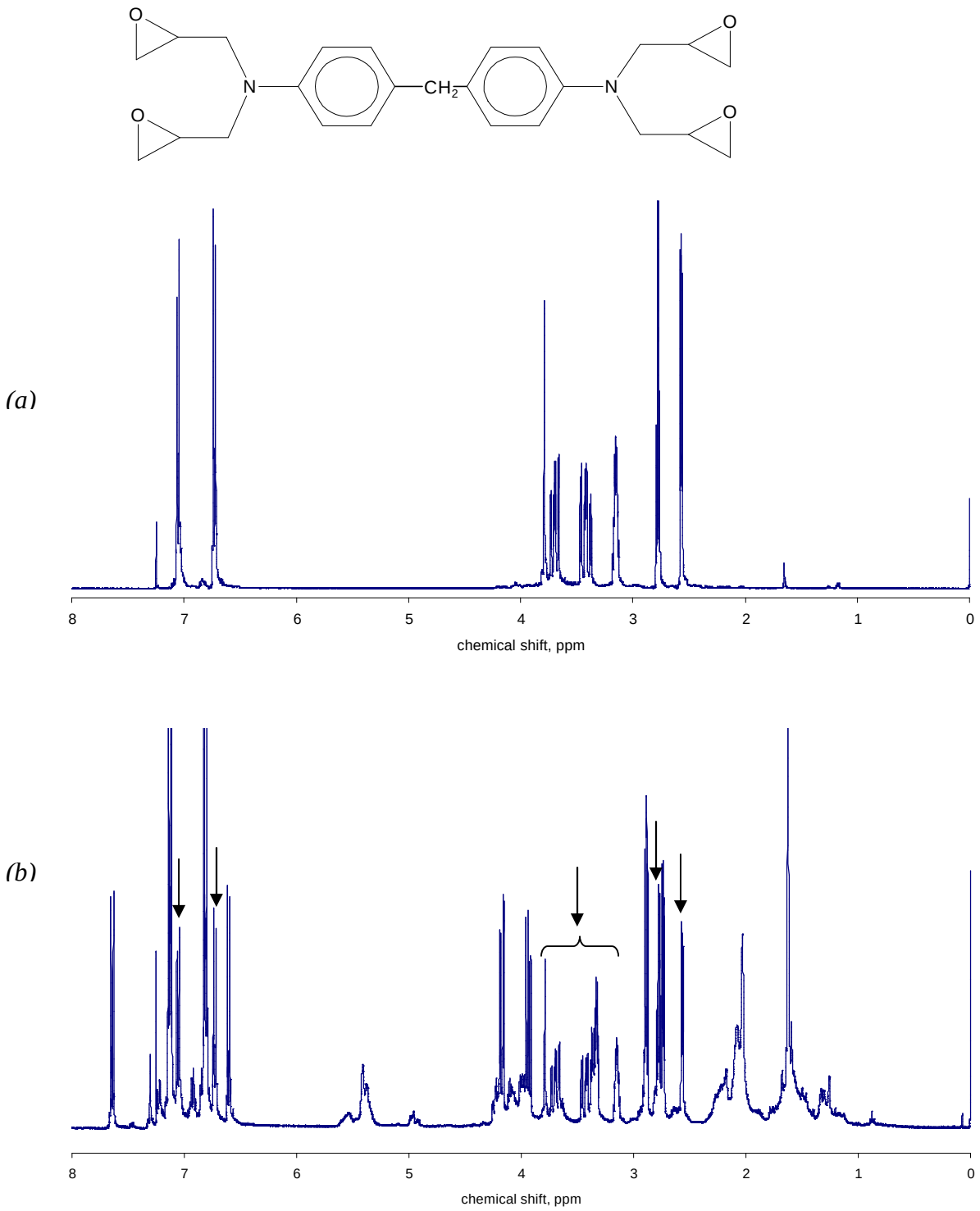

Figure 2.4. Comparison of ^{1}H NMR spectrum of *(a) N,N,N'N'*-tetraglycidyl-4,4'-diamino diphenylmethane (TGDDM) epoxy resin to that of the film adhesive (*b*) in $CDCl_3$.

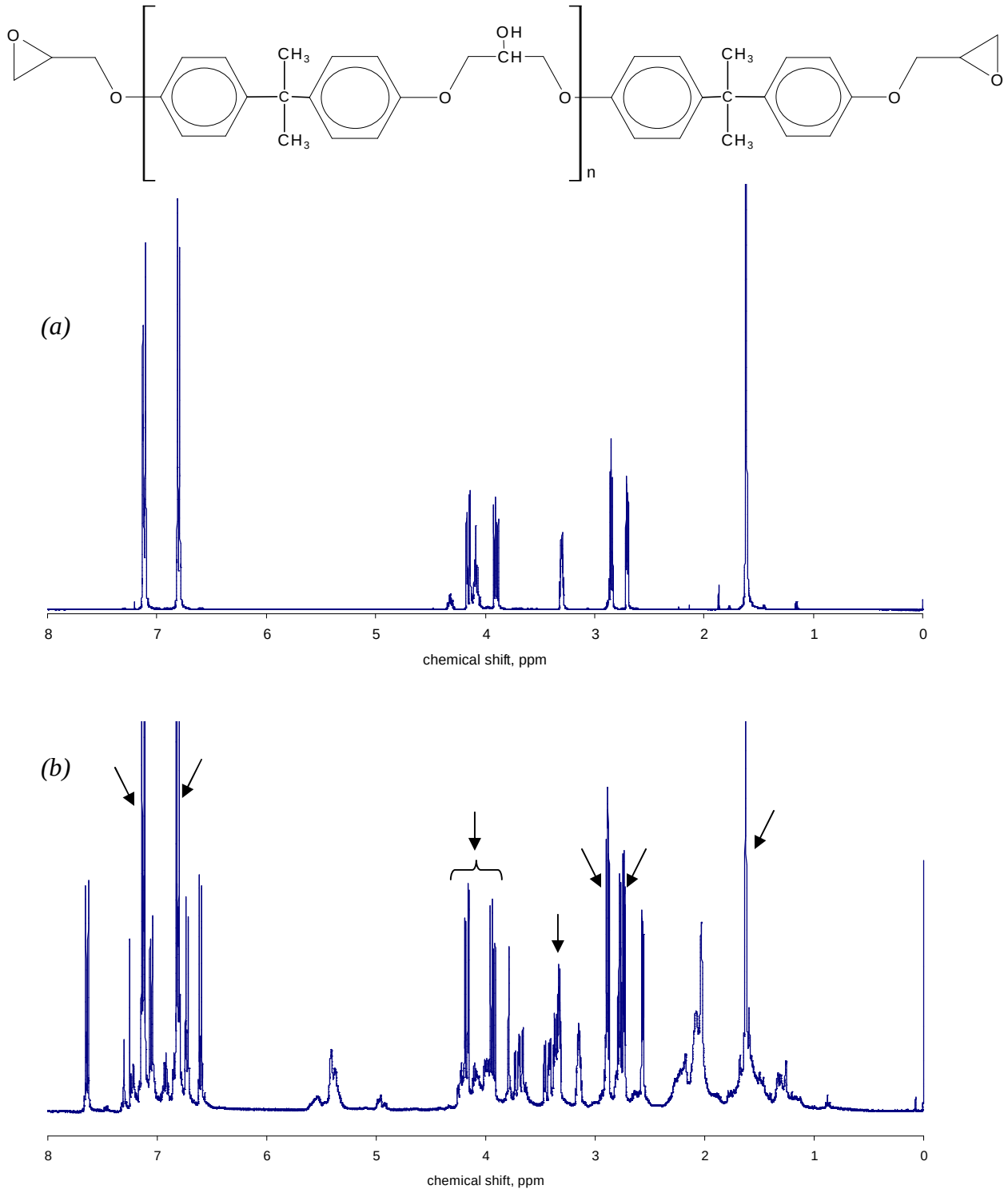

Figure 2.5. Comparison of ¹H NMR spectrum of *(a)* diglycidyl ether of bisphenol A (DGEBA) epoxy resin to that of the film adhesive (*b*) in $CDCl_3$.

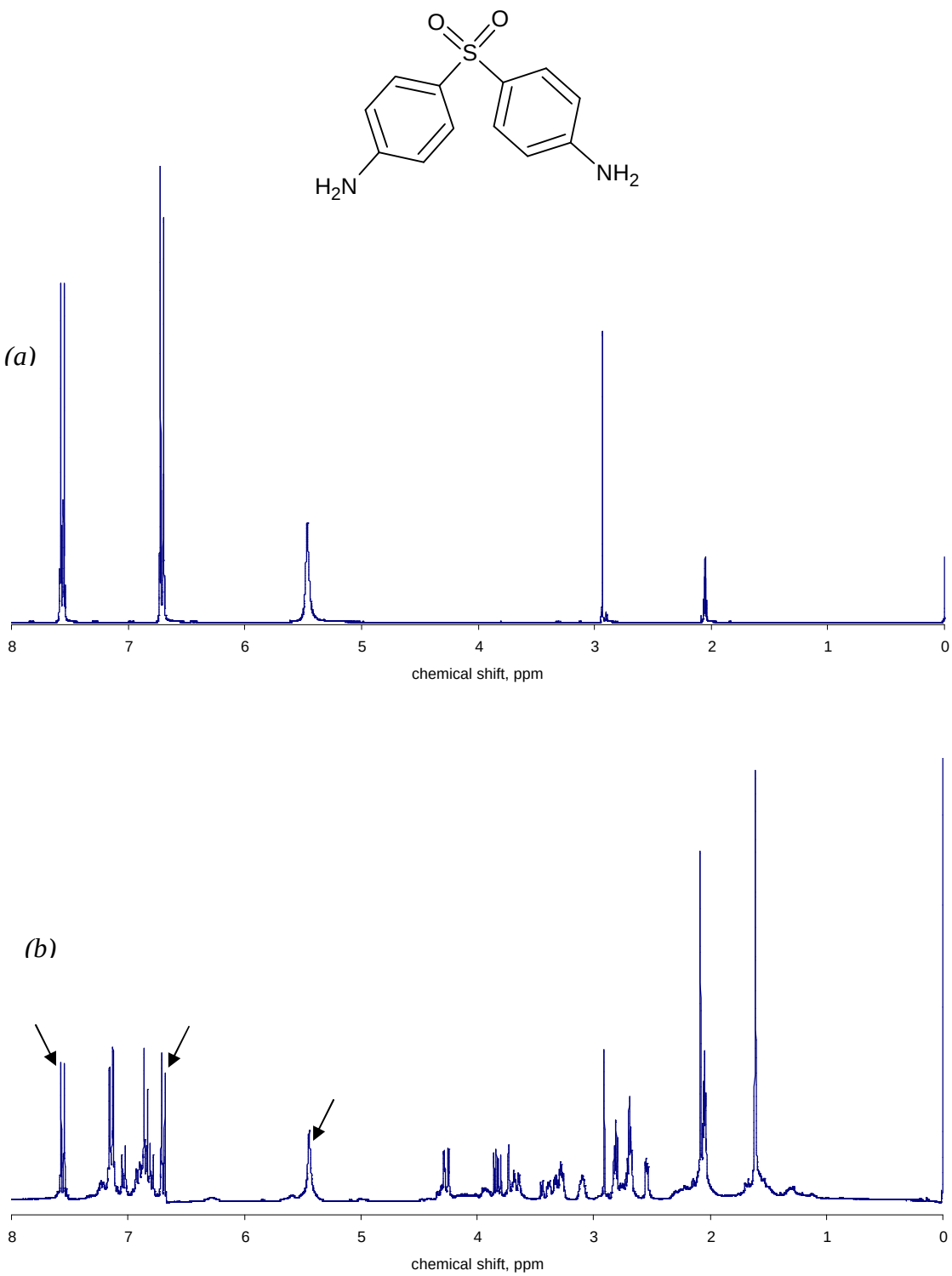

Figure 2.6. Comparison of ^{1}H NMR spectrum of the curing agent 4,4'-diaminodiphenylsulfone (DDS) (*a*) to that of the film adhesive (*b*) in CD_3COCD_3.

reduces the extent to which resin spreads out between parts that are being bonded. The viscosity of epoxy resin minimizes above 100°C but gradually increases as the reaction progresses.

DDS has been a preferred curing agent in preformulated epoxy-based adhesive and pre-impregnated composite materials because it reacts very slowly with epoxy at room temperature. The sulfone group decreases the basicity of the amino groups. However, DDS will react with epoxy groups at elevated temperatures. Having a functionality of 4, it also gives a highly cross-linked cured material. A relatively smaller amount of dicyandiamide (DICY), another curing agent, is also present in the adhesive as detected in the FT-IR spectrum. DICY (functionality = 4) is a latent curing agent. It is relatively unreactive towards epoxy at ambient conditions. Thus, epoxy systems with DICY can have a long shelf life of up to six months when mixed with epoxy resin. DICY possesses a reactivity between that of aliphatic and aromatic amine, and can, therefore help boost viscosity in the early stages of cure.

The presence of peaks due to the methylene protons of the repeating unit of DGEBA indicates that it is a mixture of monomer and oligomers. The “distance” between the two epoxy end groups, or the chain length of DGEBA, is a function of the ratio of bisphenol A and epichlorohydrin used during DGEBA manufacture. A small value of n *(minimum = 0)* imparts a high crosslink density and modulus but produces a resin that is more crack sensitive. Increasing the value of n improves fracture toughness and lowers resin Tg by decreasing crosslink density, and enhances adhesion due to the creation of hydroxyls on the chain. The value “n” could not be estimated directly from the ^{1}H NMR spectrum due to overlapping signals. With reference to Figure 2.7 (*a*) spectrum, signals

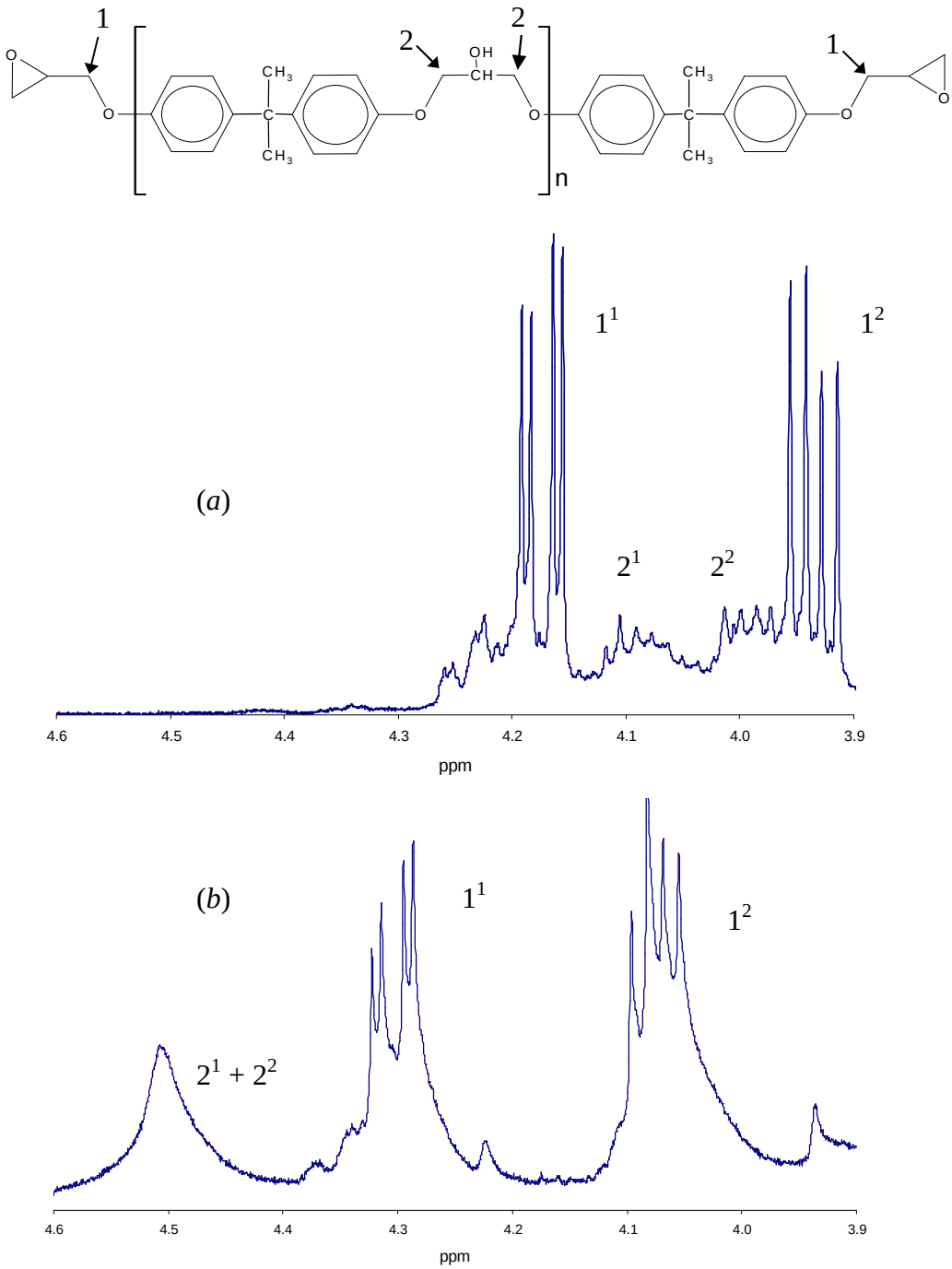

Figure 2.7. Determination of the average oligomer length of the DGEBA component of the film adhesive. ^{1}H NMR spectra of the film adhesive without (*a*) and with (*b*) added Eu(FOD) shift reagent in $CDCl_3$. The base number refers to the carbon atom; the superscript refers to the protons attached to the carbon atom. Hence, 2^1 refers to proton #1 on carbon #2.

from methylene protons on atoms labeled as carbon **1** (terminal) and **2** (repeating unit) overlap in the NMR spectrum and are difficult to integrate. However, by titrating with Europium FOD Lanthanide shift reagent, the signals from protons attached to carbon **2** (2^1 and 2^2) moved downfield and away from those on carbon **1** due to complex formation of the shift reagent with the central hydroxyl group. Although signals from both types of protons shifted downfield, the ones on carbon **2** did more; and hence, value of *n* was estimated to be about 0.4 from the ratio of the peak areas. This corresponded to an epoxy equivalent weight of ~230 which was similar to that of EPON™ 834 DGEBA resin manufactured by Resolution Performance Products.

2.3.3 Elemental Analysis

The elements C, H, N, S, and Al in the adhesive were determined by standard methods of analysis. Since more than 1 component of the mixture contained C, H, and N, those analyses did not provide much information. In contrast, the levels of aluminum filler as 33.8 % and the amount of DDS as 9.92 % by weight of the adhesive were determined from the analysis of aluminum and sulfur in the mixture, respectively. Aluminum filler is believed to help dissipate the heat produced from the exothermic curing reaction of epoxy, and hence, prevent the possibility of localized charring. Inductively Coupled Plasma – Mass Spectroscopy (ICP-MS) was used to scan for other constituents in the adhesive to check the presence of other common inorganic fillers, such as TiO_2, $CaCO_3$, SiO_2, mica, etc. The level of aluminum in the adhesive by elemental analysis agreed to within ˜ $\pm$ 1% of the level determined by weighing the insoluble

material collected after dissolving the uncured adhesive in a good solvent. The level of aluminum filler was very consistent on a sample to sample basis.

2.3.4 Thin-Layer Chromatography

A sketch of a developed TLC plate is shown in Figure 2.8. The separated components from the preparative TLC plates were recovered but the resulting spectra of the fractions revealed that they were still mixtures. Distinctive functional groups like the nitrile for the CTBN rubber component and the sulfone for the DDS curing agent were prominent in fractions 1 and 2, respectively. Aromatic ether bands were intense in fraction 4. In addition, by developing TLC profile of the film adhesive side by side with reference materials, it was confirmed that the CTBN rubber was contained in fraction 1, DDS in fraction 2, TGDDM in fraction 3 and DGEBA in fraction 4.

2.3.5 Composition of the Film Adhesive

Based on the results of the elemental analyses, the ^{1}H NMR, FT-IR and preparative TLC experiments, an approximate compositional breakdown for the adhesive was derived. The relative amounts of TGDDM, DDS and DGEBA were determined from non-overlapping peaks in the aromatic region of the ^{1}H NMR spectrum of the adhesive in d_6-acetone. Integration of the aromatic protons assigned to TGDDM, DDS and DGEBA gave a mole ratio of 1:1.33:2.28. From the sulfur content (1.28 %) as determined by elemental analysis and contained only in DDS, the relative amounts of the major components of the adhesive were calculated. Resulting values are shown in Table 2.1. Their structures are drawn in Figure 2.9.

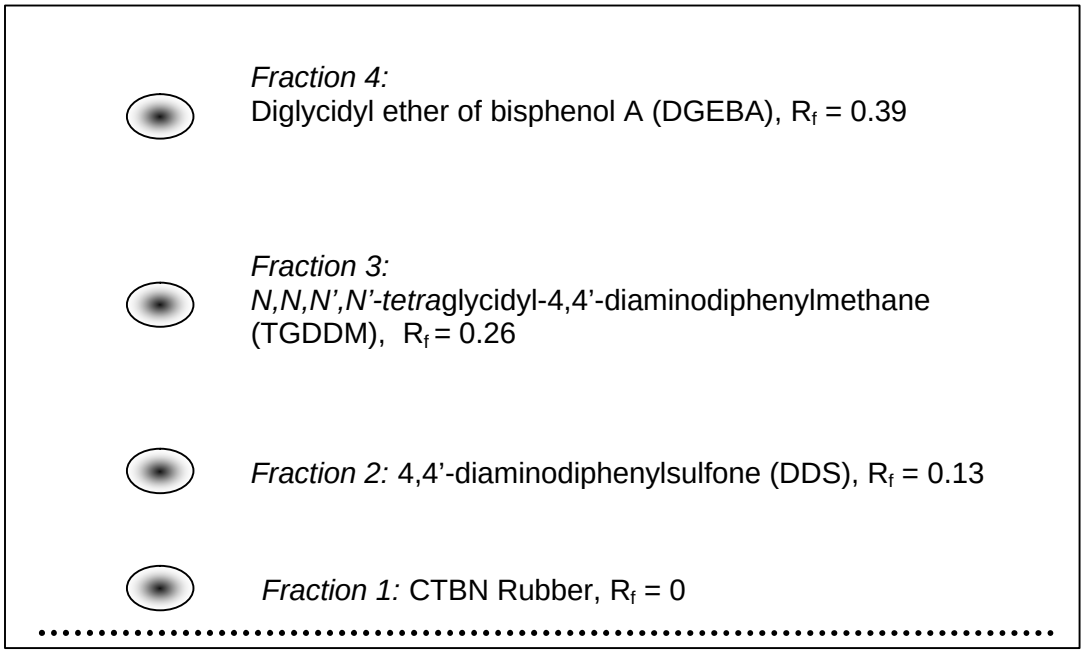

Figure 2.8. Sketch of a developed thin-layer chromatography (TLC) plate using the solvent system cyclohexane:ethyl acetate:isopropyl alcohol (6:3:1).

Table 2.1

Approximate composition of the film adhesive

Component	**Mass %**
Aluminum Filler	34 %
DGEBA epoxy resin *(n=0.4)*	32 %
TGDDM epoxy resin	13 %
DDS curing agent	10 %
Other Components (DICY, CTBN rubber, etc)	11 %

(*a*)

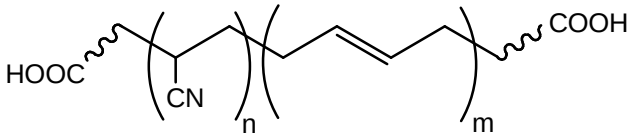

(*b*)

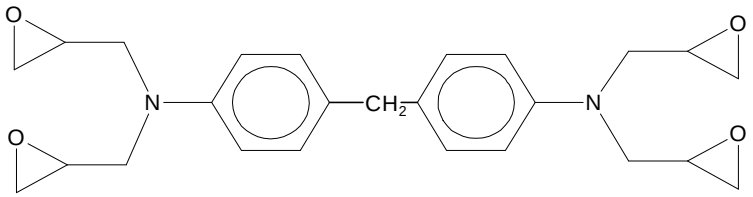

(*c*)

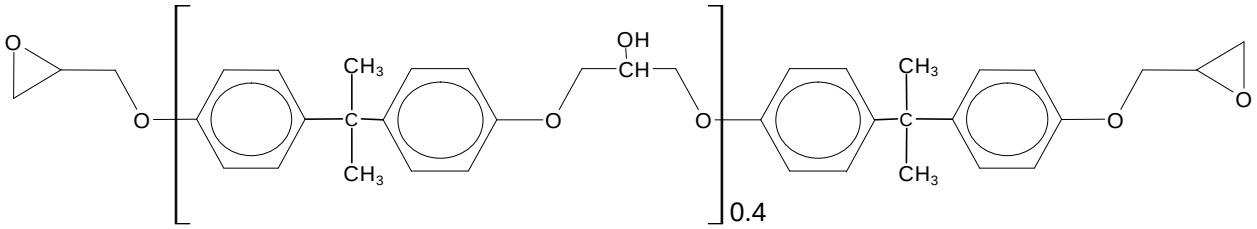

(*d*)

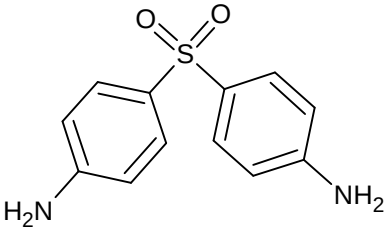

(*e*)

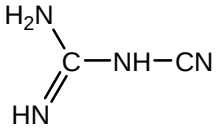

Figure 2.9. Structures of the major components of the film adhesive. (*a*) CTBN rubber (*b*) TGDDM epoxy resin (*c*) DGEBA epoxy resin (*d*) DDS curing agent (*e*) DICY curing agent.

CHAPTER 3

CURE KINETICS OF THE FILM ADHESIVE

3.1 Introduction

Parts prepared using epoxy-based high performance adhesives co-cured with pre-impregnated composite materials form a mainstay in the aerospace industry. The preparation of parts made from these materials involves vacuum bagging and curing in a pressurized autoclave. An example of a cure cycle for epoxy thermosets is shown in Figure 3.1. The autoclave is heated from ambient temperature to about 121°C (250°F) at a rate of 3°C (5.4°F)/min (step I), and held there for 30 min to equalize temperatures throughout the autoclave (step II). The autoclave is then heated to 176°C (350°F) at a rate of 3°C (5.4°F)/min (step III), and held there for 180 min (step IV). The entire cure cycle, excluding time required for loading and unloading the autoclave, and cooling down from 350°F to ambient temperature, takes a minimum of 4.3 hours. Therefore, a single autoclave load can be assembled, cured and removed in 1-2 “shifts” of labor.

This cure cycle, in general, works quite well for curing a majority of epoxy-based materials. However, demands for better performing adhesive and composite materials for higher temperature applications result in changing formulations to enhance certain desired properties. This causes some problems with the use of a standard one-cycle-fits-all process. All reagents may be epoxy-based but cure behavior may vary. The presence of property-enhancing additives can make the epoxy resin cure faster or slower allowing viscosity to build up earlier or later, etc.

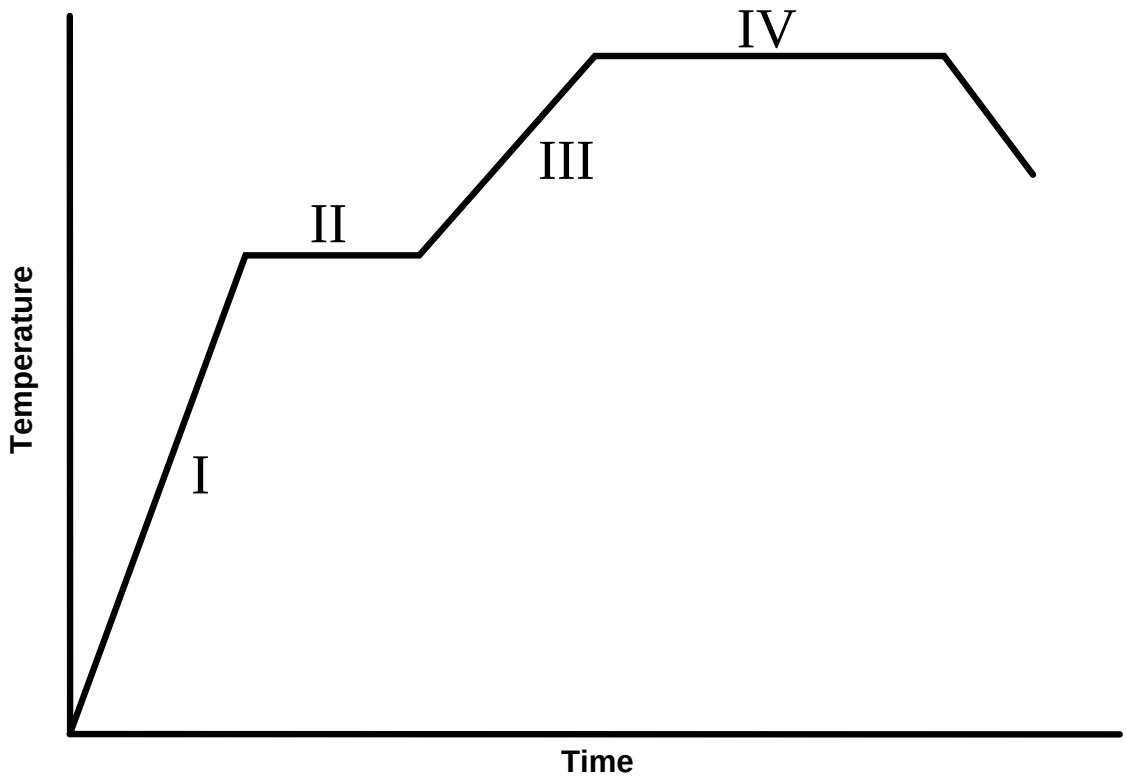

Figure 3.1. An example of a cure cycle for epoxy-based thermosets.

This high performance, high shear film adhesive under investigation is used for making major load-bearing parts in the aerospace industry. In some cases, a substandard material is produced with this adhesive using the cure cycle described in Figure 3.1. Determining an optimized cure cycle for this adhesive becomes, therefore, a priority.

To properly understand the behavior of this adhesive in a commercial autoclave, it is not sufficient to perform isolated dynamic temperature and isothermal scanning cure experiments as is commonly undertaken in research and quality control laboratories. Rather, the two must be combined to fully follow the curing process similar to the way it is actually cured in an industrial setting.

The approach to the problem was divided into three sets of experiments:

(1) dynamic temperature scan or ramp over a range of heating rates (0.5 to 20°C/min);

(2) isothermal scan or soak (110 to 180°C) until no appreciable curing was observed; &

(3) combined dynamic temperature and isothermal scanning to mimic an actual ramp and soak cure cycle.

To begin with, if there is an appreciable curing at segments I and II of the cure cycle, the problem would become intractable. Fortunately, this was simplified because it was found that the cure achieved during segments I and II of the cycle was negligible. The entire cure cycle was then modeled around combined ramp and soak segments.

3.2 Experimental

3.2.1 Thermal analysis

Thermal analysis of the film was performed using a Perkin Elmer DSC6. Samples were cured in hermetically sealed aluminum pans. Sample sizes were in the range of 10-20 mg. For all DSC runs, the instrument was pre-set at a starting temperature of 30°C. For dynamic temperature scanning, variable heating rates were used (0.5°C/min to 20°C/min) from the starting temperature to about 300°C wherein the adhesive was considered completely cured. The cured sample was cooled down to 30°C and then rescanned up to 300°C at 10°C/min to get the ultimate glass transition temperature (Tg).

Isothermal scanning was done from 110°C to 180°C. The sample was placed in the DSC at 30°C; the temperature was then quickly ramped up to the cure temperature at 50°C/min and held there until the signal returned to the baseline. The sample was cooled down to 30°C and rescanned up to 300°C at 3°C/min to determine the intermediate Tg and any residual exotherm. For the ultimate Tg, the sample was cooled down again to 30°C and then rescanned up to 300°C at 10°C/min.

For the ramp and soak DSC experiments, samples of the adhesive were cured as follows:

(1) dynamic temperature scan at various heating rates (0.5°C/min to 5°C/min at 0.5°C increments) from 30°C to an isothermal cure temperature;

(2) cool down sample to 30°C, quick temperature ramp (50°C/min) to the isothermal cure temperature and then isothermal cure at that temperature until signal returns to the baseline;

(3) cool down sample to 30°C and then rescan up to 300°C at 3°C/min for the intermediate Tg and residual exotherm; and

(4) cool down to 30°C and then rescan to 300°C at 10°C/min to get the ultimate Tg.

The isothermal cure temperatures were 140 - 180°C in 5°C increments.

Data analysis and 2D plots were obtained using MS Excel and Origin 6.1 (Origin Lab Corporation). Three dimensional plots and surface fitting were constructed using TableCurve® 3D version 4.0 (Systat Software).

3.2.2 Dynamic Shear Rheometry

Dynamic shear rheometry experiments were performed by Fluids Dynamics, Inc using a TS2R® rheometer in isothermal scanning mode with a fixed frequency. The rheometer with the sample cup was pre-equilibrated at the test temperature. The sample was then added to the sample cup and allowed to melt. The test probe was quickly inserted and allowed to equilibrate for about 1 minute before the start of the measurement. Five data points per minute were collected using the oscillation frequency of 2 Hz. Dynamic shear rheometry experiments were done at 130, 135, 140 and 150°C.

3.3 Results and Discussions

3.3.1 Dynamic Temperature Scanning

Dynamic temperature scanning DSC experiments were performed in order to characterize the cure kinetics during the ramped portion of the cure cycle. The adhesive sample was ramped from 30°C to an end temperature of about 300°C at various heating rates. A representative programmed DSC trace of the adhesive, at a heating rate of 3°C/min, is reproduced in Figure 3.2. The cure reaction exotherm is well defined and ends at around 280°C, below the onset of higher temperature degradation reactions of the resin.

The DSC cell with the cured sample was then cooled to room temperature and re-heated to 300°C at a standard heating rate of 10°C/min (Figure 3.3). The absence of a residual exotherm in the second scan affirmed that the cure reaction was completed during the first scan. The degree of cure (α), rate of cure ($d\alpha/dt$) and ultimate Tg values were calculated and plotted against temperature. In this experiment, Tg was measured for samples of adhesive that had been previously cured in the DSC pan. It is more difficult to measure Tg for such samples than to measure Tg for cured samples that are crushed into the DSC pan. In the first instance, passage through Tg gives only a baseline slope change (Figure 3.3). In the second instance, passage through Tg relieves stress and marks the transition with a baseline translation.

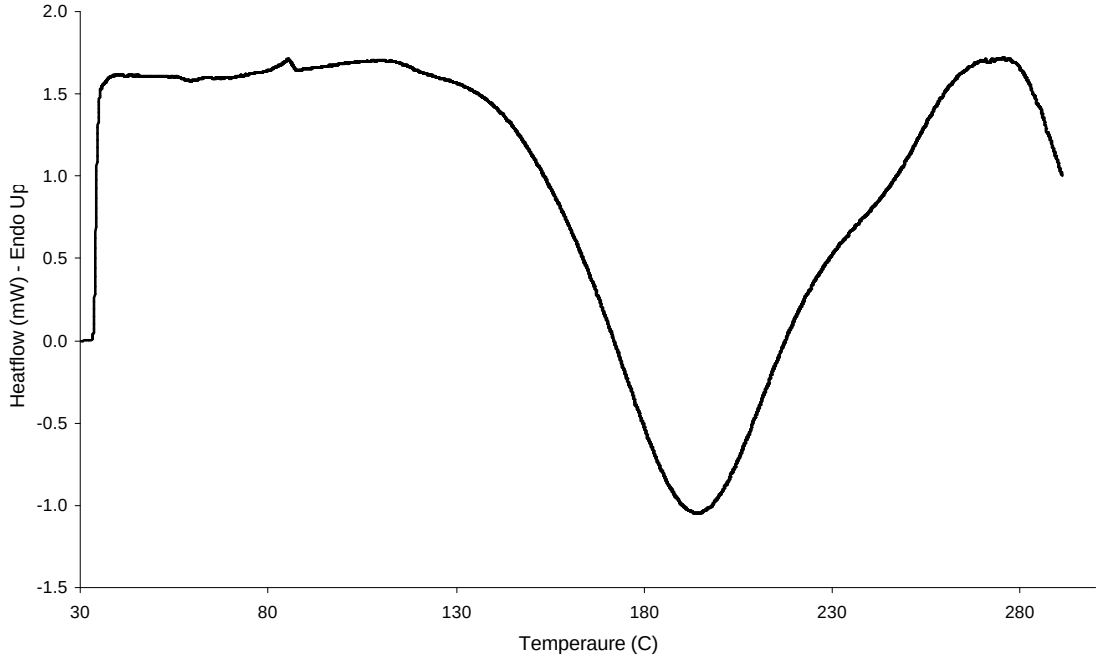

Figure 3.2. An exotherm generated from dynamic temperature scanning of the film adhesive at 3°C/min from 30°C to 300°C.

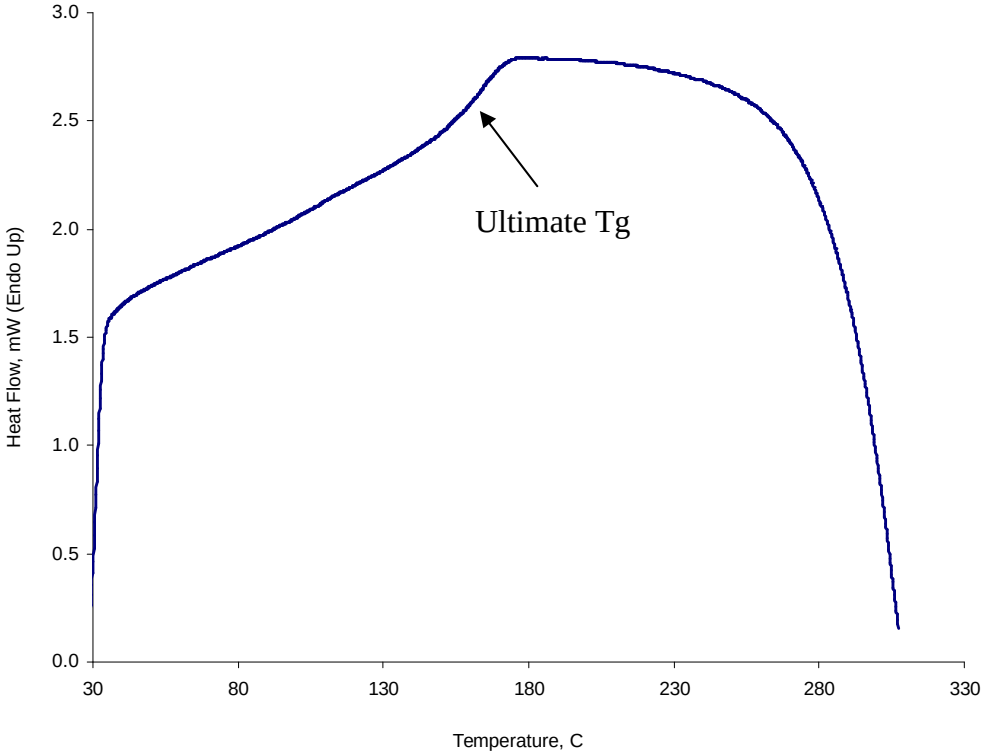

Figure 3.3. DSC trace from the rescan of the film adhesive previously cured from 30°C to 300°C at 3 ^{o}C/min. Note the absence of residual exotherm. Rescanning was done at 10°C/min from 30°C to 300°C.

The degree of cure attained at a fixed point in the reaction was calculated as the ratio of the partial area of the exotherm up to that point to the total area (Figure 1.3). A set of data points (time, temperature and degree of cure) for every heating rate was generated. Plots of the degree of cure (α) as a function of temperature over a range of heating rates from 0.5°C/min to 20°C/min are shown in Figure 3.4. Each curve is an average over two experiments. If a significant difference between the two experiments was observed, the experiment was repeated. As expected, the cure reaction is shifted to higher temperatures at higher heating rates. At very high heating rates (15-20°C/min), a significant portion of the adhesive cure reaction takes place above 300°C. As will be pointed out later, degradation reactions that occur in epoxy resins above 300°C changed the apparent heat of reaction. By differentiating the plot of the degree of cure versus time, rate of cure profiles were generated for the cure reaction under dynamic temperature scanning conditions, as reproduced in Figure 3.5.

Using TableCurve 3D software, three dimensional plots of α and $d\alpha/dt$ as functions of heating rate and temperature were generated (Figures 3.6 and 3.7, respectively). The software itself generated equations that best describe the data. Using these curves, values of α and $d\alpha/dt$ for intermediate linear heating rates and temperatures can be interpolated. It must be noted that the cure reaction of the film adhesive is irreversible. For example, choose a heating rate (dT/dt), vary temperature (T) and generate a 2D plot of α or ($d\alpha/dt$) as a function of temperature. In contrast, applying a non-linear ramp such that heating rate is a function of temperature, α or $d\alpha/dt$ versus temperature or time cannot be generated from the graph.

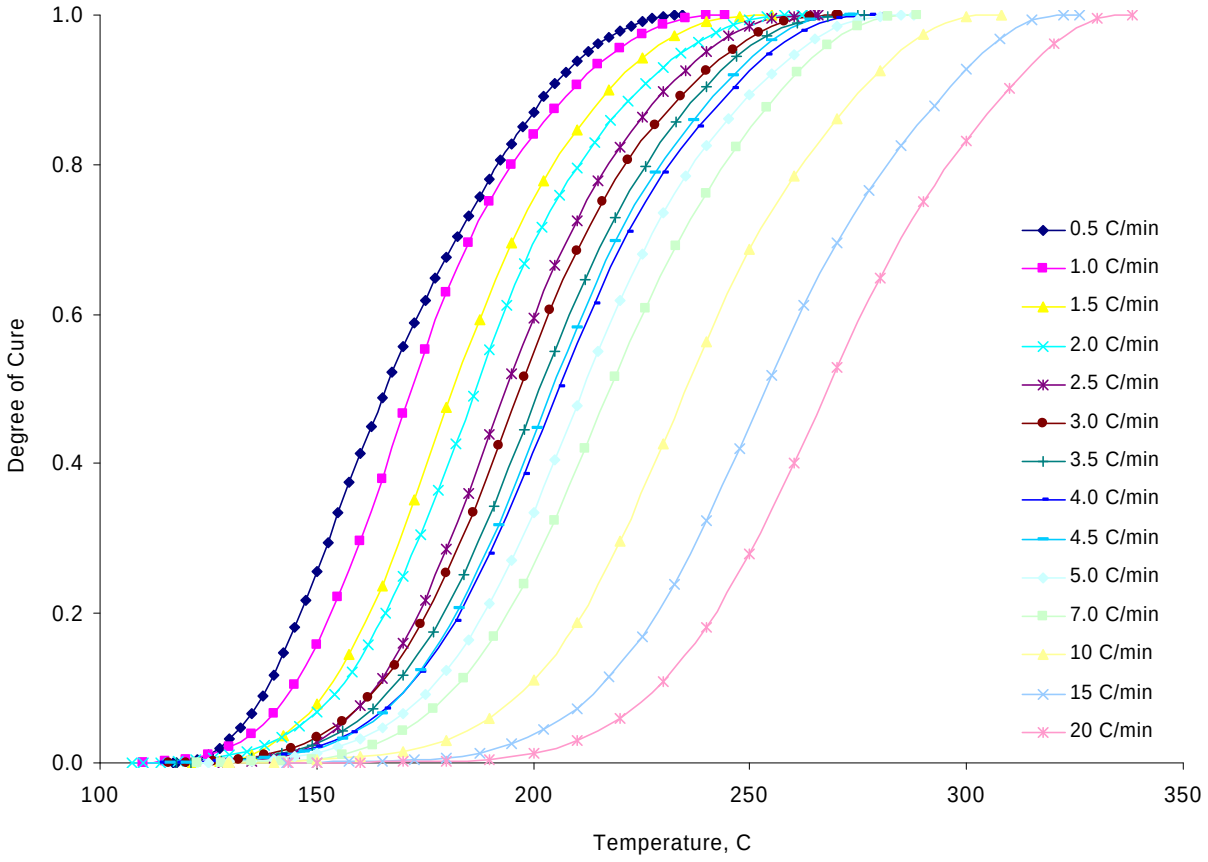

Figure 3.4. Degree of cure (α) of the film adhesive versus temperature over a range of heating rates.

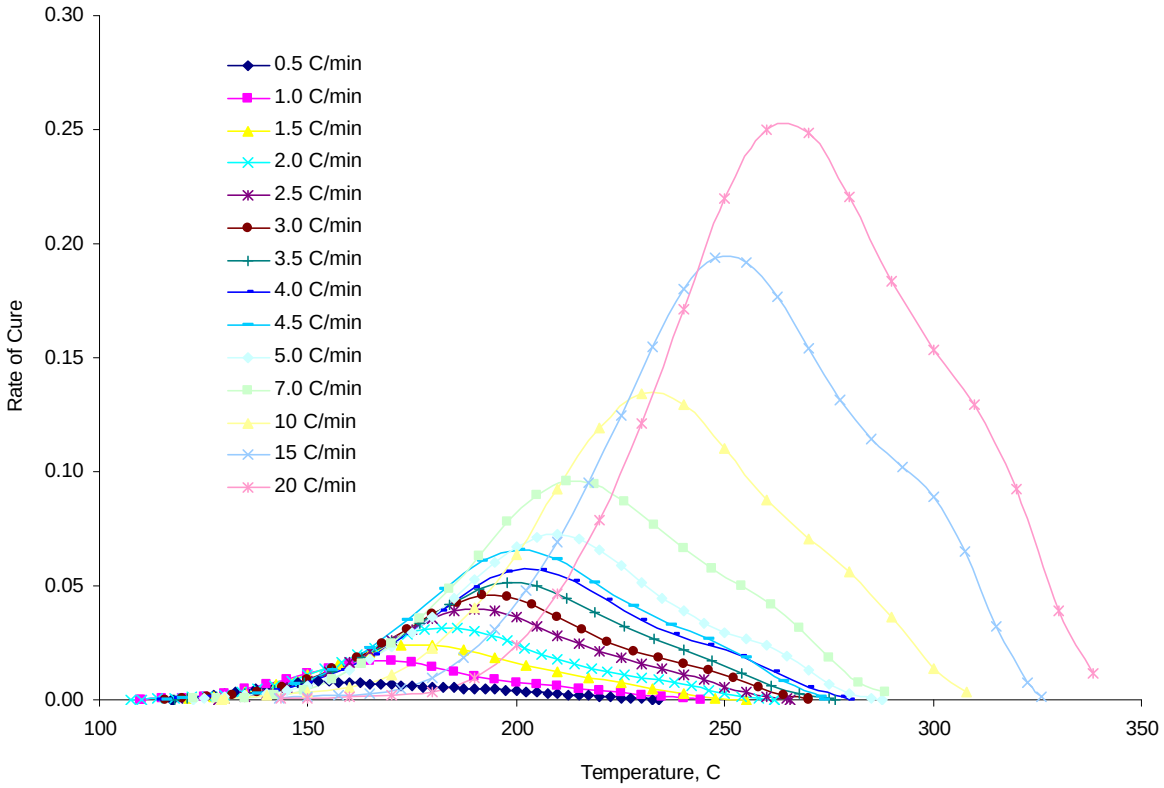

Figure 3.5. Rate of cure (*da/dt*) of the film adhesive versus temperature over a range of heating rates.

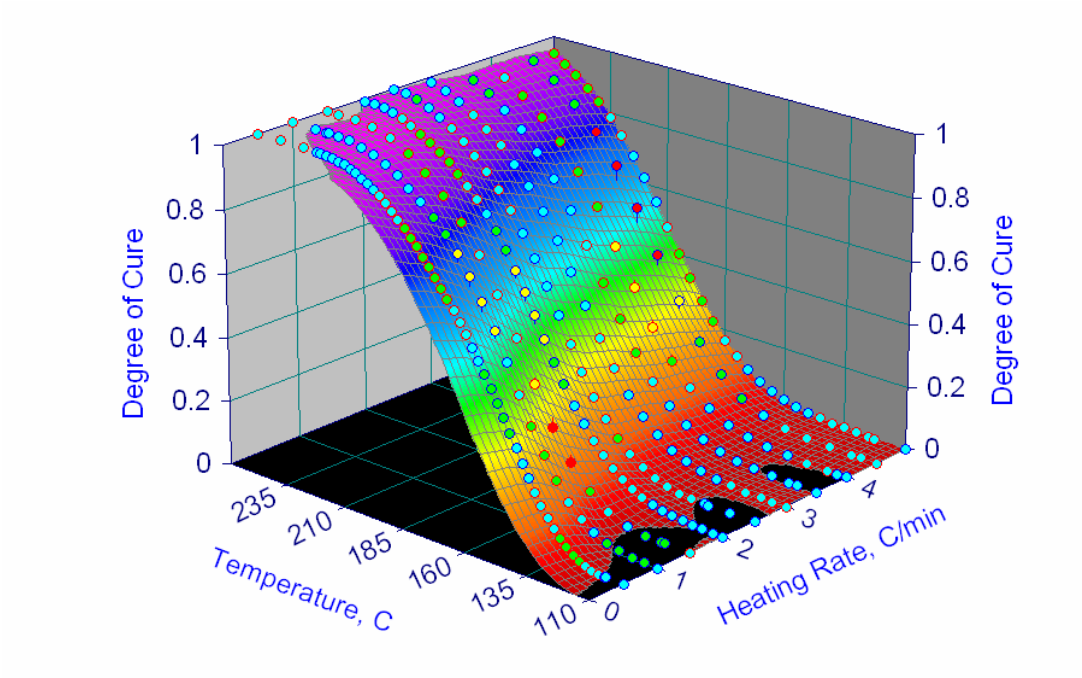

Figure 3.6. Plot of degree of cure (α) of the adhesive as a function of heating rate and temperature.

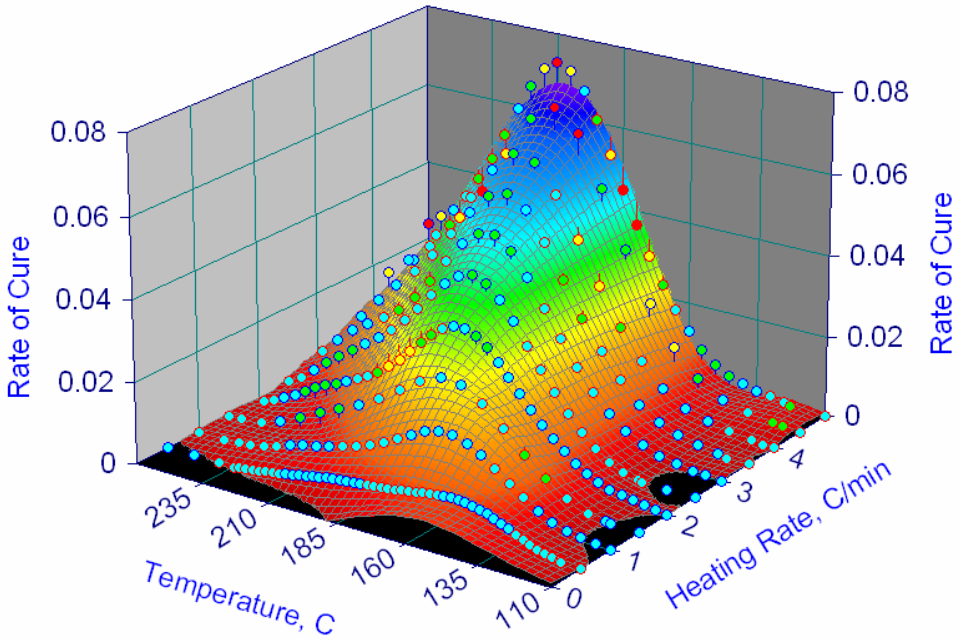

Figure 3.7. Plot of rate of cure (dα/dt) of the adhesive as a function of temperature and heating rate.

It has been mentioned that an appreciable portion of the cure reaction in the adhesive takes place above 300°C at faster heating rates. At these elevated temperatures, it is entirely possible that the cure reaction overlaps higher temperature degradation reactions. DDS has been reported to start to volatilize and degrade at about 250°C[60]. Epoxy has also been found to degrade at temperatures near 300°C with the phenolic ether linkage being the site of scission [61]. If the apparent heat of cure (J/g of adhesive) is plotted as a function of heating rate, and if these higher temperature degradation processes are accompanied by a heat change, said overlap would affect the apparent heat of reaction, as is observed in Figure 3.8. In this plot, each data point is an average of two experiments. Using the seven values generated between heating rates of 1°C/min and 4°C/min, the heat of reaction was estimated as 213 $\pm$ 12 J/g of adhesive. This is considerably lower than apparent heats of reaction measured for other epoxy resins, and is most likely due to the presence of unreactive filler and toughening agents. Since approximately 45 % of the adhesive is considered inert, the apparent heat of reaction is about 387 $\pm$ 22 J/g of reactive epoxy resin in the adhesive.

Using the data from the dynamic temperature scanning experiment at 3°C/min, the observed degree of cure up to 121°C was less than 1%. This means that the extent of conversion from step I of the cure cycle described in Figure 3.1 is negligible.

By combining the results of isothermal DSC experiments with isothermal dynamic shear rheometry, as discussed in a later section, the extent of cure at the gel point of the adhesive was determined. The gel point corresponds to the extent of cure at which there is a complete loss of flow in the adhesive. The gel point temperature is plotted as a function of heating rate for the adhesive in Figure 3.9.

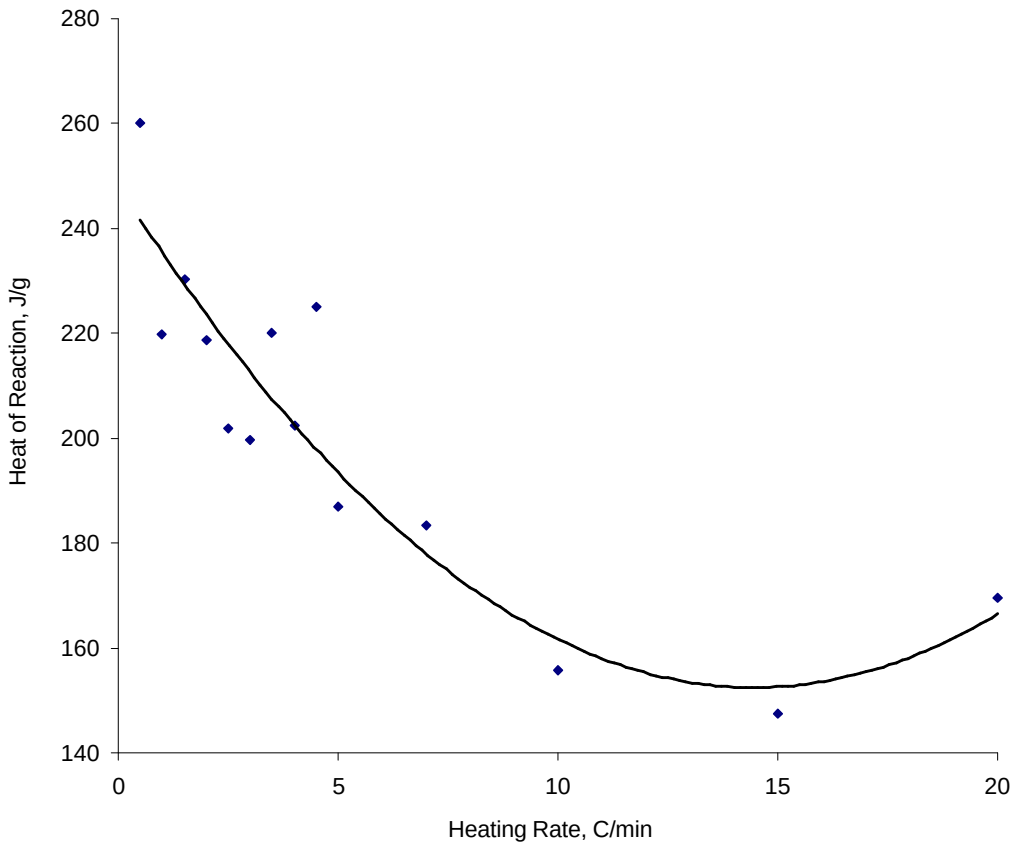

Figure 3.8. Apparent exothermic heat of reaction of the adhesive as determined by dynamic temperature scanning over a range of heating rates.

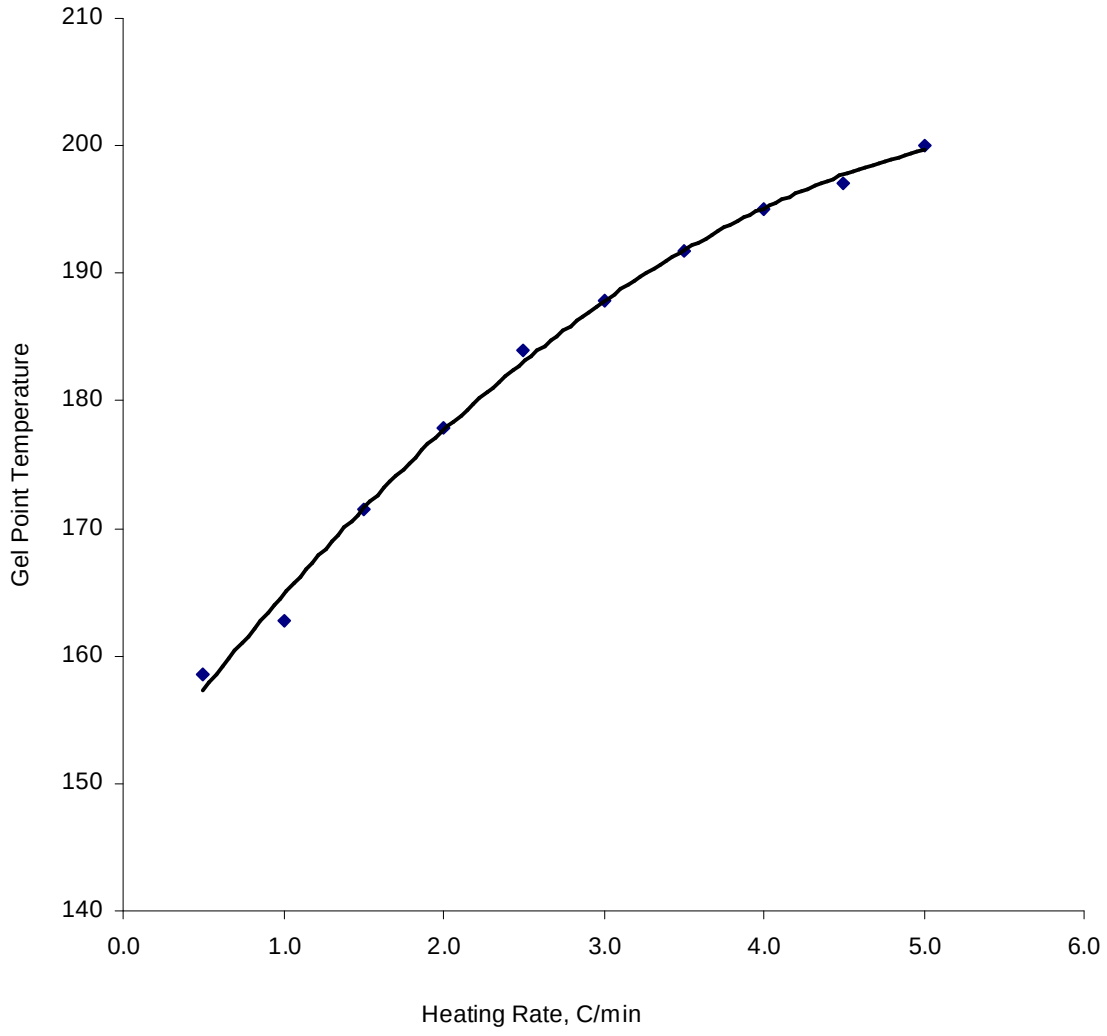

Figure 3.9. The gel point temperature for the adhesive, (or the temperature at which the degree of cure is 0.36) as a function of programmed heating rate.

Under dynamic temperature scanning conditions, at a heating rate of 3°C/min (close to the standard heating rate of 5°F/min employed in the industrial autoclave cure cycle), the gel point temperature is close to 188°C. The significance of this is that the gel point is reached sometime after the final soak temperature has been achieved (step IV in Figure 3.1). At heating rates below 2°C/min, the gel point is reached during the second ramped segment (step III) and before the final soak segment (step IV) of the cure cycle. The position of the gel point in a combined dynamic and isothermal cure cycle is explored more fully in a later section.

The measurement of the ultimate glass transition temperature (Tg) of the cured adhesive is illustrated in Figure 3.3. In Figure 3.10, the ultimate Tg of the cured adhesive is plotted against the heating rate during cure. The measured ultimate Tg's were remarkably unaffected by the rate of programmed warm up during the previous cure cycle and were averaged at 167 $\pm$ 3°C over all heating rates. The measured Tg is a function of heating rate during rescan. For this reason, all Tg's were recorded at a heating rate of 10°C/min.

The apparent activation energy (*Ea*) can be measured for a resin cure reaction as a function of the degree of cure (α). Under favorable conditions, *Ea* can yield insight into changes in the mechanism of cure. As the cure reaction progresses, the reaction medium changes - it becomes more polar due to the creation of hydroxyl functionality and more viscous due to the buildup of oligomers and ultimately a gel fraction. The former accelerates cure, while the latter retards the cure reaction. Hydroxyl groups can act as catalyst in the ring-opening of the epoxy ring by the amine group. As the viscosity of the

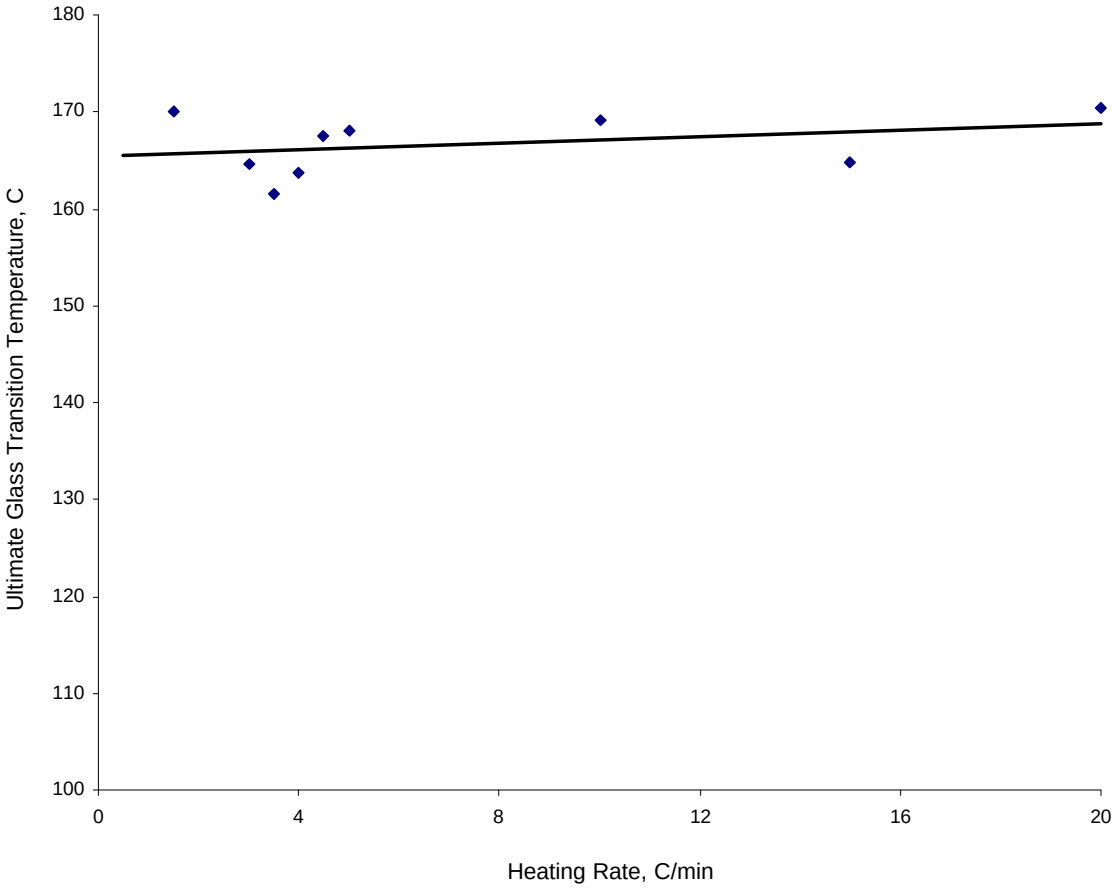

Figure 3.10 Ultimate glass transition temperatures (Tg) of adhesive measured at a heating rate of 10°C/min from 30°C to 300°C, after curing over a range of heating rates.

resin builds up, it will become more difficult for the functional groups to find each other, and hence, the apparent *Ea* will increase. In such case, the reaction is said to be diffusion-controlled. In addition, the cure reaction can be influenced by the decomposition of catalyst and other residues that accelerate cure. A plot of *Ea* versus α for the adhesive can be generated using the data plotted in Figures 3.5 and 3.6.

The rate of cure (*da/dt*) for systems described by an Arrhenius type behavior follow equation (12) where *f(a)* is a function of the degree of cure. It is an empirical function that defines the relationship between the rate of cure and the concentrations and chemical environment of functional groups in the resin. *f(α)* can be complicated and difficult to determine for most types of system. It can vary at different stages of cure.

$$\frac{da}{dt} = K\ f(a) \tag{12}$$

$$K = Ae^{\left(\frac{-E_a}{RT}\right)} \tag{13}$$

$$\ln\left(\frac{da}{dt}\right) = \ln A + \ln\left(f(a)\right) - \frac{E_a}{RT} \tag{14}$$

The Arrhenius rate constant *K* is described by equation (13) where *A* is the pre-exponential shape factor, *Ea* is the activation energy, *R* is the gas constant, and *T* is the temperature in Kelvin. Substituting *K* in equation (12) with equation (13) and taking logarithm yields equation (14). This equation describes the dependence of the rate of cure on the degree of cure and temperature. Fortunately, values of *Ea* can be calculated

without having to determine the form of $f(\alpha)$ by plotting $\ln(d\alpha/dt)$ versus 1/(T) for a fixed value of α. By doing so, the terms ln *A* and ln f(α) can be considered as constants.

Equation (14) was used to determine the apparent *Ea* from dynamic temperature scanning data. The time and rate of cure values from different heating rates were determined at a fixed degree of cure. Plotting these data according to equation (14) for every fixed value of α gave linear graphs from which the apparent *Ea* was calculated (see Figure 3.11 for a sample plot). The plots for other α values can be found in Appendix A. In each case, a good linearity was achieved. Consequently, the variation of *Ea* values with degree of cure is shown in Figure 3.12.

From Figure 3.12, the apparent activation energy for the cure of the adhesive is a smoothly increasing function of α without unusual features. The absence of a "bump" at the earlier stage of cure is typical for systems without low temperature catalyst. As expected, a large increase in *Ea* is observed in the final stages of cure, consistent with the massive increase in micro-viscosity near the completion of the reaction making the reaction diffusion-controlled. The gel point at α = 0.36 is not associated with any significant change in the nature of the cure reaction as it signifies only the first appearance of an infinite network that is swollen with large amounts of mobile, reactive non cross-linked material.

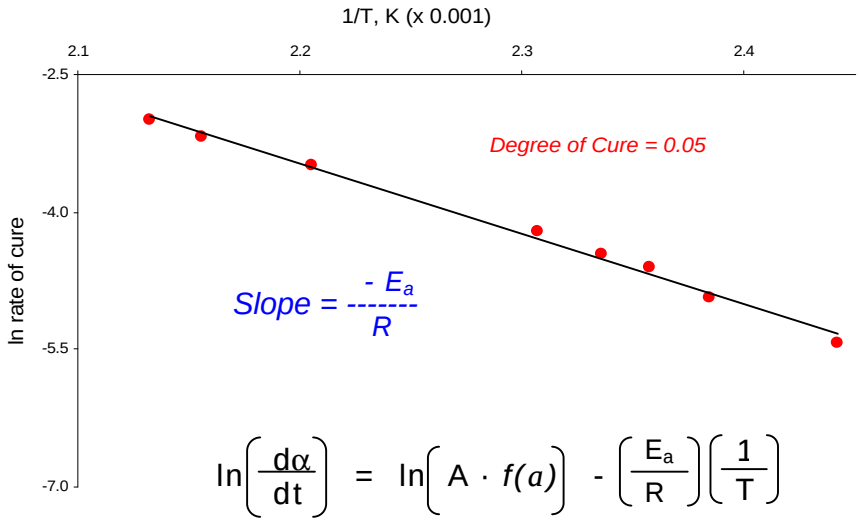

Figure 3.11. A plot of ln($d\alpha/dt$) versus 1/T for the adhesive at α = 0.05. Plots for other values of *a* are reproduced in Appendix A.

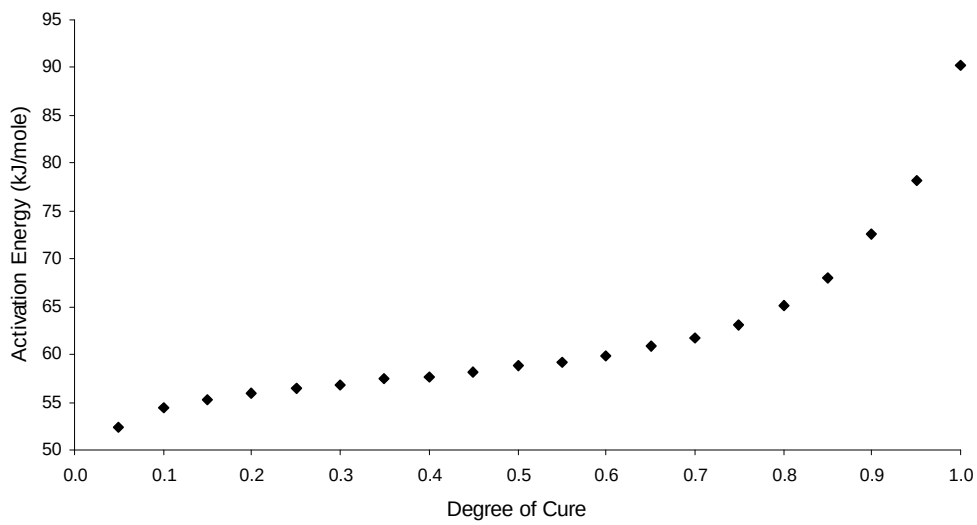

Figure 3.12. Plot of the apparent activation energy (*Ea*) of the adhesive cure reaction as a function of the degree of cure (α) as determined from dynamic temperature scanning data.

3.3.2 Isothermal Scanning

As a preliminary to modeling the autoclave cure of the adhesive under ramp and soak conditions, thermal behavior of the adhesive under isothermal conditions was investigated. The sample at 30°C was quickly heated to the soak temperature at a rate of 50°C/min, then held at that temperature for a prolonged period of time until the exotherm returned to the baseline. A sample of an exotherm from isothermal curing is illustrated in Figure 3.13. The adhesive cure reaction at 165°C was first accelerated to a maximum rate then slowed with time. This is indicative of autocatalytic reactions that are accelerated by products of reaction, in this instance, the polar hydroxyls formed upon attack of amine functionality on epoxy groups.

At intermediate temperatures, the adhesive can vitrify and the cure reaction is essentially stopped at an intermediate cure state. Even after an extended exposure at the isothermal cure temperature, no additional curing was observed. For this reason, the isothermal scanning was followed by a dynamic temperature scan to measure the intermediate Tg and the “residual exotherm” (Figure 3.14). This was done at 3°C/min from 30°C to 300°C. A second dynamic temperature scan verified that the cure reaction had been completed and measured the “ultimate” Tg of the adhesive (Figure 3.15). This ultimate Tg was measured from the final scan at 10°C/min from 30°C to 300°C.

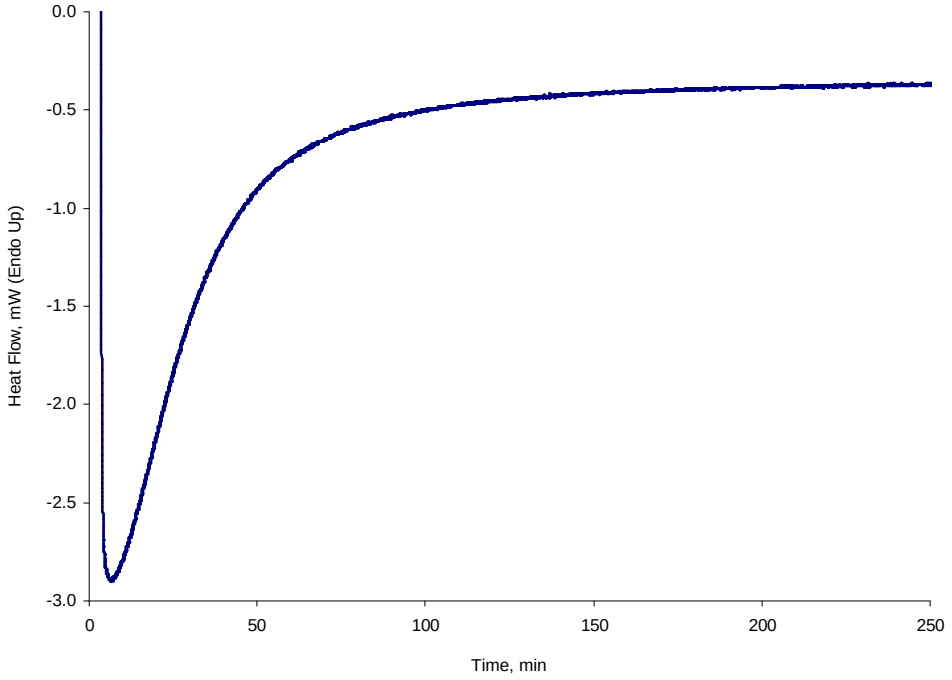

Figure 3.13. An exotherm produced from isothermal scanning of the adhesive at 165 ^{o}C for 8 hours after a rapid jump to that temperature from 30°C.

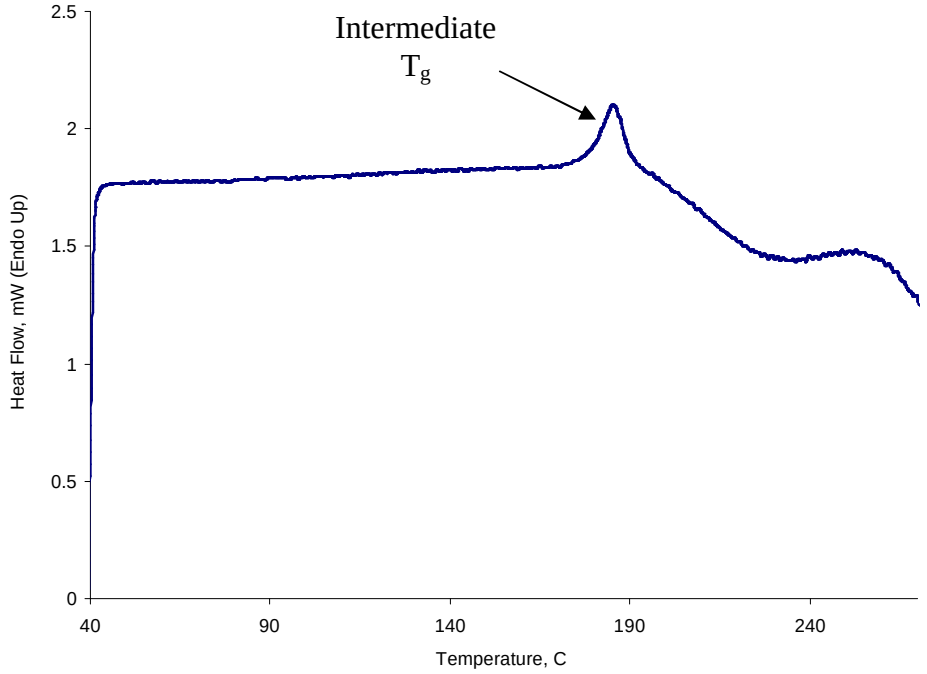

Figure 3.14. Intermediate Tg and residual exotherm produced from the rescan of the adhesive partially cured at 165°C for 8 hours. This rescan was done from 30°C to 300°C at 3°C/min.

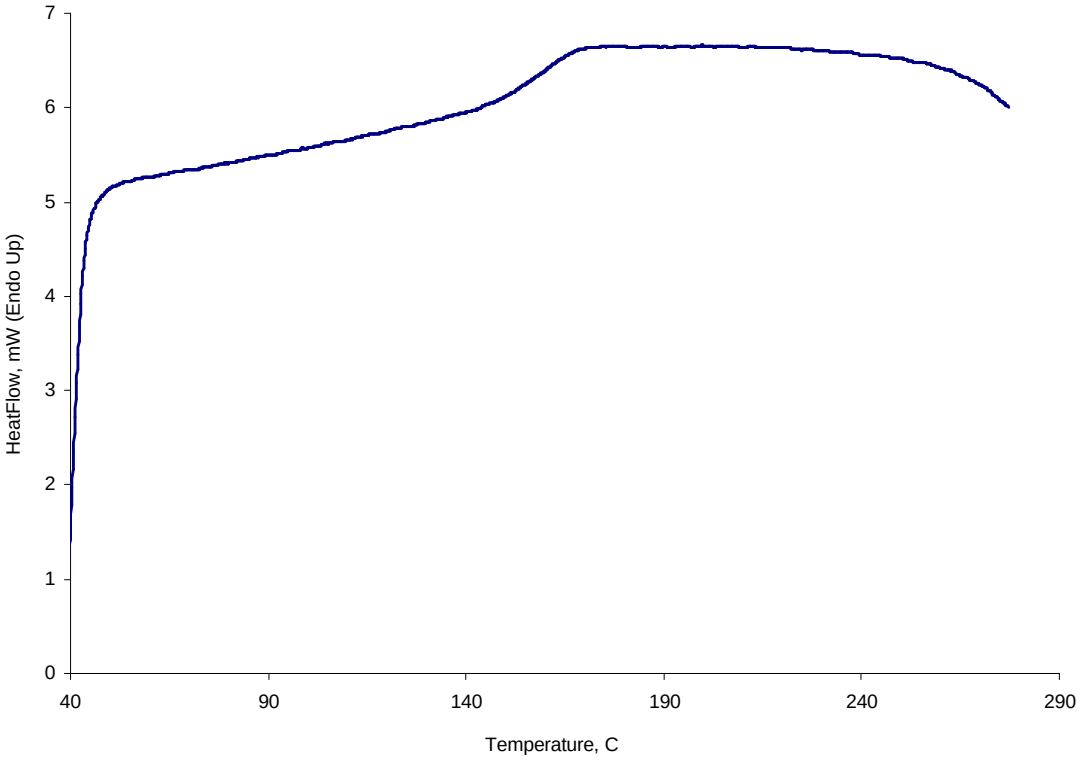

Figure 3.15. Ultimate Tg of the adhesive isothermally cured at 165°C for 8 hrs followed by dynamic temperatures scanning at 3°C/min from 30°C to 300°C to complete the cure. This DSC trace showing the ultimate Tg was generated from the dynamic temperature scanning at a heating rate of 10°C/min from 30°C to 300°C of the fully cured sample.

The total cure exotherm (total heat of reaction) was obtained by adding the cure achieved during both the isothermal and the following ramp exotherms. The degree of cure (α) under isothermal conditions as a function of time was then calculated from the partial area of the isothermal exotherm up to a certain time *t* divided by the total cure exotherm. In this way, intermediate cure states of the adhesive as a function of time over a series of isothermal temperatures between 110°C and 180°C were determined. This is plotted in Figure 3.16.

As expected, the cure reaction proceeded rapidly at 180°C but dropped off at lower cure temperatures. Likewise, the maximum degree of cure that can be attained from isothermal scan was a function of the isothermal cure temperature. For example, the cure reaction was 95 % complete from isothermal scanning at 160°C or above. The measured maximum degree of cure under isothermal conditions is plotted against isothermal cure temperature in Figure 3.17. This figure reveals that appreciable curing of the adhesive can be achieved at temperatures even as low as 110°C (α_{max} ~ 0.78, isothermal scanning for 27 hours), provided that cure reaction is allowed to proceed over an extended period of time.

Going back to the cure cycle described in Figure 3.1, the degree of cure after a 30 minutes soak at 120°C (step II) is about 7 %. As mentioned in the preceding section, the degree of cure for step I is negligible (< 1%).This means that, in the case of the adhesive, the majority of curing in this cycle occurs in steps III and IV. So, the industrial cure cycle can be modeled by a simple ramp and soak experiment.

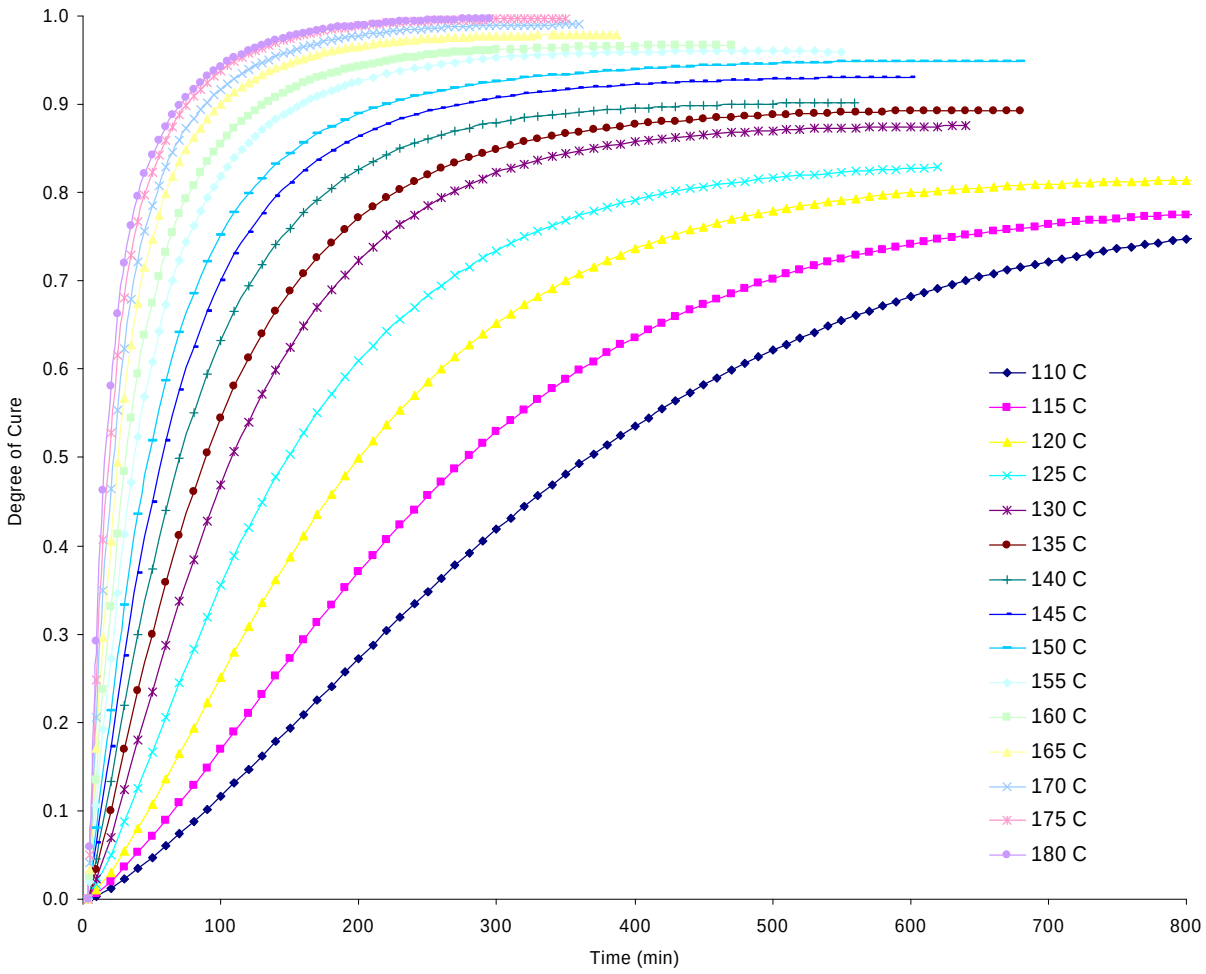

Figure 3.16. 2D plot of the degree of cure (α) as a function of time for the film adhesive isothermally cured over a range of temperatures.

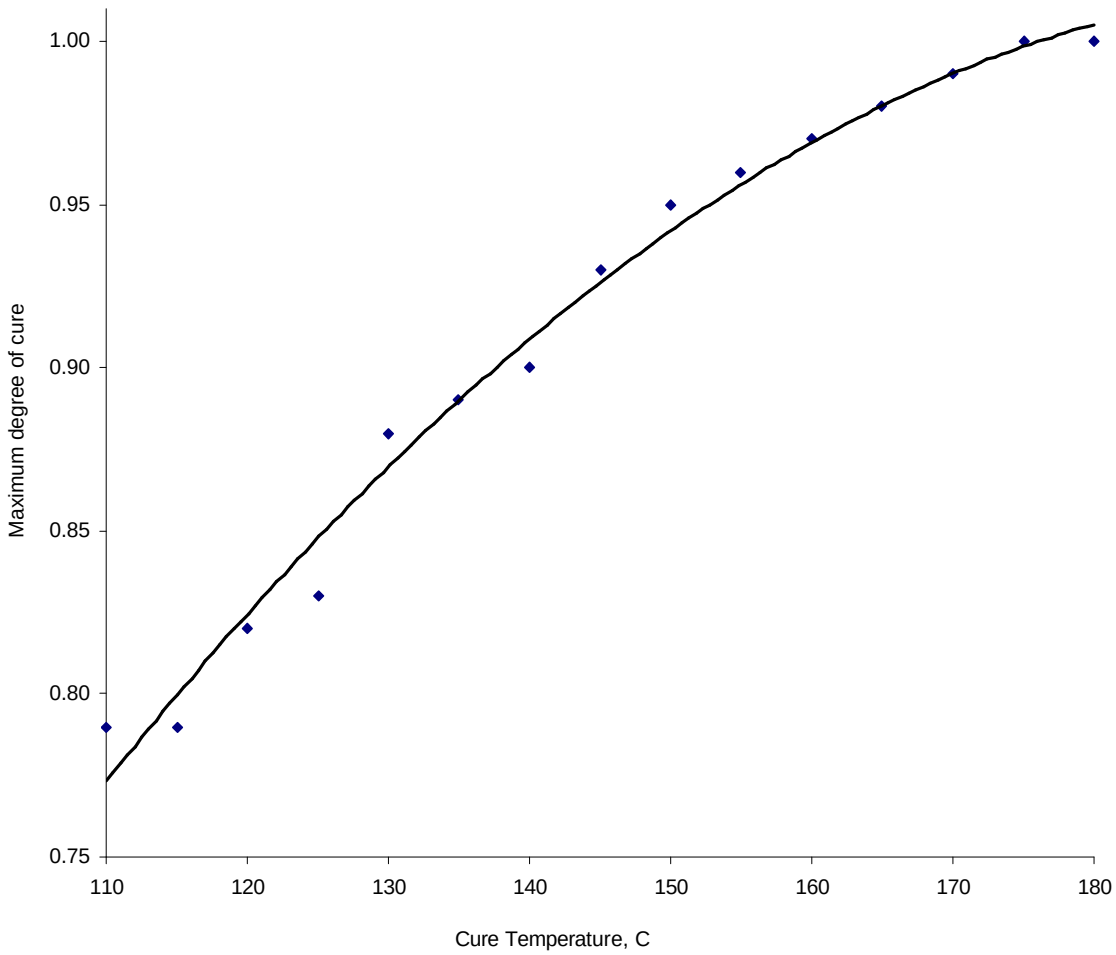

Figure 3.17. Maximum degree of cure (α_{max}) attained after isothermal scanning.

Plots of reaction rate ($d\alpha/dt$) versus time as a function of cure temperature for isothermal cure, following a quick jump to that temperature, are shown in Figure 3.18. It can be seen that the magnitude of the initial spike in the rate of the cure reaction is a strong function of cure temperature. This rate "spike" indicates the extent of heat evolution from the cure reaction. If this is high, it can cause localized charring. This has been found to occur during actual curing of parts made with this film adhesive. Obviously, in order to reduce the possibility of overheating the resin, this rate maximum must be moderated.

The limitations of isothermal cure, following a fast jump to that temperature, as a safe and efficient commercial cure cycle are illustrated in Figure 3.19. The upper curve represents the maximum extent of cure (α_{max}) of the adhesive as a function of isothermal cure temperature. The lower curve represents the maximum rate of cure observed at that cure temperature normalized to the maximum rate of cure at 180°C. In order to drop the initial cure rate and lessen the possibility of charring, the reaction temperature must be decreased. By dropping the reaction temperature, the maximum degree of cure that will be attained is accordingly lowered as well. In order to build up good mechanical properties, the cure state must exceed 95%. A small drop in reaction temperature can produce materials that may not be able to function properly. This problem can be partly circumvented by ramping more slowly to the isothermal cure temperature.

The degree of cure is re-plotted as a function of both isothermal cure temperature and cure time in Figure 3.20 to allow us to interpolate the extent of cure as a function of time and temperature. As outlined previously, one of the two variables can be fixed while varying the other to get the degree of cure. Both variables may not be changed at the

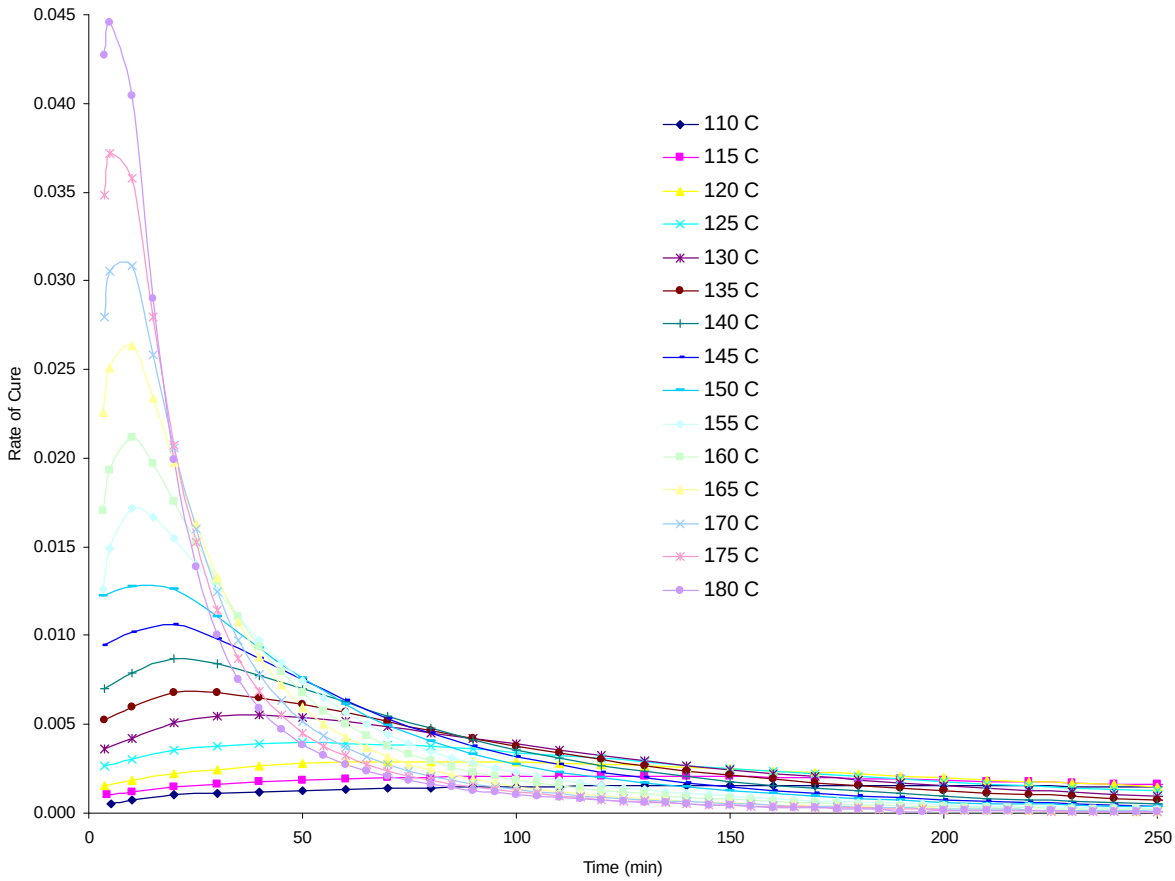

Figure 3.18. 2D plot of the rate of cure ($d\alpha/dt$) as a function of time for the film adhesive isothermally cured over a range of temperatures.

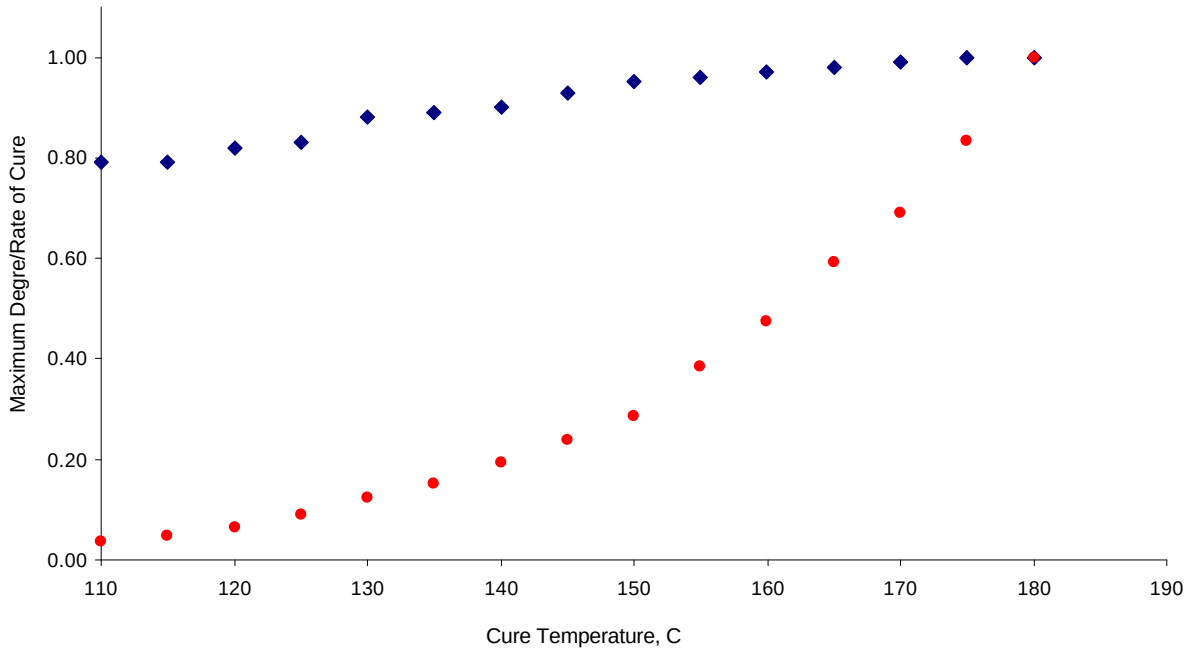

Figure 3.19. Maximum degree of cure (α_{max}) of the adhesive attained after prolonged isothermal scanning after a rapid jump to that temperature (upper curve). Maximum reaction rate attained at the cure temperature normalized to that attained at 180°C (lower curve).

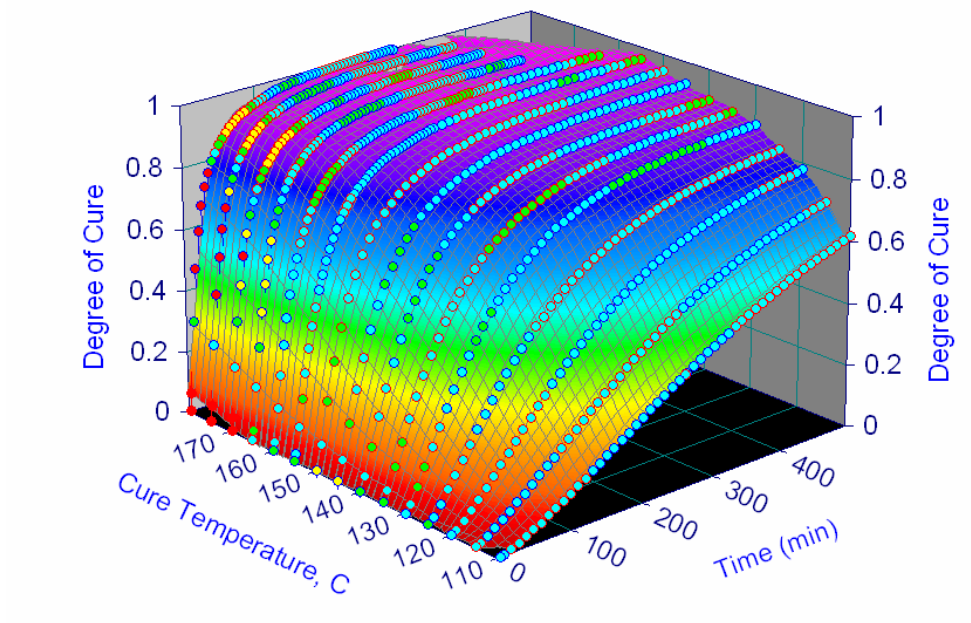

Figure 3.20. 3D plot of the degree of cure (α) as a function of time and isothermal cure temperature.

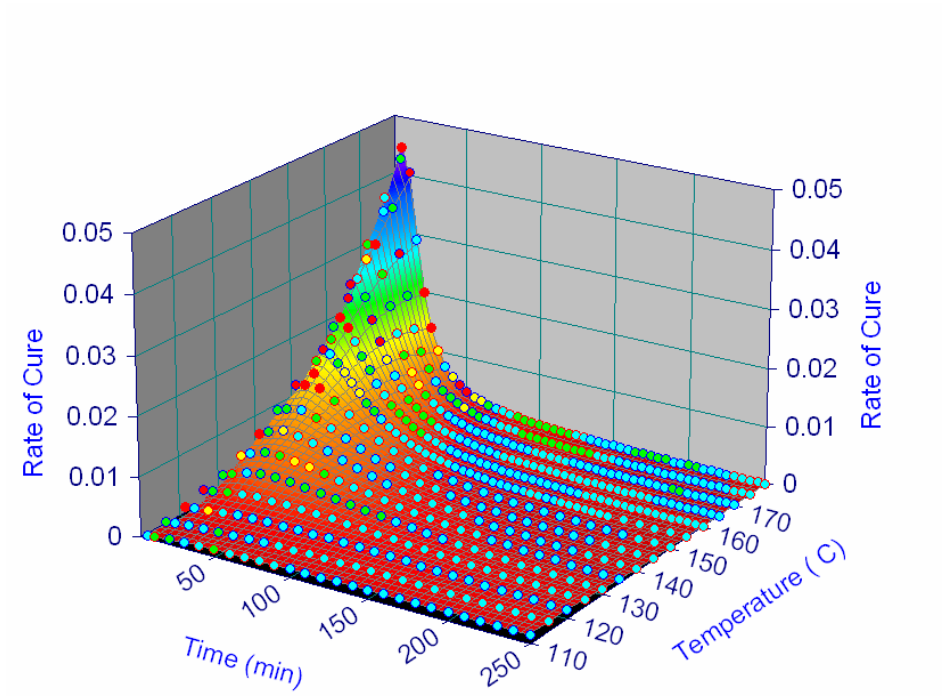

Figure 3.21. 3D plot of the rate of cure (*dα/dt*) as a function of time and isothermal cure temperature.

same time. Similarly, the cure rate is re-plotted as a function of isothermal cure temperature and time in Figure 3.21. The same limitations apply to this plot.

Figure 3.22 shows the intermediate Tg of the adhesive obtained after a prolonged isothermal cure as a function of the cure temperature. It will be noted that, at least for this material, the simplistic “rule of thumb” statement that the cure reaction progresses until the intermediate glass transition temperature reaches the cure temperature, does not apply. Over most of the range of cure temperatures, the cure reaction proceeds until the intermediate glass transition temperature drifts to over 20°C above the cure temperature.

It is shown previously (Figure 3.17) that the maximum attainable extent of cure (α_{max}) under isothermal conditions after long times, is a strong function of the isothermal cure temperature. Considering that the area of the exotherm is directly proportional to the extent of cure, then it will come as no surprise that the measured heat of reaction from the isothermal scan increases with the cure temperature, as shown in Figure 3.23. Taking into consideration the numerous sources of experimental error in these multistage experiments, a good correlation between extent of cure and heat of reaction was achieved. For example, assuming that the adhesive is completely cured after a long time at 180°C ($\alpha \sim 1$), then the heat of reaction becomes about 271 J/g. If α_{max} at 120°C reaches 0.81 at long times, as was measured, and if the heat of reaction scales with the degree of cure, then the heat of reaction at 120°C should equal to 220 J/g, which is close to the measured value (208 J/g).

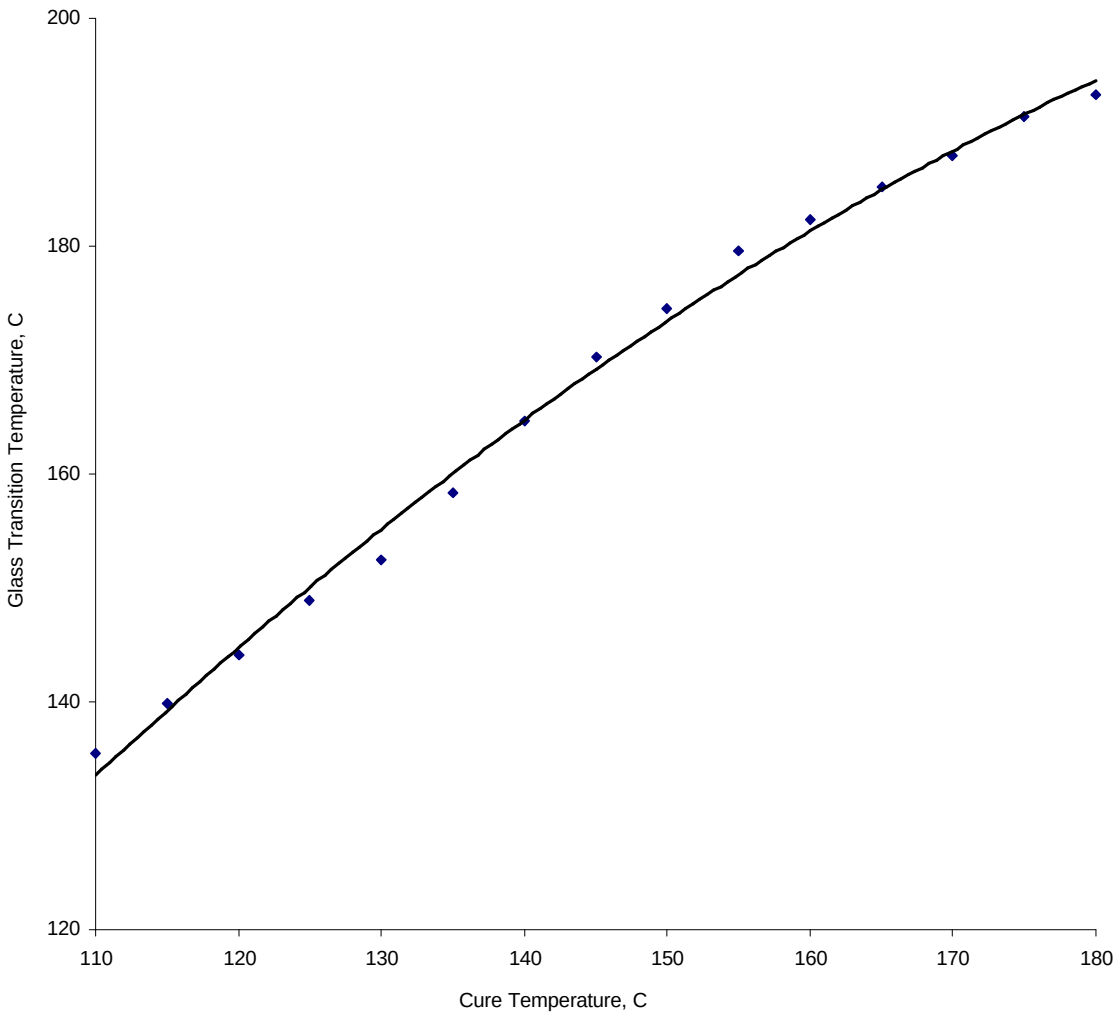

Figure 3.22. Intermediate Tg of the adhesive attained after prolonged isothermal heating, determined as 3°C/min post ramp from 30-300°C to complete the cure reaction.

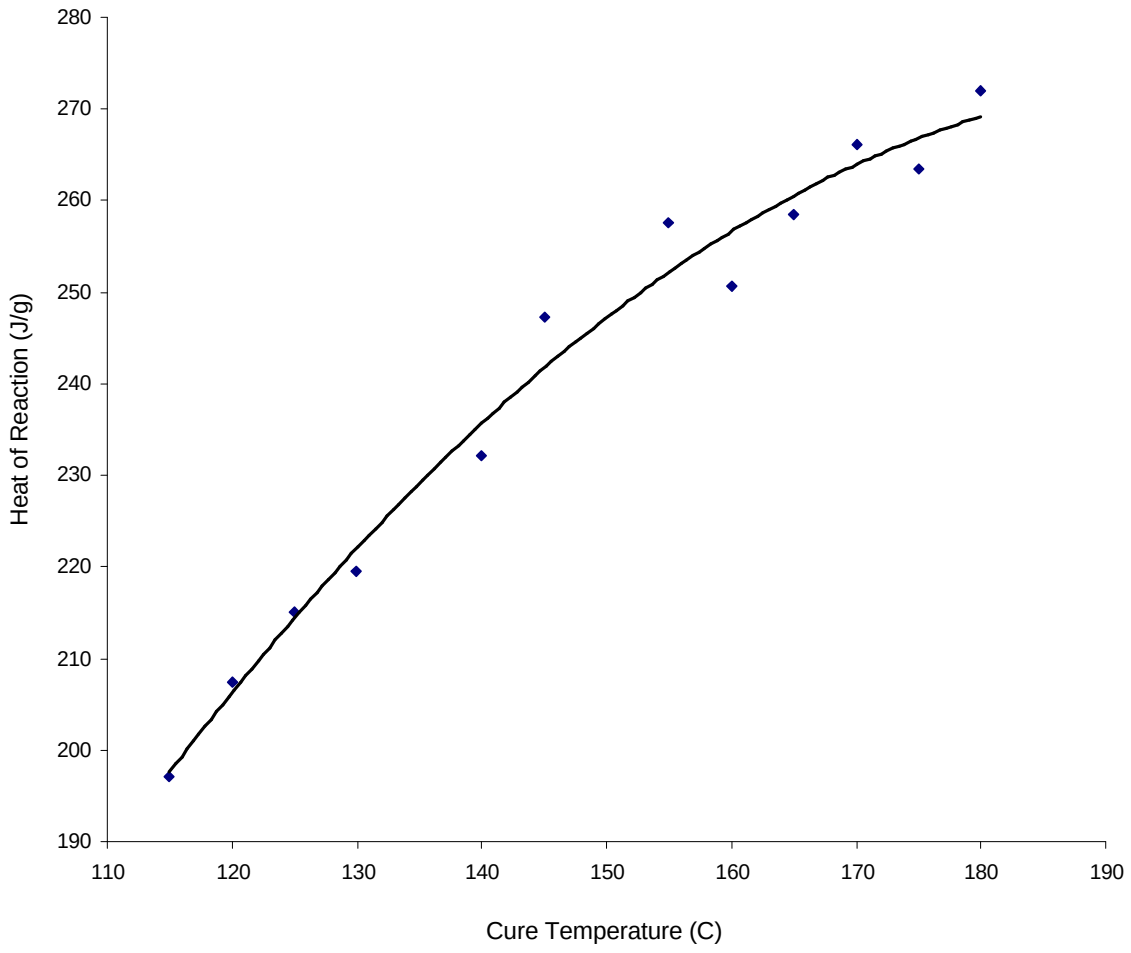

Figure 3.23. Apparent heat of reaction (J/g) released during isothermal cure of the adhesive over a range of temperatures.

From examination of the results shown in Figure 3.23, the apparent reaction enthalpies, as measured from isothermal scanning experiments, are considerably higher than predicted by comparison with the results obtained from dynamic temperature experiments. For example, the averaged heat of reaction measured from dynamic temperature scanning at lower heating rates is 213 $\pm$ 12 J/g, dropping to even lower values at higher heating rates that shift the cure reaction to higher temperatures. In contrast, the heat of reaction produced by complete cure of the resin under isothermal conditions at 180°C is 271 J/g. This can be explained by the existence of higher temperature endothermic processes in the adhesive that overlap and reduce the apparent exotherm of reaction at temperatures above 200°C.

As previously shown in Figure 3.10, the ultimate Tg of the film adhesive cured under dynamic temperature conditions is remarkably insensitive to the rate of cure. In similar fashion, the ultimate Tg measured after prolonged isothermal cure followed by dynamic temperature scanning to complete the cure reaction, is not affected by the isothermal cure temperature. A plot of ultimate Tg of the adhesive versus isothermal cure temperature is shown Figure 3.24. The ultimate Tg values that averaged at 184 $\pm$ 2°C from isothermal scanning are considerably higher than those measured from dynamic temperature scanning (167 $\pm$ 3°C). The resin cure reaction is actually a supposition of two overlapping reactions – that of the primary amine with an epoxy group at lower temperatures, and that of the secondary amine with an epoxy group at higher temperatures. By curing under isothermal conditions, lower temperature reactions are favored over higher temperature degradation reactions resulting in structurally different cured material.

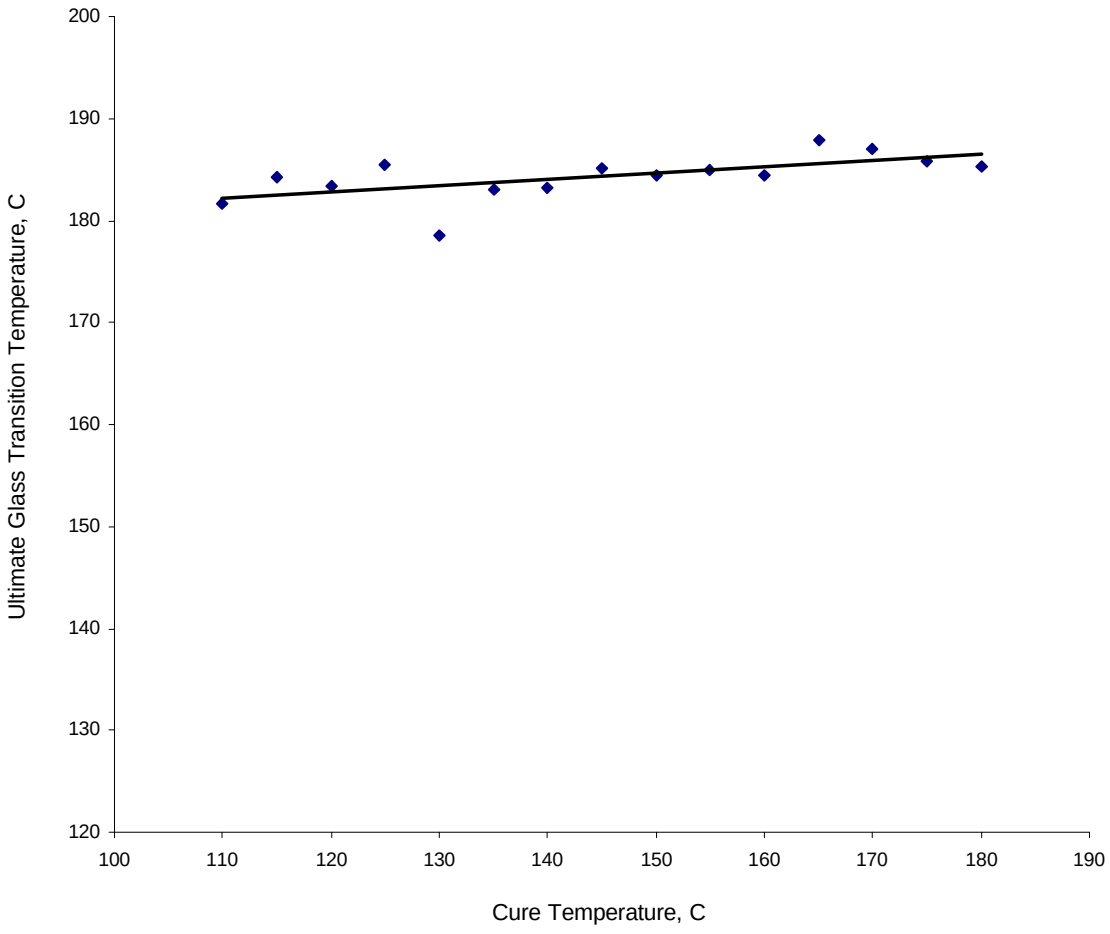

Figure 3.24. Ultimate Tg of the adhesive after prolonged isothermal cure over a range of temperatures followed by a post cure scan at 3°C/min from 30°C to 300°C to complete the cure reaction. Ultimate Tg was determined by a second scan at 10°C/min from 30°C to 300°C.

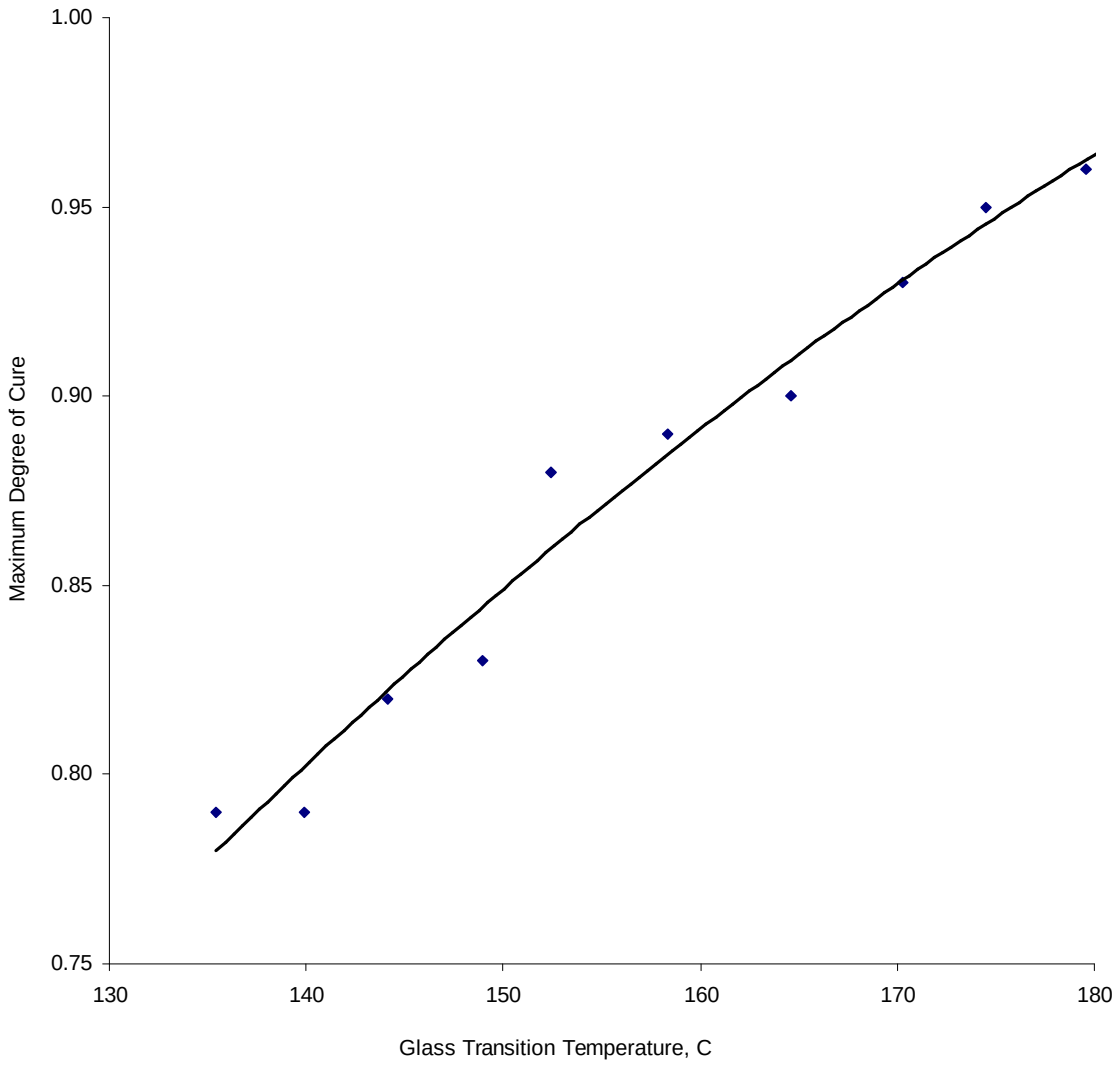

Figure 3.25. Maximum degree of cure (α_{max}) of the adhesive partly cured after an extensive isothermal soak as a function of the Tg attained during that isothermal scanning. This was measured from a 3°C/min post scanning from 30°C to 300°C.

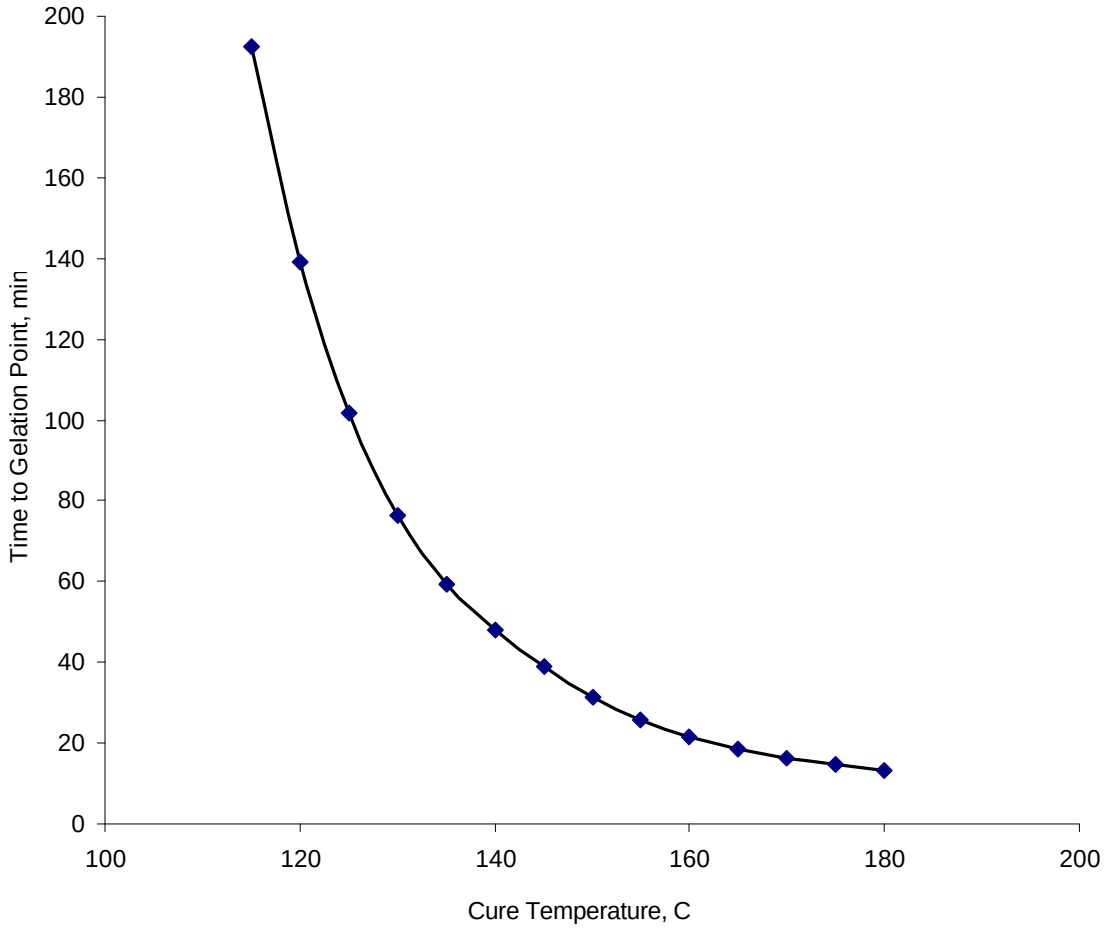

Figure 3.26. Time to reach the gel point (α_{gel} = 0.36) for the adhesive cured under isothermal conditions.

By combining the results of Figures 3.17 and 3.22, a correlation between the maximum degree of cure attainable under isothermal conditions and the intermediate Tg values achieved at that temperature was generated (see Figure 3.25).

Time to reach the gel point for this adhesive as a function of isothermal cure temperature is plotted in Figure 3.26. An inverse relationship between time to gel and cure temperature may be assumed, however, these are derived data from thermal and rheological analysis. Nonetheless, gel times are very short at higher temperatures and longer at lower temperatures.

Isothermal data were fitted into the kinetic model of Kamal [3, 30] (*equation (15)*). Fitting was done in Origin 6.1 software which uses Levenberg-Marquardt minimization algorithm. Good correlation was observed for the entire temperature range (refer to Figure 3.27).

$$\frac{da}{dt} = \left(K_1 + K_2 a^m\right)\left(a_f - a\right)^n \qquad (15)$$

Table 3.1 shows the tabulated kinetic parameters for all the temperatures. All four parameters were found to vary with temperatures and degree of cure. The maximum degree of cure achieved at the cure temperature was used in the model. Assuming K_1 and K_2 follow Arrhenius rate constant dependence, activation energies and pre-exponential factors were also calculated. K_1 is the rate constant for the reaction catalyzed by groups initially present in the resins, while K_2 is the rate constant for the reaction catalyzed by newly formed groups and represents the influence of the reaction products on the rate of reaction.

$$\ln\left(K_1\right) = \frac{-E_{a1}}{RT} + \ln\left(A_1\right) \qquad (16)$$

$$\ln(K_2) = \frac{-E_{a2}}{RT} + \ln(A_2) \qquad (17)$$

From the isothermal data, E_{a1} annd E_{a2} were found to be 82 and 67 kJ/mole while pre-exponential factors were 1.56 x 10^8 and 4.31 x 10^6 min^-, respectively.

Table 3.1

Kinetic parameters for the isothermal data fitted into equation (15).

Temperature (°C)	a_{max}	K_1	K_2	*m*	*n*
110	0.79	0.00070	0.00404	0.463	0.953
120	0.82	0.00185	0.00688	0.538	1.043
130	0.88	0.00402	0.01017	0.538	1.134
140	0.90	0.00788	0.01277	0.601	1.186
150	0.95	0.01298	0.01376	0.600	1.314
160	0.97	0.01767	0.03149	0.584	1.493
170	0.99	0.02941	0.10501	1.066	1.960
180	1.00	0.04249	0.09356	0.866	1.869

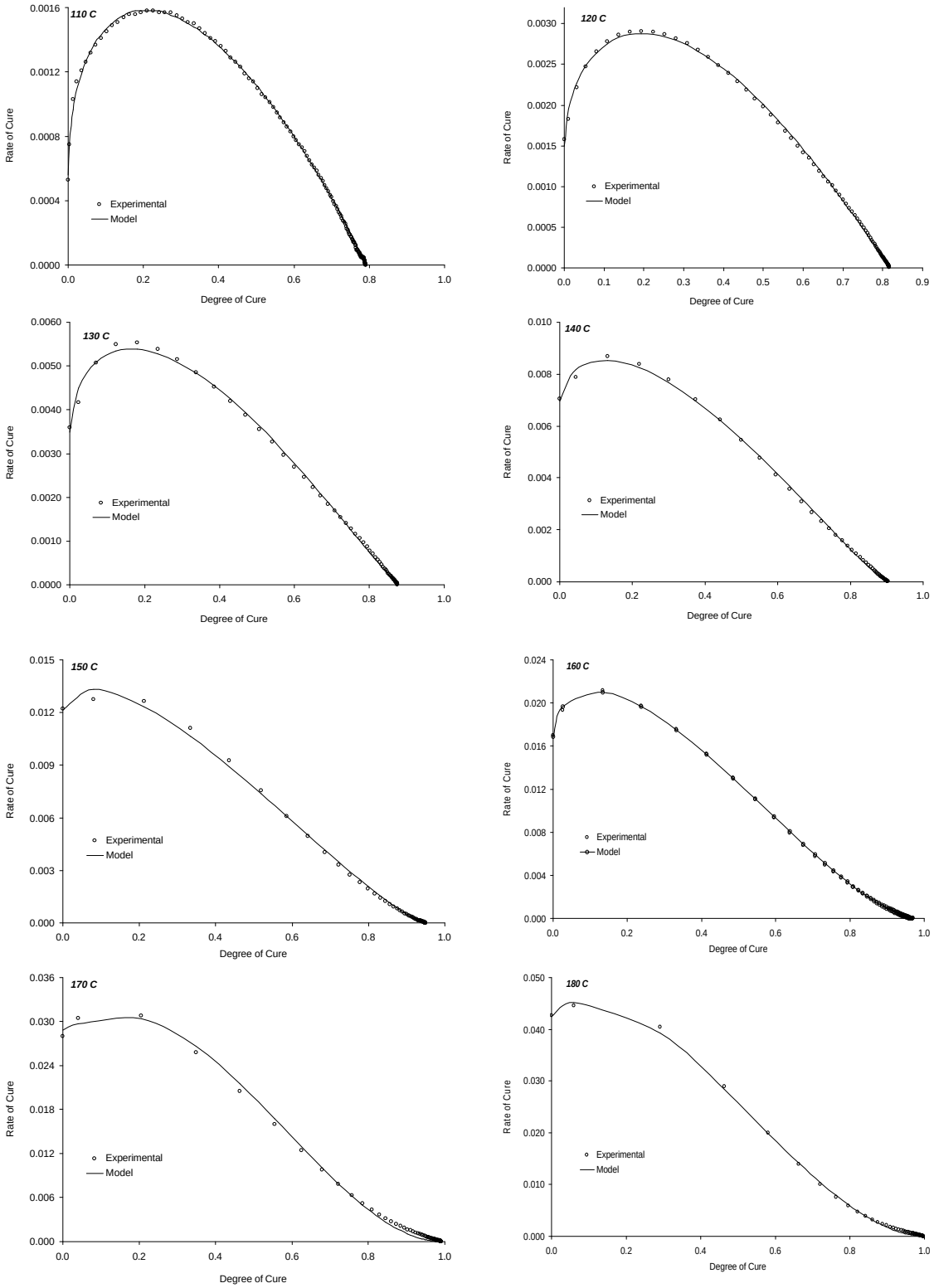

Figure 3.27. Rate of cure versus degree of cure. Model prediction compared to isothermal data at 110 to 180°C.

3.3.3 Combined Ramp and Soak Experiments

Having completed the thermal analysis of the film adhesive under both dynamic temperature and isothermal conditions, experiments were performed to combine the two to determine the conversion profile and kinetics of cure under conditions similar to a typical autoclave cure cycle (Figure 3.1). In a classical isothermal cure experiment, the sample is scanned at a defined temperature after a very rapid jump to that temperature with the result that α can be set at zero at the start of the isothermal scan. In a combined dynamic temperature and isothermal scanning experiment, the sample reaches the isothermal cure temperature partially cured. In other words, the degree of cure at t_o is not zero. There is no analytical model that can be used to factor in the influence of cure history on an isothermal cure experiment. Therefore, our only recourse was to perform the required experiments.

Combined dynamic temperature and isothermal scanning experiments were done in 4 steps:

(1) the sample was heated from 30°C to the isothermal cure temperature (140°C, 150 to 180°C at 5°C increment) over a range of heating rates (0.5 to 5°C/min);

(2) the sample was rapidly cooled to 30°C and then heated up to the same isothermal cure temperature at 50°C/min and held there until the DSC trace returned to the baseline;

(3) the sample was cooled down to 30°C and heated up to 300°C at 3°C/min to determine intermediate Tg and residual exotherm; and

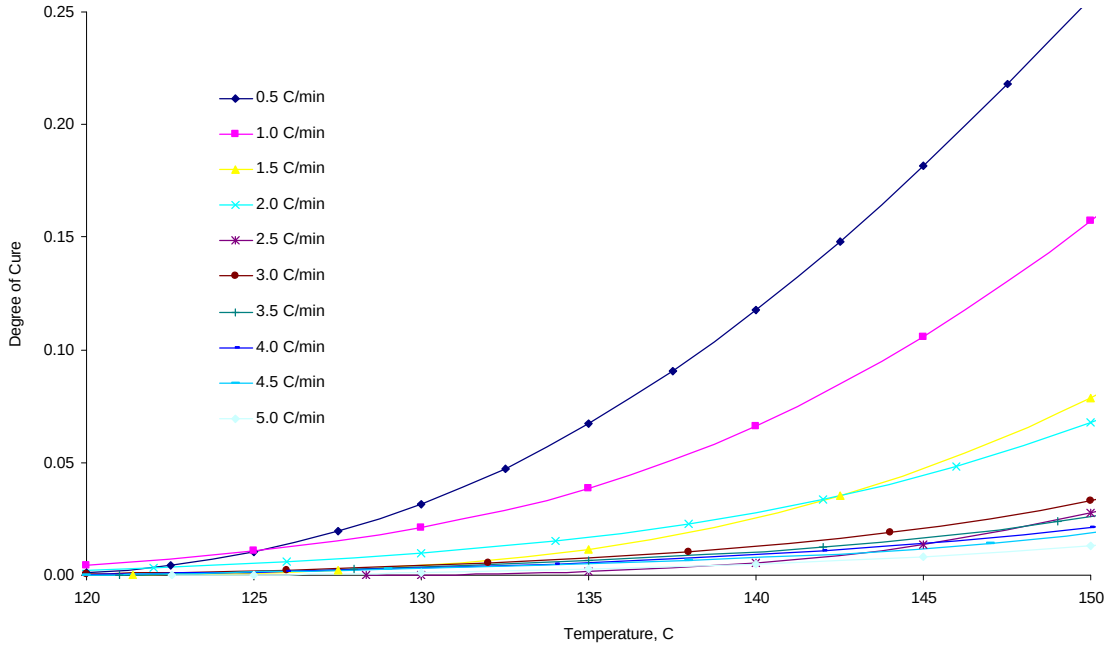

Figure 3.28. Extent of cure (α) as a function of temperature up to 150°C at various heating rates (step 1).

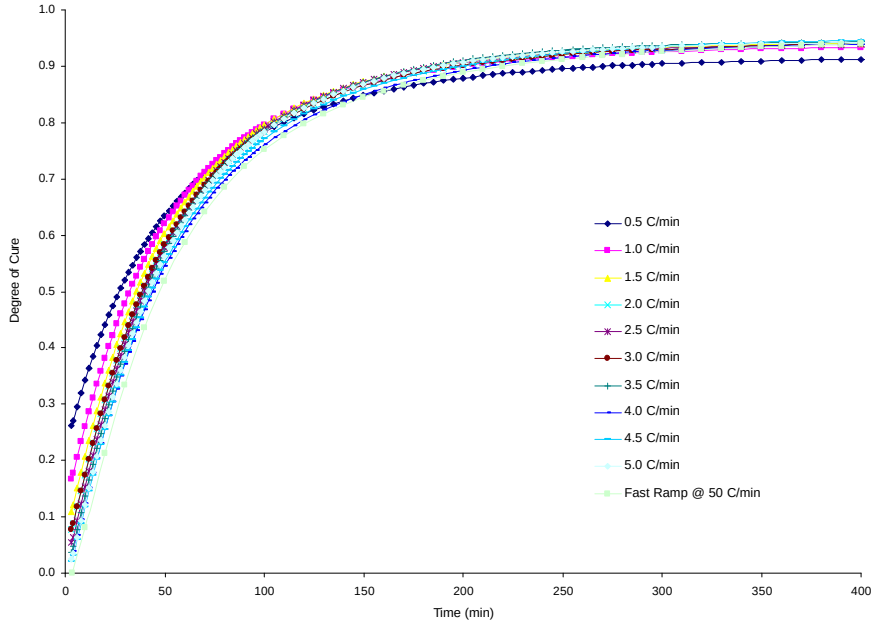

Figure 3.29. Degree of cure as a function of time for the isothermal portion (step 2) at 150 ^{o}C after ramping to that temperature over a range of linear heating rates.

(4) the sample was cooled down to 30°C/min and heated up to 300°C at 10°C/min for the ultimate Tg.

The extent of cure (α) and rate of cure ($d\alpha/dt$) were calculated as a function of time to follow the cure process of the adhesive during the ramp and soak experiment. However, it was found that the exotherm from step (1) was rather difficult to integrate. The previously generated data from the dynamic temperature scanning experiments were therefore used. For illustrative purposes, Figure 3.28 was generated as a plot of α as a function of temperature up to 150°C for different heating rates.

For the isothermal scanning portion, degree of cure and rate of cure data were calculated by dividing the partial area of the isothermal exotherm from step 2 of the combined run with the total area. The total area, in this case, was the sum of the areas from step 1 (dynamic temperature scanning), step 2 (isothermal scanning) and step 3 (dynamic temperature scanning for residual exotherm). Plot of the degree of cure as function of time for step 2 is shown in Figure 3.29. Note that a slower heating rate in step (1) leads to a greater initial conversion (α at t_0) at the beginning of step (2). Note also that the conversion curves converge at long times. In other words, the ultimate conversion ($a_{¥}$), measured during an isothermal cure after linear heating to that temperature with different heating rates, is a function of isothermal cure temperature and not of thermal history or initial degree of cure. Two dimensional plots of α versus time for isothermal scanning for a range of temperatures following dynamic temperature ramp using various heating rates to that isothermal cure temperature can be found in Appendix B.

a for the isothermal scanning portion of the combined run was also plotted as a function of the initial cure (extent of cure from step 1) and time at the isothermal temperature scan. Again, this can be used to interpolate the extent of cure occurring during isothermal scanning (step 2) for intermediate soak times and heating rates. Such a plot is shown in Figure 3.30 for isothermal cure at 150°C. With reference to Figure 3.6, α at t_o can be determined for any combination of heating rate and target isothermal cure temperature (for example, a 3°C/min ramp up to 150°C). Inputting the initial a_0 into the best fit equation for the following isothermal cure (for example, at 150°C as in Figure 3.30), the development of the degree of cured during soak at 150°C (step 2) can be modeled. 3D plots of α versus time and initial degree of cure for a range of cure of temperatures (140°C to 180°C) following linear heating up to the cure temperature for various heating rates are reproduced in Appendix C.

In similar fashion, the rate of cure ($d\alpha/dt$) during step (1) for the combined dynamic and isothermal scanning experiment was also determined. This was accomplished by differentiating the corresponding degree of cure curves (Figure 3.28 for the experiment at 150°C) and plotting the rate of cure data as shown in Figure 3.31.

Furthermore, by differentiating the conversion curves in Figure 3.29, the rates of reaction for step (2) of the combined dynamic and isothermal scanning at 150°C were determined and plotted (Figure 3.32). Also, two dimensional plots of ($d\alpha/dt$) versus time for step 2 over a range of soak temperatures from 140°C to 180°C, following ramp at different heating rates to the isothermal cure temperatures can be found in Appendix D.

The rates of reaction for step (2) were plotted also as a function of the initial degree of cure (a_0) and time at the soak temperature, for example at 150°C as shown in

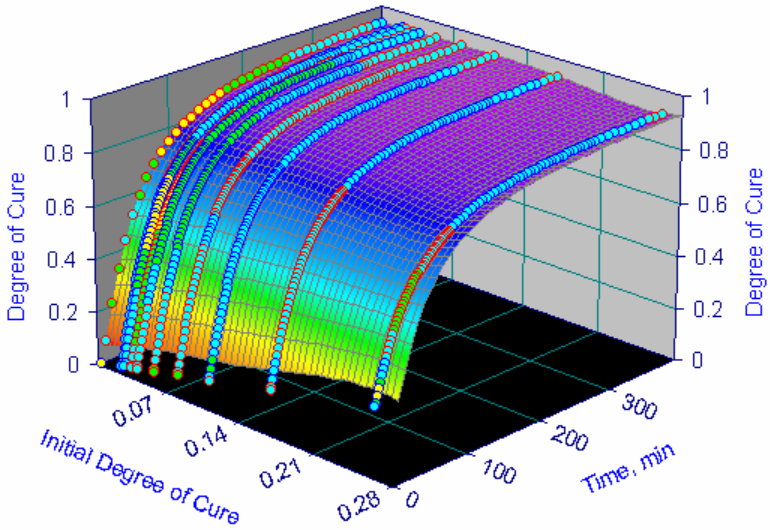

Figure 3.30. Degree of cure as a function of time and initial degree of cure (from step 1 for various heating rates) for isothermal scanning at 150°C (step 2).

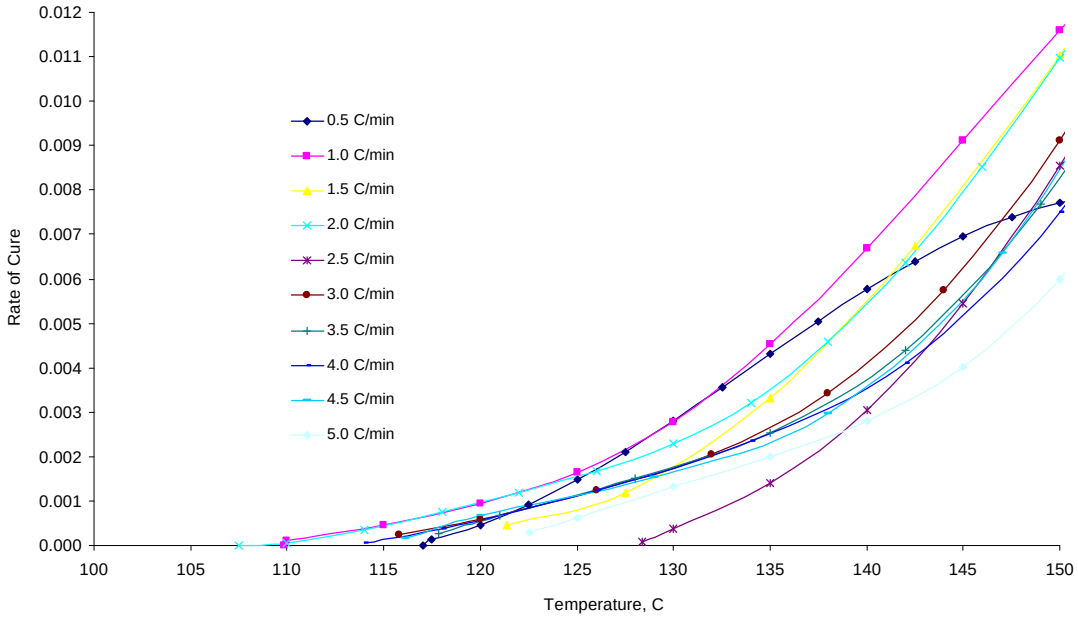

Figure 3.31. Rate of reaction ($d\alpha/dt$) of as a function of temperature for dynamic temperature scanning up to 150°C for a range of linear heating rates (step 1).

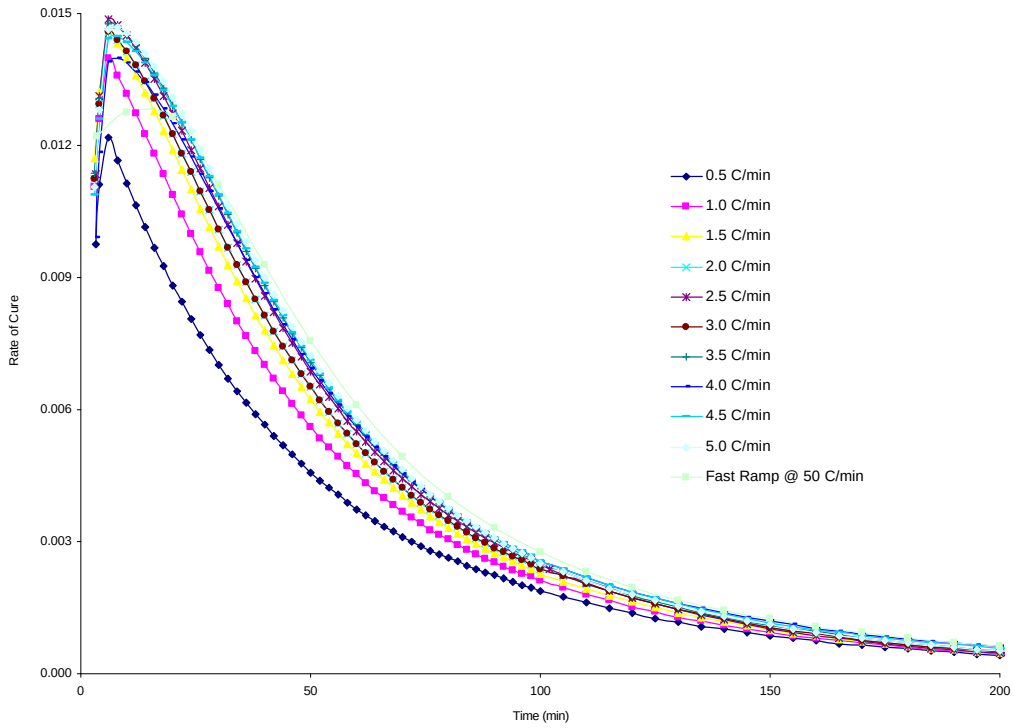

Figure 3.32. Reaction rate ($d\alpha/dt$) as a function of time during isothermal scanning at 150°C (step 2) after ramping to that temperature over a range of linear heating rates.

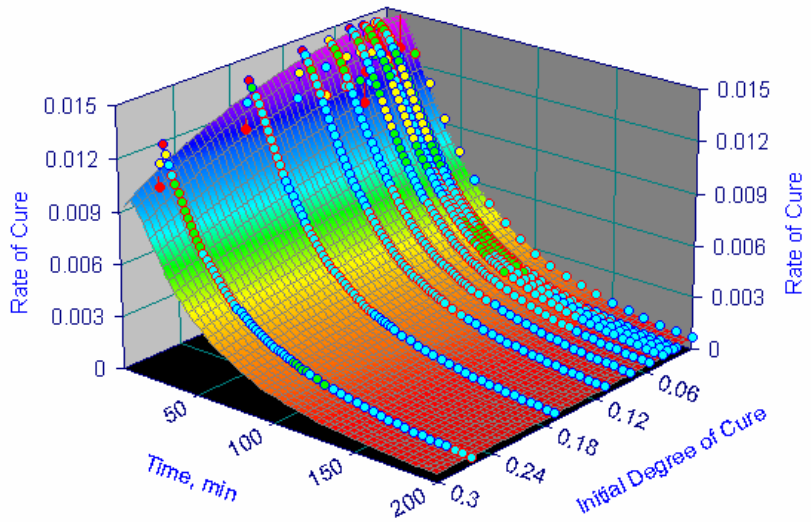

Figure 3.33. Reaction rate ($d\alpha/dt$) versus time and initial degree of cure for the isothermal scanning (step 2) at 150°C after ramping to that temperature over a range of linear heating rates.

Figure 3.33. A best fit equation that describes the plot surface was obtained. Again, this plot allows the interpolation for the reaction rate value after ramping to the isothermal cure temperature at any heating rate from 0.5 to 5°C/min. Three dimensional plots of ($d\alpha/dt$) versus time and the initial degree of cure for the combined dynamic and isothermal scanning experiments for 140°C to 180°C are shown in Appendix E.

After analyzing separately the cure profiles for steps (1) and (2) of the combined ramp and soak experiment, the next step of data analysis was to integrate the data for steps (1) and (2). This was done, in the hope, of creating a visual representation of the entire cure cycle.

A plot of the extent of cure (a) versus time for a combined dynamic and isothermal scanning experiment at 175°C over a range of heating rates is shown in Figure 3.34. Times to the left of the y axis correspond to the ramp segment of the cure cycle (step 1). Times to the right of the y axis correspond to the soak segment (step 2). The horizontal bar represents the gel point of the adhesive.

Significant cure is achieved during the ramped segment for heating rates below 2°C/min. The gel point is achieved during the ramped segment for heating rates less than 1.5°C/min. Similar plots for the experiments at 170°C and 180°C are reproduced in Appendix F. As would be expected, pre-isothermal cure is somewhat less pronounced for cure cycles ending at 170°C and more pronounced for cure cycles ending at 180°C.

Likewise, rate of reaction profiles for steps (1) and (2) of combined ramp and soak experiments were plotted to show how reaction rate (and, therefore, the exotherm) develops throughout the entire autoclave cure cycle. A plot of rate of cure versus time for the experiment at 175° C over a range of heating rates is shown Figure 3.35. It can be

deduced from the plot that the rate spike observed at the beginning of the isothermal segment is a strong function of previous heating rate. A heating rate of 1°C/min to 175°C is unique for the adhesive in that it minimizes ramp time while producing a symmetrical low intensity exotherm that extends from step 1 to step 2 of the cure cycle reaction without any observed autoacceleration at the beginning of the isothermal scanning segment. Two dimensional plots of reaction rate versus time for dynamic and isothermal scanning for experiments at 170°C and 180°C are reproduced in Appendix G. For cure cycles ending at 170°C, the rate maximum for heating at, for example, 1°C/min is displaced marginally to the right of the time curve into the isothermal segment. For cure cycles ending at 180°C, the rate maximum for heating at 1°C/min is displaced marginally to the left of the time curve, both with reference to the 175°C rate curve.

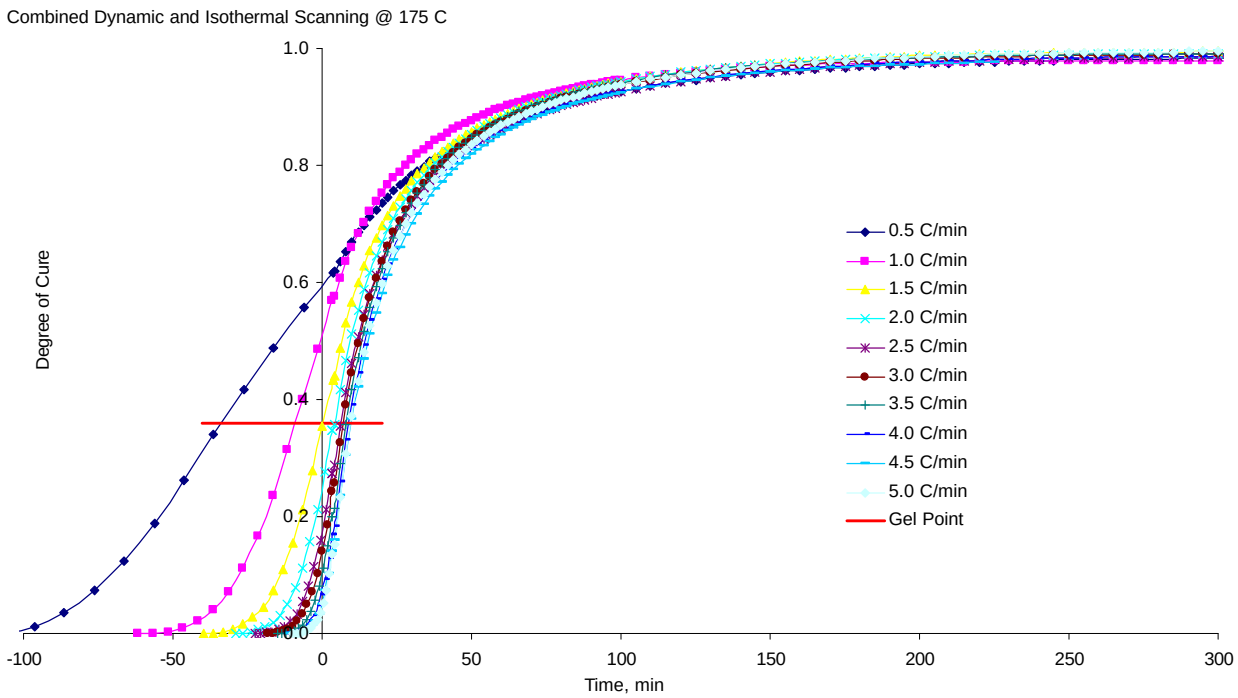

Figure 3.34. Development of the degree of cure for steps 1 and 2 of the combined dynamic and isothermal scanning experiment at 175°C. Times to the left of the y-axis correspond to ramp segment (step 1) while those to the right correspond to the soak segment (step 2).

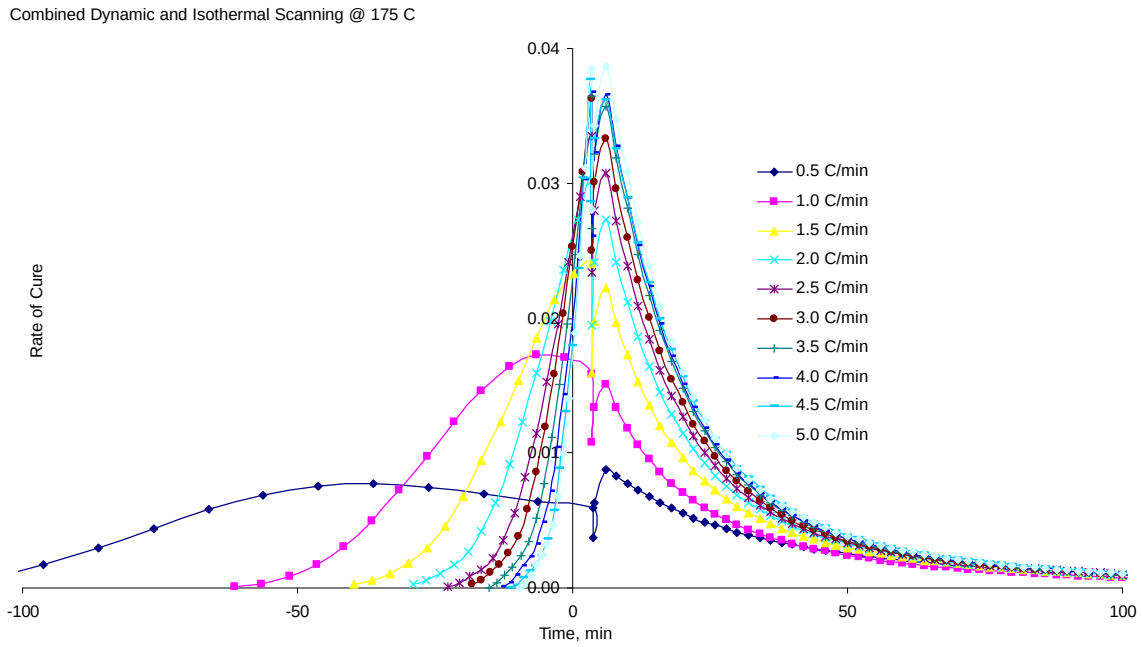

Figure 3.35. Rates of cure ($d\alpha/dt$) for steps 1 and 2 of the combined dynamic and isothermal scanning experiment at 175°C. Times to the left of the y-axis correspond to the ramp segment (step 1) while those to the right correspond to the soak segment (step 2).

3.3.4 Dynamic Shear Rheometry

The gel point of the adhesive signals the first appearance of an infinite network, and the conversion beyond which all flow ceases [62, 63]. In order to measure the gel point conversion of the adhesive, the results of DSC experiments were combined with those from dynamic mechanical analysis (DMA). In the DMA experiment, the adhesive was sandwiched between two circular flat platens. The assembly was placed in an oven and allowed to thermally equilibrate at the test temperature. Shear moduli were then obtained at a forced frequency. Due to the slow temperature equilibration, this type of instrument cannot be used to obtain measurements under dynamic temperature conditions with any efficiency. For this reason, the buildup of the viscosity was monitored under isothermal conditions as the adhesive was cured. The gel point was assumed to have been reached when the storage (G') and loss (G") moduli became equal in magnitude [24]. In order to minimize pre-cure during temperature equilibration, data were collected at lower temperatures. The development of G' (storage), G"(loss), and G*(complex modulus) of the adhesive during isothermal cure at 130°C is shown in Figure 3.36. The gel point was reached after 4433 sec at this temperature.

Plots of G', G", and G* versus time for all other isothermal cure experiments can be found in Appendix H. Plots of the ratio between G" and G' (tan delta) as a function of time at 130°C, 135°C, 140°C and 150°C are illustrated in Figure 3.37. As expected, the time to reach the gel point drops appreciably as the cure temperature is raised. At each temperature, the conversion at the gel point was obtained with reference to Figure 3.20. With the extent of cure at the gel point (α_{gel}) for a particular isothermal cure temperature, the time at which gelation is expected to occur can be calculated.

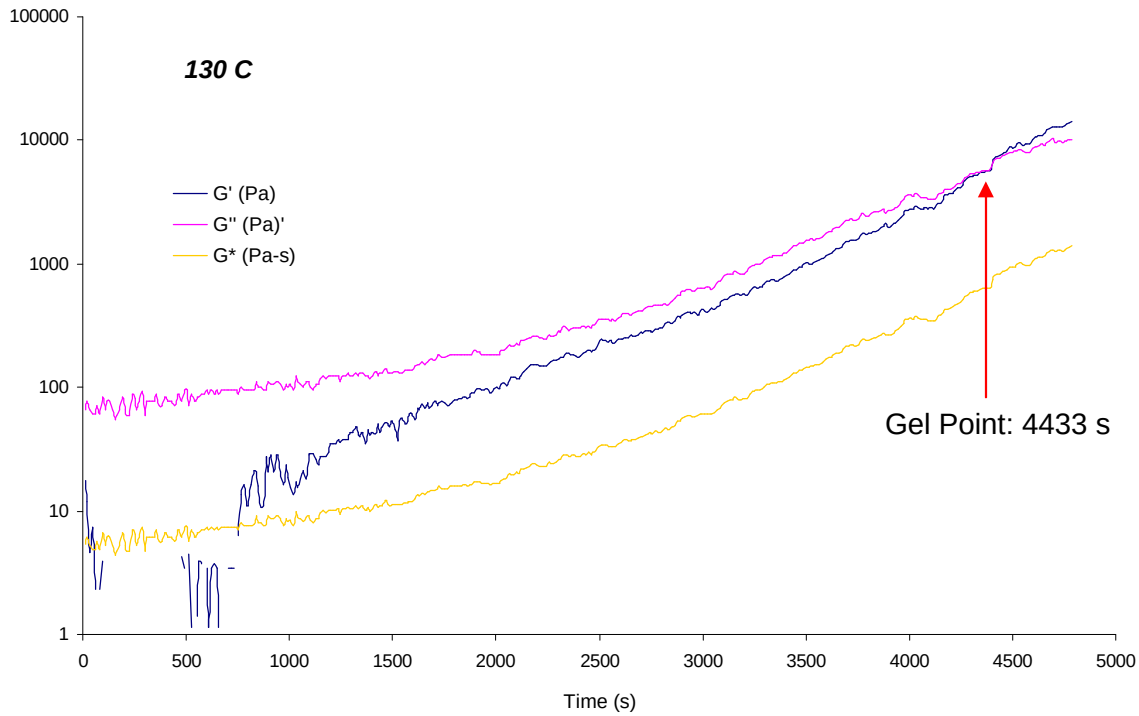

Figure 3.36. Plot of storage modulus (G'), loss modulus (G'') and complex modulus (G*) for the initially uncured adhesive as a function of time during isothermal cure at 130°C. The gel point (arrowed) is reached at 4433 sec.

Values of apparent α_{gel} are plotted in Figure 3.38 as a function of cure temperature. Gel point conversions measured from 130°C to 140°C are numerically close. The apparent gel point conversion measured at 150°C is significantly lower. The rate of cure, at or close to 150°C, is significantly higher than those at the two lower temperatures. This discrepancy can, therefore, be explained as a consequence of a pre-cure of the adhesive during the temperature equilibration for about 1 minute before the measurement started, thus lessening the time measured to reach the gel point. From these measurements, the conversion at the gel point was taken as the average of the gel points measured at 130°C, 135°C, and 140°C and set at $\alpha_{gel} = 0.36$.

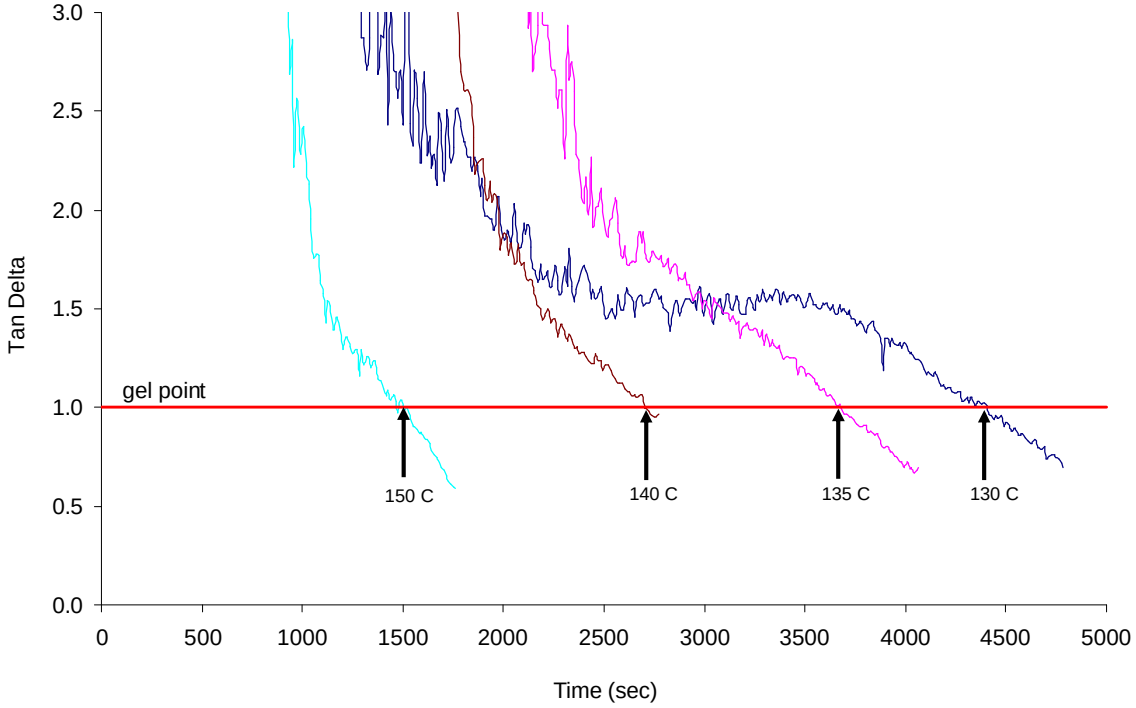

Figure 3.37. Development of tan delta with time for the adhesive cured under isothermal conditions at 130°C, 135°C, 140°C, and 150°C. Arrows mark the gel point at each temperature.

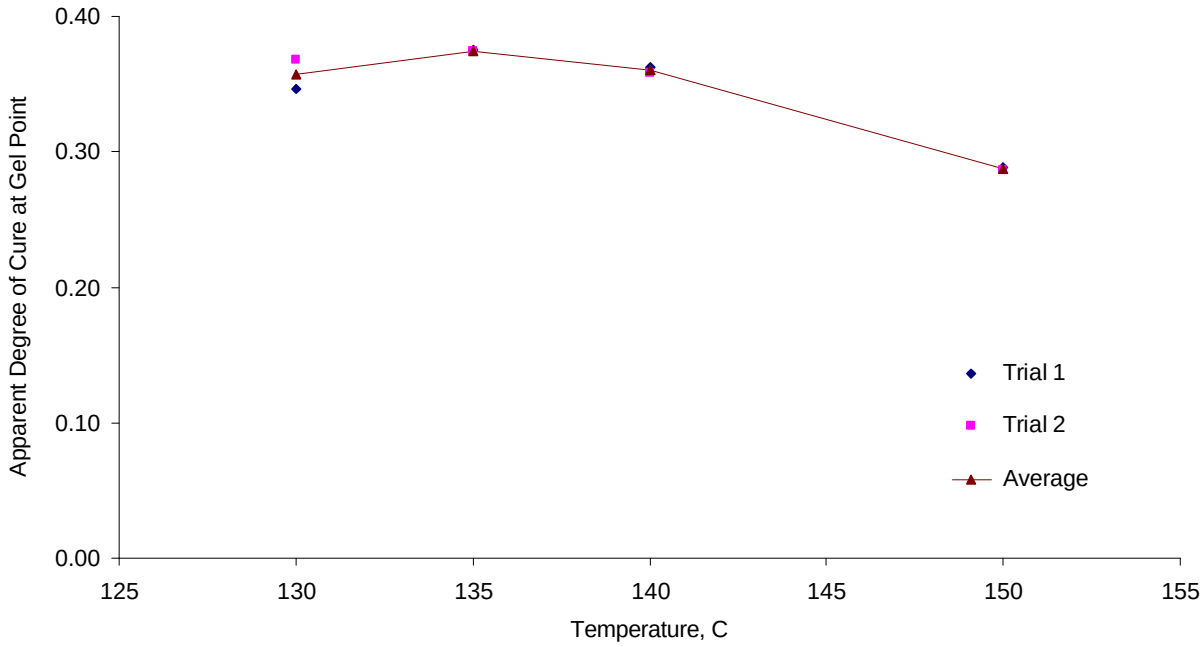

Figure 3.38. Apparent degree of cure at the gel point as a function of isothermal cure temperature. Average degree of cure at the gel point for the curing at 130, 135 and 140°C was 0.36.

CHAPTER 4

CONCLUSIONS

The major components of a high performance epoxy adhesive system were determined using chromatography and spectroscopic analytical methods. The epoxy precursors were found to be DGEBA and TGDDM. As a one pot system, the adhesive contained DDS and DICY as curing agents. These amine-based hardeners are relatively unreactive at ambient conditions giving the adhesive a long shelf life. The adhesive also contained aluminum filler. The filler enhances the thermal conductivity of the adhesive and minimizes heat concentration during cure. The adhesive was toughened with carboxy terminated poly(acrylonitrile-*co*-butadiene) rubber.

The kinetics of cure of the adhesive was investigated using DSC. Three sets of DSC experiments were performed: dynamic temperature scanning, isothermal scanning and combined dynamic temperature and isothermal scanning. In the dynamic temperature scanning experiments, the cure reaction of the adhesive shifted to higher temperatures with faster heating rates (10-20°C/min) as expected. The epoxy is known to degrade at temperatures near 300°C. Therefore the adhesive must be cured at lower temperatures and using slower heating rates. A decrease in the apparent heat of reaction was observed with faster heating rates and this was attributed to such thermal degradation reactions. The apparent energy of activation for the cure was found to vary with the degree of cure. It increased dramatically at later stages of the reaction due to the build up of resin viscosity. The ultimate Tg for the adhesive cured under dynamic temperature scanning was averaged at 167 $\pm$ 3°C.

Isothermal scanning experiments were performed from 110°C to 180°C. It was found that the maximum attainable degree of cure under isothermal conditions was a strong function of the cure temperature. However, a significant cure was observed even at 110°C if the adhesive was allowed to soak at that temperature for an extended period of time. A 95 % completion was attained from an extended soaking at 160°C and above. The intermediate Tg varied accordingly with the extent of cure. The ultimate Tg from isothermal scanning was found to be 184 $\pm$ 2°C. This is higher than the ultimate Tg observed from dynamic temperature scanning experiments. The reaction of primary amine and epoxide could be favored under isothermal conditions at lower temperatures while that of the secondary amine and epoxide could be favored in dynamic temperature scanning at higher temperatures. This could result in different network structures and, hence, Tg. The averaged heat of reaction from isothermal scanning was 271 J/g of adhesive. This is higher than that measured in dynamic temperature scanning experiments (213 $\pm$ 12 J/g). Again, this shows that the cure of the adhesive under dynamic temperature scanning may result in a different network than obtained under isothermal conditions.

The isothermal data were found to fit the kinetic model proposed by Kamal [3, 30]. Kinetic parameters and apparent activation energies were calculated. The Arrhenius rate constants K_1 and K_2 were found to vary with temperature. The values *m* and *n* are usually temperature independent. However in the entire range of isothermal temperatures reported here, kinetic parameters *m* and *n* did vary with temperature and degree of cure. Less variation was observed at lower temperatures (110 to 140°C).

From dynamic shear rheometry, the gel point was determined to occur at 36 % conversion under isothermal conditions. This is an important parameter during the cure process as it controls the flow property of the adhesive. The adhesive must reach this gel point as soon as possible in a multi-step cure cycle. Otherwise, resin will run out of the assembly to produce a resin poor product. This can be achieved using a ramp rate less than 2°C/min.

To follow the cure kinetics of a multi-step cure cycle, a series of combined ramp and soak experiments was performed. This set of experiments showed that extent of cure in the soak portion of a 2-step cure cycle at intermediate times is not a function of cure history or initial degree of cure. At long times, conversions converge to a common value, irrespective of the heating rate used in the previous ramp segment. It was shown that the cure profile during soaking at an intermediate temperature can be predicted if the initial degree of cure at the start of the soak cycle is known. This was accomplished using 3-dimensional surface-fitting software. Such plots can be used to predict values of a and da/dt for intermediate times and initial degrees of cure at a given soak temperature. This is an empirical model. Building upon previous kinetic studies on epoxy systems, this study has shown that it is possible to predict the degree of cure and rate of cure at any point of a two-step cure cycle of type commonly used in an industrial setting.

REFERENCES

LIST OF REFERENCES

[1] B. Ellis, *Chemistry and Technology of Epoxy Resins*, Blackie Academic and Professional, **1993**, p. 332.

[2] A. R. Meath, *Epoxy Resin Adhesives, in: Handbook of Adhesives*, Van Nostrand Reinhold, **1990**, p. 347-358.

[3] J. M. Barton, *Advances in Polymer Science* **1985**, pp. 111-154.

[4] N. S. Enikolopiyan, *Pure and Applied Chemistry* **1976**, *48*, 317-328.

[5] D. O. Bowen and R. C. Whiteside, Jr, *in: Epoxy Resins*, American Chemical Society, **1968**, p. 48-59.

[6] H. Liu, A. Uhlherr, R. J. Varley and M. K. Bannister, *Journal of Polymer Science: Part A: Polymer Chemistry* **2004**, *42*, 3143-3156.

[7] I. T. Smith, *Polymer* **1961**, *2*, 95-108.

[8] J. Mijovic, A. Fishbain and J. Wijaya, *Macromolecules* **1992**, *25*, 979-985.

[9] L. Shechter, J. Wynstra and R. P. Kurkjy, *Journal of Industrial and Engineering Chemistry* **1956**, *48*, 94-97.

[10] H. J. Flammersheim, *Thermochimica Acta* **1998**, *310*, 153-159.

[11] E. Girard-Reydet, C. C. Riccardi, H. Sautereau and J. P. Pascault, *Macromolecules* **1995**, *28*.

[12] J. Mijovic and J. Wijaya, *Macromolecules* **1994**, *27*, 7589-7600.

[13] K. C. Cole, *Macromolecules* **1991**, *24*, 3093-3097.

[14] K. C. Cole, J. J. Hechler and D. Noel, *Macromolecules* **1991**, *24*, 3098-3110.

[15] Y. Tanaka and T. F. Mika, *Epoxide curing reactions, in: Epoxy Resins*, Marcel Dekker, NY New York, **1973**, p. 135-238.

[16] J. J. King and J. P. Bill, *in: Epoxy Resin Chemistry*, American Chemical Society, **1979**, p. 225-257.

[17] M. K. Um, I. M. Daniel and B. S. Hwang, *Composite Science and Technology* **2002**, *662*, 29-40.

[18] K. Horie, H. Hiura, M. Sawada, I. Mita and H. Kambe, *Journal of Applied Polymer Science: Part A-1* **1970**, *8*, 1357-1372.

[19] I. P. Aspin, I. Hamerton, B. J. Howlin, J. R. Jones and M. J. Parker, *Surface Coatings International* **1998**, *81*, 68-71.

[20] J. Wei, M. Hawley and M. Demeuse, *Polymer Engineering and Science* **1995**, *35*, 461-470.

[21] P. L. Chiou and A. Letton, *Ceramic Transactions* **1991**, *19*, 59-65.

[22] S. Swier and B. v. Mele, *Thermochimica Acta* **2004**, *411*, 149-169.

[23] G. V. Kozlov, A. A. Bejev and Y. S. Lipatov, *Journal of Applied Polymer Science* **2004**, *92*, 2558-2568.

[24] N. A. St John and G. A. George, *Progress in Poymer Science* **1994**, *19*, 755-795.

[25] S. R. White, P. T. Mather and M. J. Smith, *Polymer Engineering and Science* **2002**, *42*, 51-67.

[26] W. I. Lee, A. C. Loos and G. S. Springer, *Journal of Composite Materials* **1982**, *16*, 510-520.

[27] M. Opalicki, J. M. Kenny and L. Nicolais, *Journal of Applied Polymer Science* **1996**, *61*, 1025-1037.

[28] D. O'brien, *Polymer Engineering and Science* **2003**, *43*, 863-874.

[29] S. Lee, M. Chiu and H. Lin, *Polymer Engineering and Science* **1992**, *32*, 1037-1046.

[30] M. R. Kamal and S. Sourour, *Polymer Engineering and Science* **1973**, *13*, 59-64.

[31] M. R. Dusi, W. I. Lee, P. R. Ciriscioli and G. S. Springer, *Journal of Composite Materials* **1987**, *21*, 243-261.

[32] J. M. Kenny, A. Trivisiano, M. E. Frigione and L. Nicolais, *Thermochimica Acta* **1992**, *199*, 213-227.

[33] S. W. Kim and J. D. Nam, *Journal of Industrial and Engineering Chemistry* **2002**, *8*, 212-217.

[34] D. J. T. Hill, G. A. George and D. G. Rogers, *Polymers for Advanced Technologies* **2002**, *13*, 353-362.

[35] S. R. White and H. T. Han, *Journal of Composite Materials* **1992**, *26*, 2402-2422.

[36] A. Yousefi, P. G. Lafleur and R. Gauvin, *Polymer Composites* **1997**, *18*, 157-168.

[37] D. D. Shin and H. T. Hahn, *Composites Part A* **2000**, *31*, 991-999.

[38] R. Seifi and M. Hojjati, *Journal of Composite Materials* **2005**, *39*, 1027-1039.

[39] M. A. Stone, B. K. Fink, T. A. Bogetti and J. W. Gillespie, Jr, *Polymer Engineering and Science* **2000**, *40*, 2489-2497.

[40] C. D. Han and K. W. Lem, *Journal of Applied Polymer Science* **1983**, *28*, 3155-3183.

[41] D. A. Shimp, *Epoxy Adhesives, in: Epoxy Resin Technology*, Interscience Publishers, **1968**, p. 159-183.

[42] M. J. Sumner in *High Performance Materials Containing Nitrile Groups, Vol. PhD* Virginia Polytechnic Institute and State University, **2003**, p. 252.

[43] J. M. Barton, *British Polymer Journal* **1986**, *18*, 37-43.

[44] J. M. Barton, *British Polymer Journal* **1986**, *18*, 44-50.

[45] J. M. Barton and D. C. L. Greenfield, *British Polymer Journal* **1986**, *18*, 196-200.

[46] H. Lee and K. Neville, *Epoxy Resins, Their Applications and Technology*, McGraw-Hill Company, Inc, **1957**, p. 305.

[47] H. Lee and K. Neville, *Handbook of Epoxy Resins*, McGraw-Hill Book Company, **1967**.

[48] J. M. Kenny and A. Trivisano, *Polymer Engineering and Science* **1991**, *31*, 1426-1433.

[49] D. Rosu, C. N. Casvacal, F. Mustata and C. Ciobanu, *Thermochimica Acta* **2002**, *383*, 119-127.

[50] J. M. Kenny, A. Trivisano and L. A. Berglund, *SAMPE Journal* **1991**, *27*, 39-45.

[51] A. D. Rogers and P. Lee-Sullivan, *Polymer Engineering and Science* **2003**, *43*, 14-25.

[52] J. Kim, T. J. Moon and J. R. Howell, *Journal of Composite Materials* **2002**, *36*, 2479-2498.

[53] J. M. Barton, I. Hamerton, B. J. Howlin, J. R. Jones and S. Liu, *Polymer* **1998**, *39*, 1929-1937.

[54] X. Buch and M. E. R. Shanahan, *Polymer Degradation and Stability* **2000**, *68*, 403-411.

[55] A. Schiraldi, *Thermochimica Acta* **1985**, *96*, 283-297.

[56] V. Nigam, D. K. Setua and G. N. Mathur, *Polymer Engineering and Science* **1999**, *39*, 1425-1432.

[57] E. Pezzati, P. Baldini and A. Schiraldi, *Thermochimica Acta* **1987**, *122*, 29-35.

[58] T. S. Chung, *Journal of Applied Polymer Science* **1984**, *29*, 4403-4406.

[59] V. Nigam, D. K. Setua and G. N. Mathur, *Rubber Chemistry and Technology* **2000**, *73*, 830-838.

[60] S. V. Levchik, G. Camino, M. P. Luda and L. Costa, *Thermochimica Acta* **1995**, *260*, 217-228.

[61] C. A. Harrison in *Spectroscopic investigation into the thermal degradation of some aromatic amine cured model epoxy resin systems*, *Vol. MS* Wichita State University, Wichita, KS, **2004**, p. 121.

[62] L. H. Sperling, *Introduction to Physical Polymer Science*, John Wiley and Sons, Inc, **1992**, p. 594.

[63] A. Apicella, P. Masi and L. Nicolais, *Rheologica Acta* **1984**, *23*, 291-296.

APPENDICES

APPENDIX A

Calculation of the Apparent Energy of Activation of Cure

Plots of ln(da/dt) versus 1/T for the film adhesive from dynamic temperature experiments. Each plot is for a fixed value of a. Apparent activation energies are calculated from the slope of the graphs.

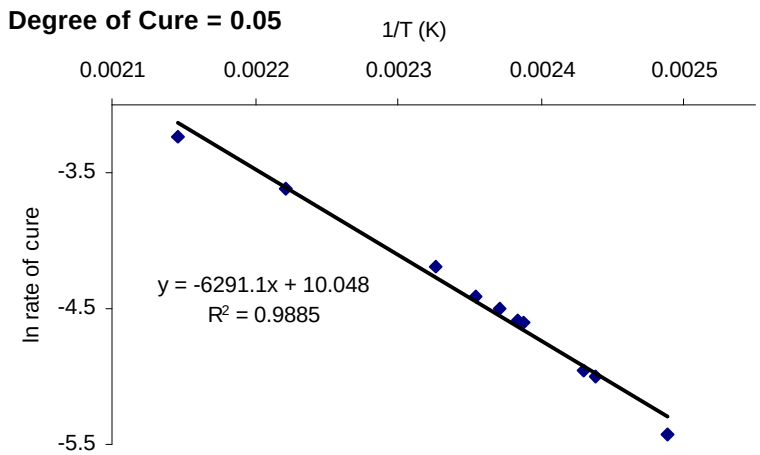

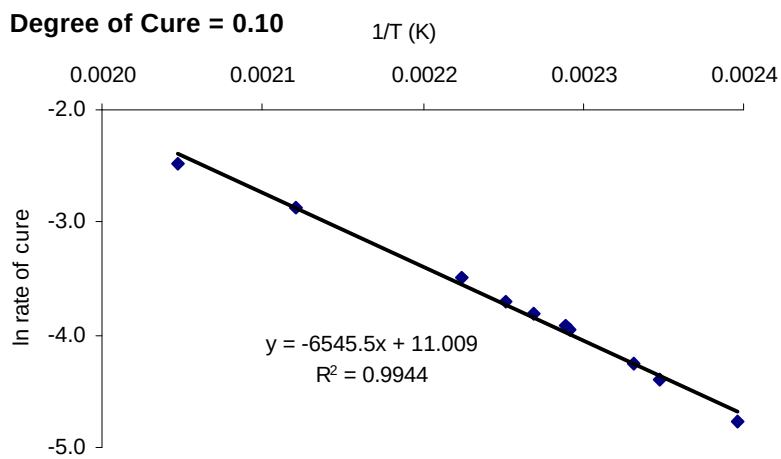

APPENDIX A *(continued)*

Calculation of the Apparent Energy of Activation of Cure

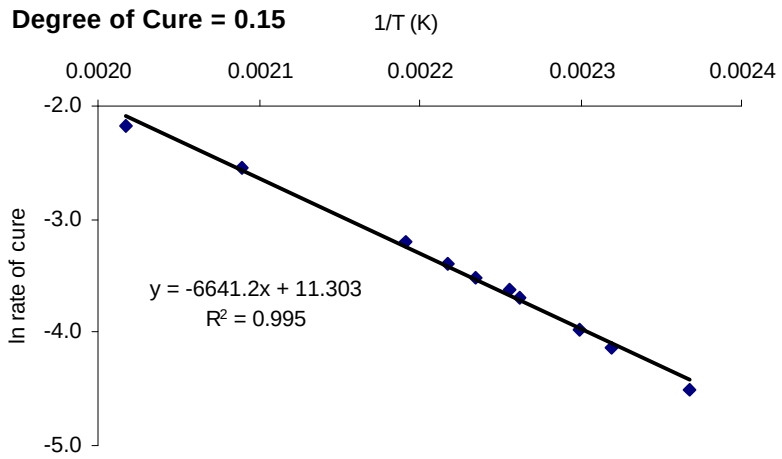

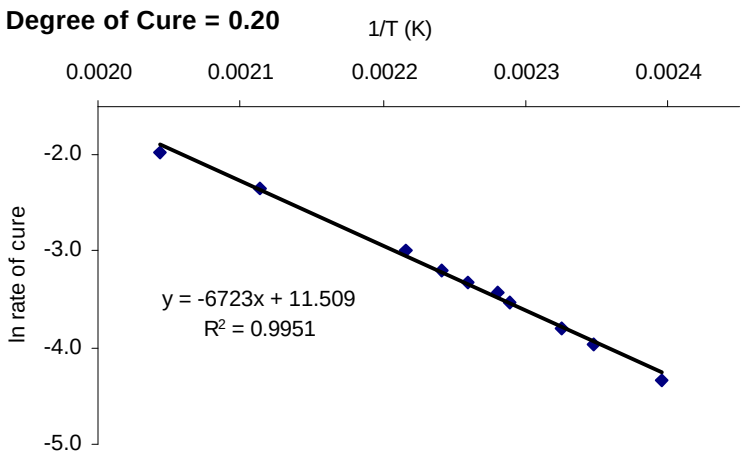

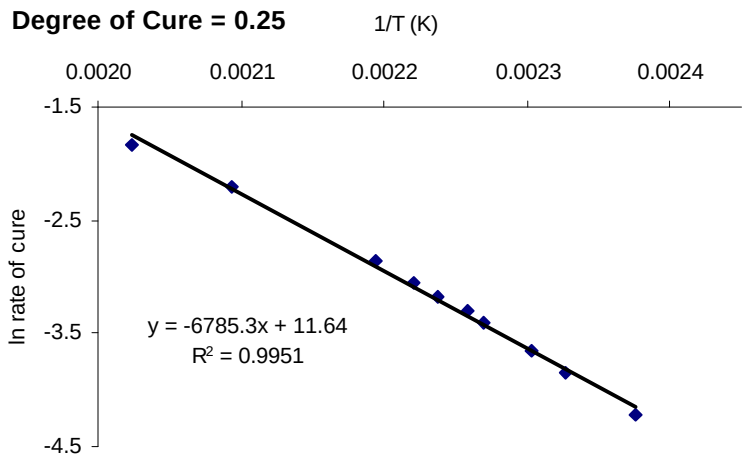

APPENDIX A *(continued)*

Calculation of the Apparent Energy of Activation of Cure

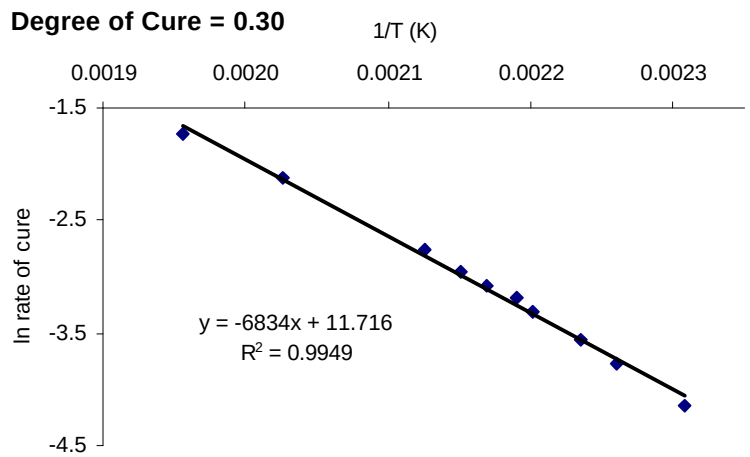

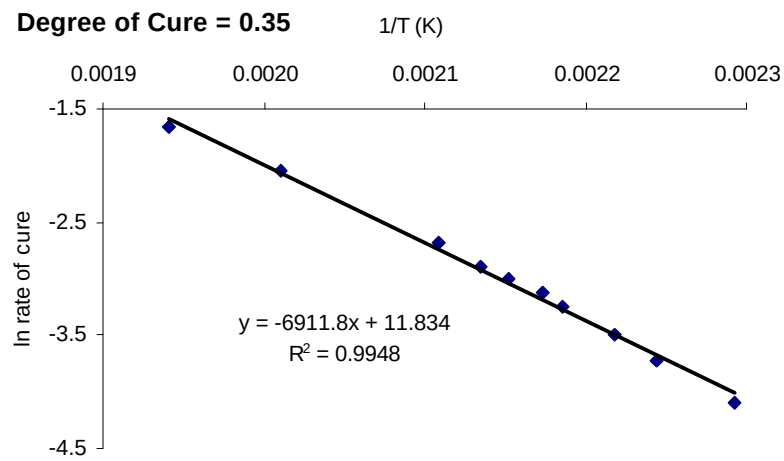

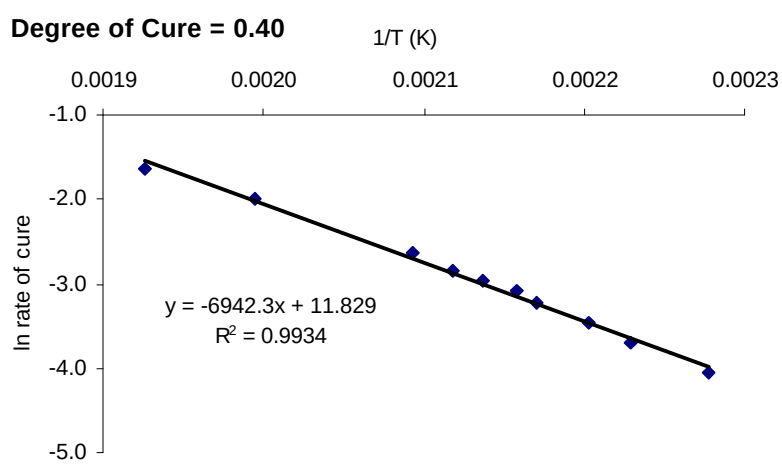

APPENDIX A *(continued)*

Calculation of the Apparent Energy of Activation of Cure

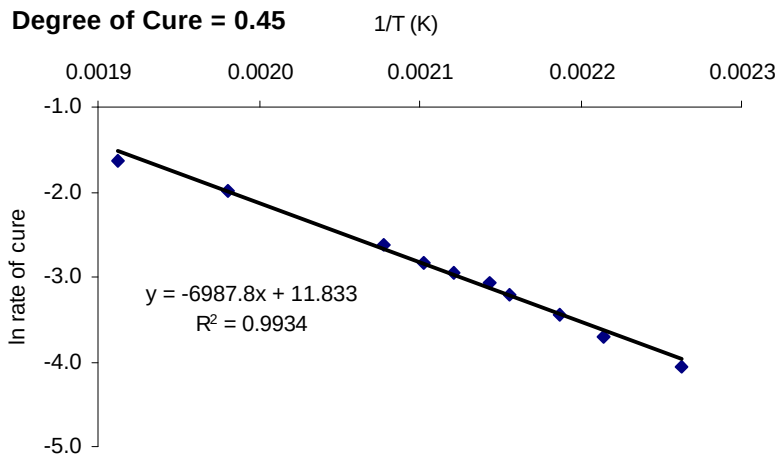

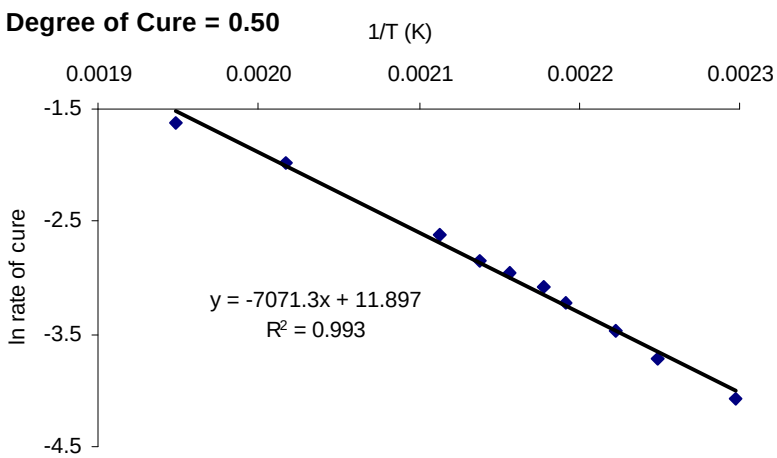

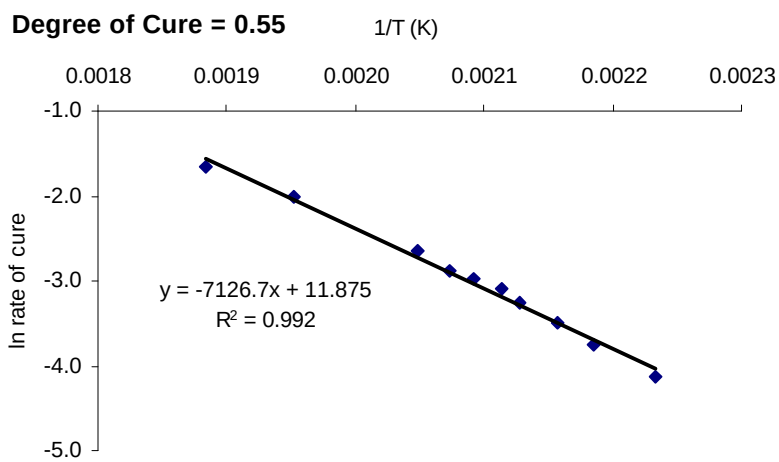

APPENDIX A *(continued)*

Calculation of the Apparent Energy of Activation of Cure

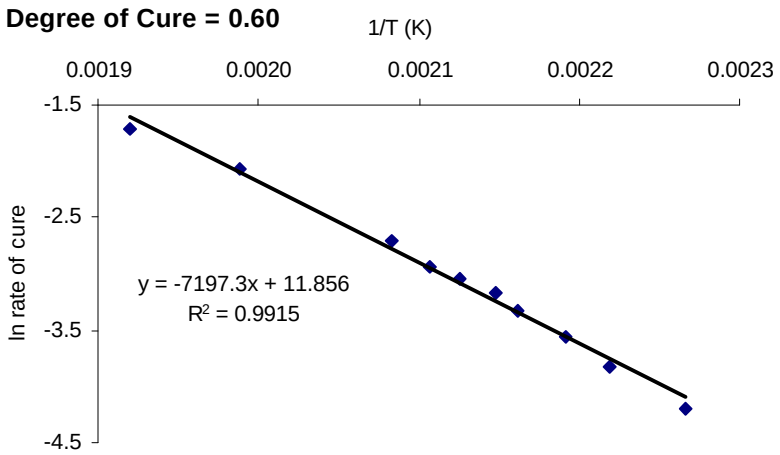

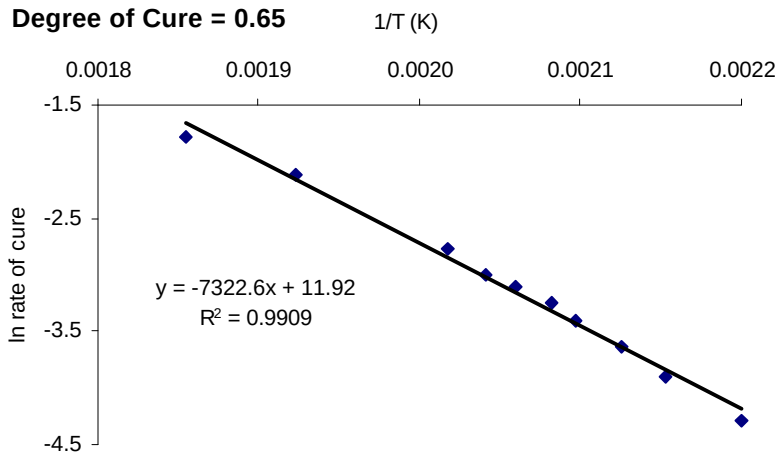

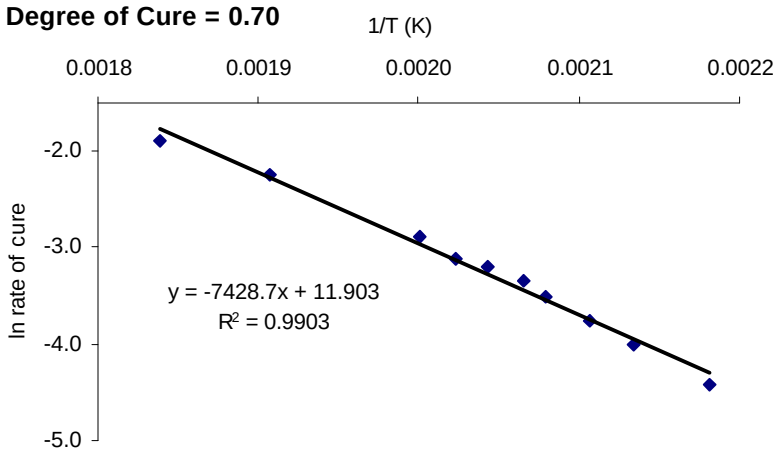

APPENDIX A *(continued)*

Calculation of the Apparent Energy of Activation of Cure

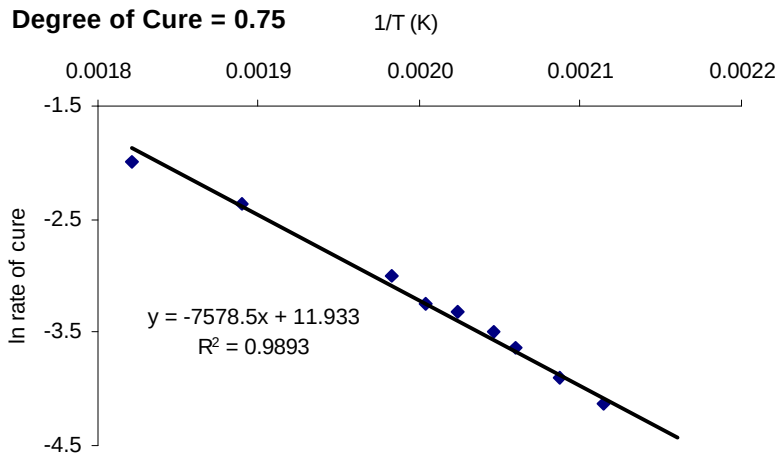

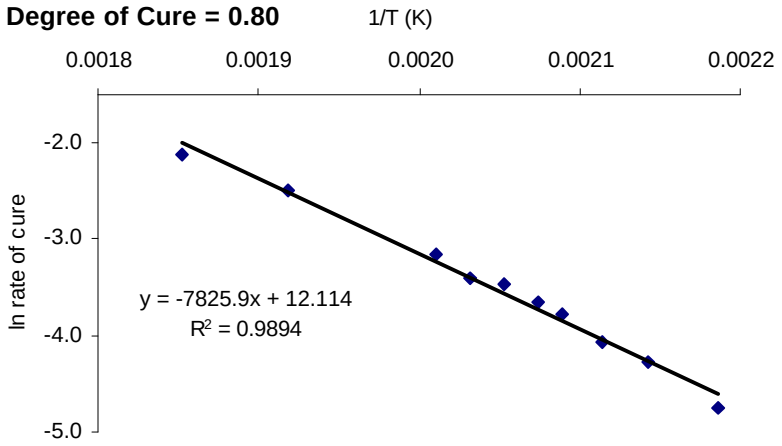

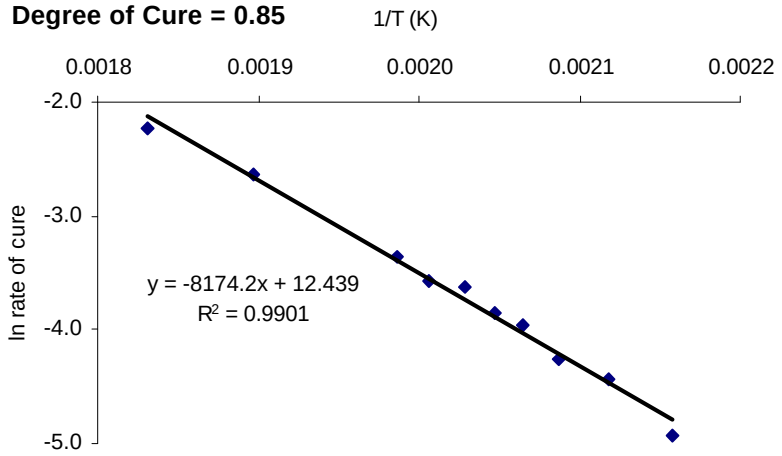

APPENDIX A *(continued)*

Calculation of the Apparent Energy of Activation of Cure

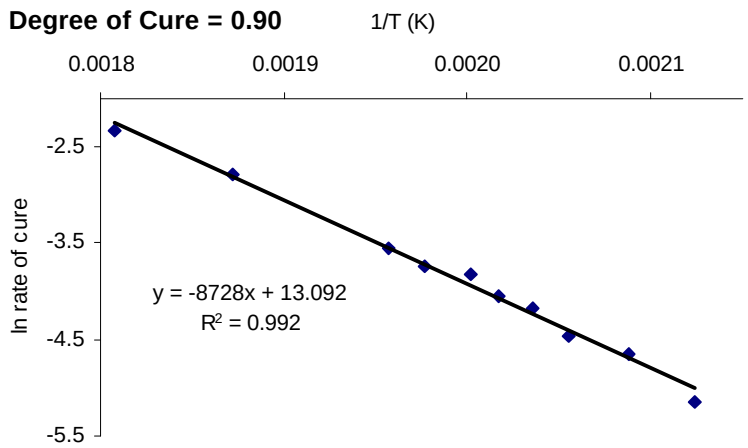

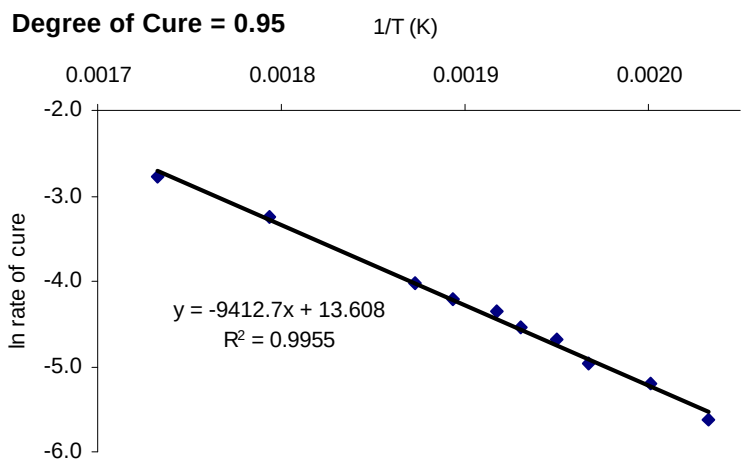

APPENDIX B

2D plot of the degree of cure (α) versus time for the film adhesive cured under isothermal conditions at 140 °C after a slow ramp to that temperature

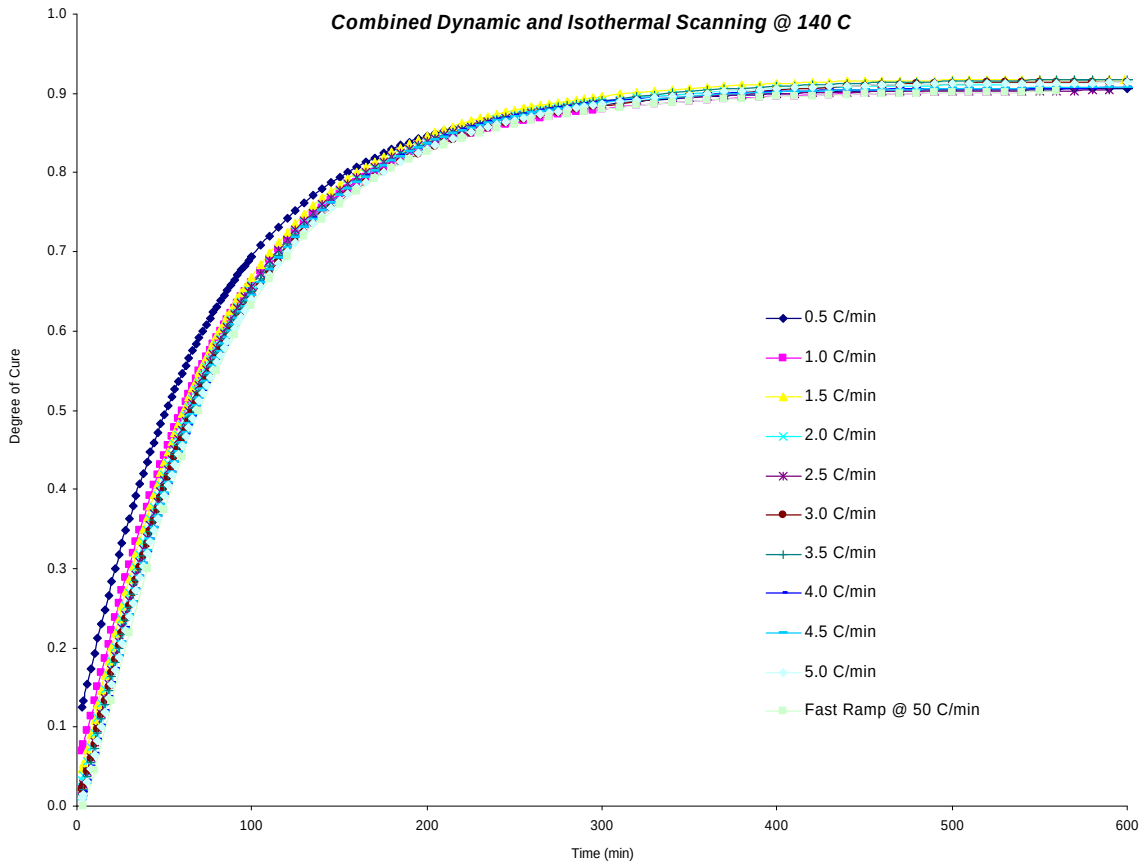

APPENDIX B *(continued)*

2D plot of the degree of cure (α) versus time for the film adhesive cured under isothermal conditions at 150 °C after a slow ramp to that temperature

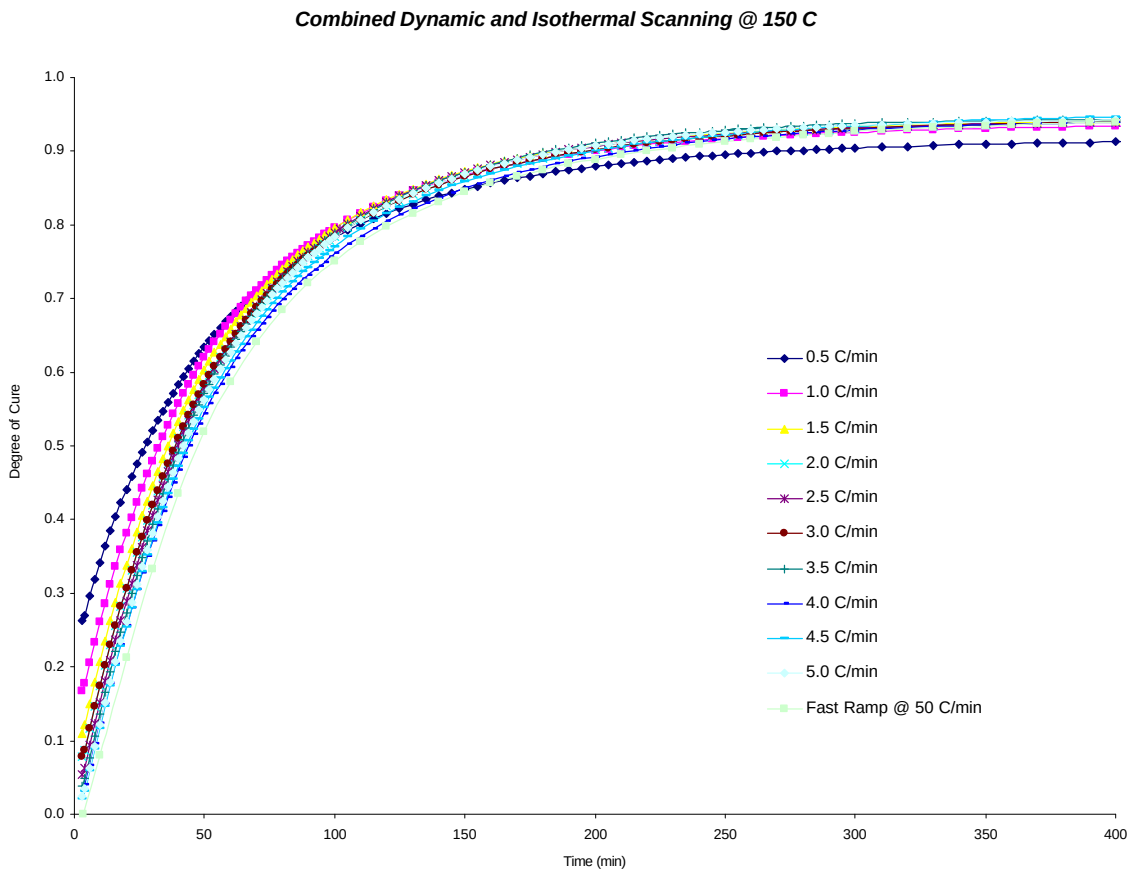

APPENDIX B *(continued)*

2D plot of the degree of cure (α) versus time for the film adhesive cured under isothermal conditions at 155 °C after a slow ramp to that temperature

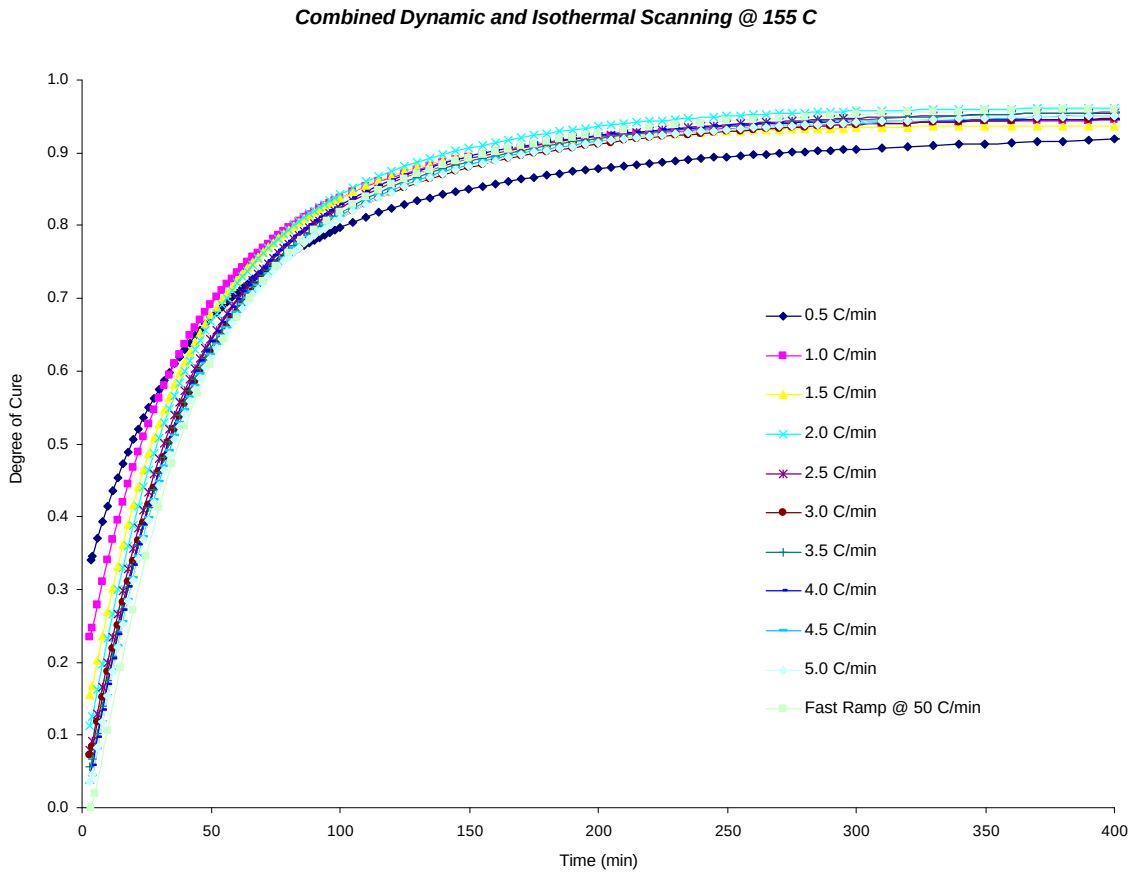

APPENDIX B *(continued)*

2D plot of the degree of cure (α) versus time for the film adhesive cured under isothermal conditions at 160 °C after a slow ramp to that temperature

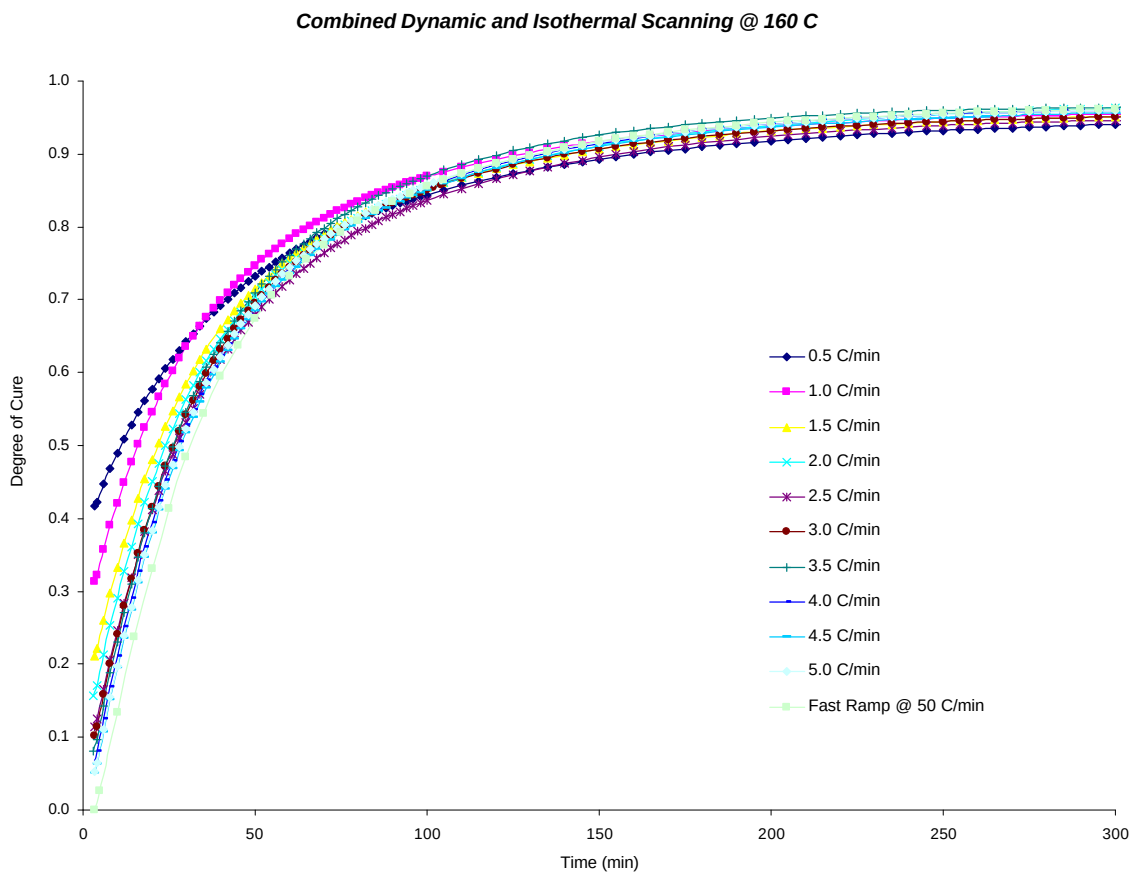

APPENDIX B *(continued)*

2D plot of the degree of cure (α) versus time for the film adhesive cured under isothermal conditions at 165 °C after a slow ramp to that temperature

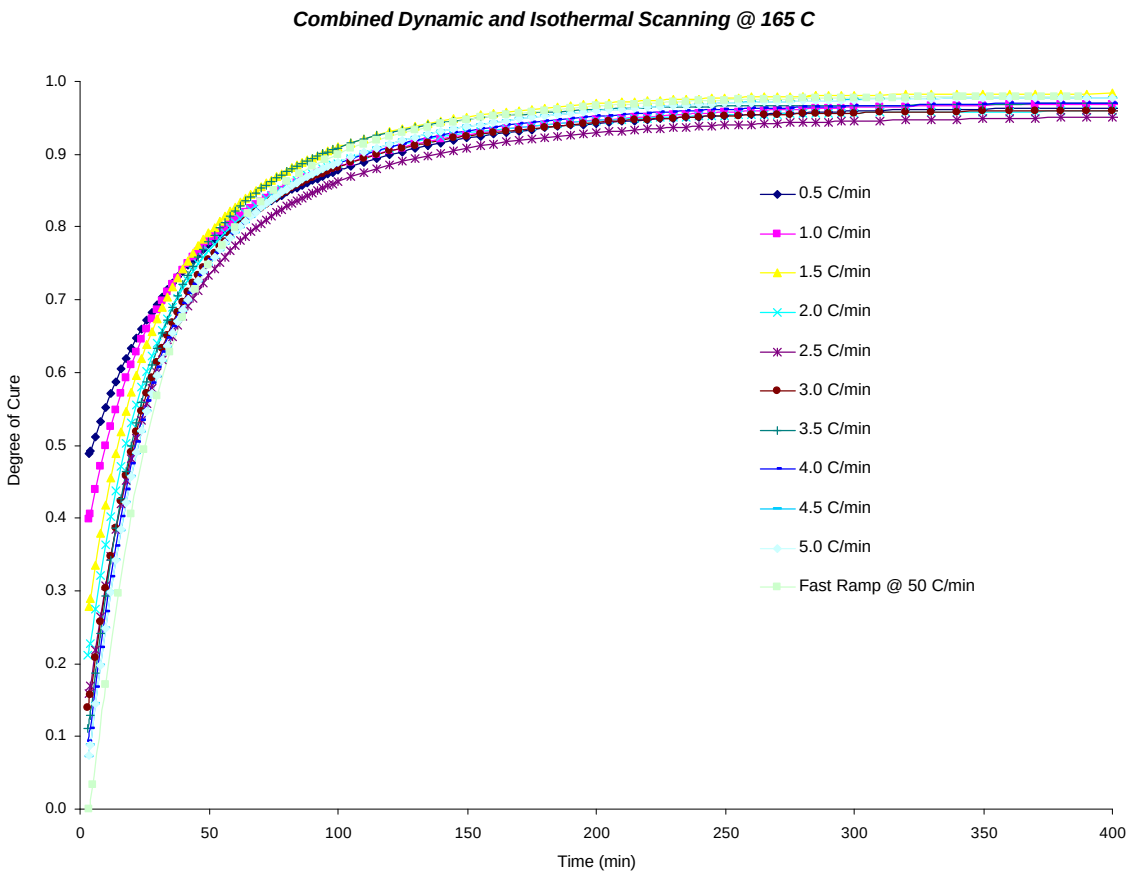

APPENDIX B *(continued)*

2D plot of the degree of cure (α) versus time for the film adhesive cured under isothermal conditions at 170 °C after a slow ramp to that temperature

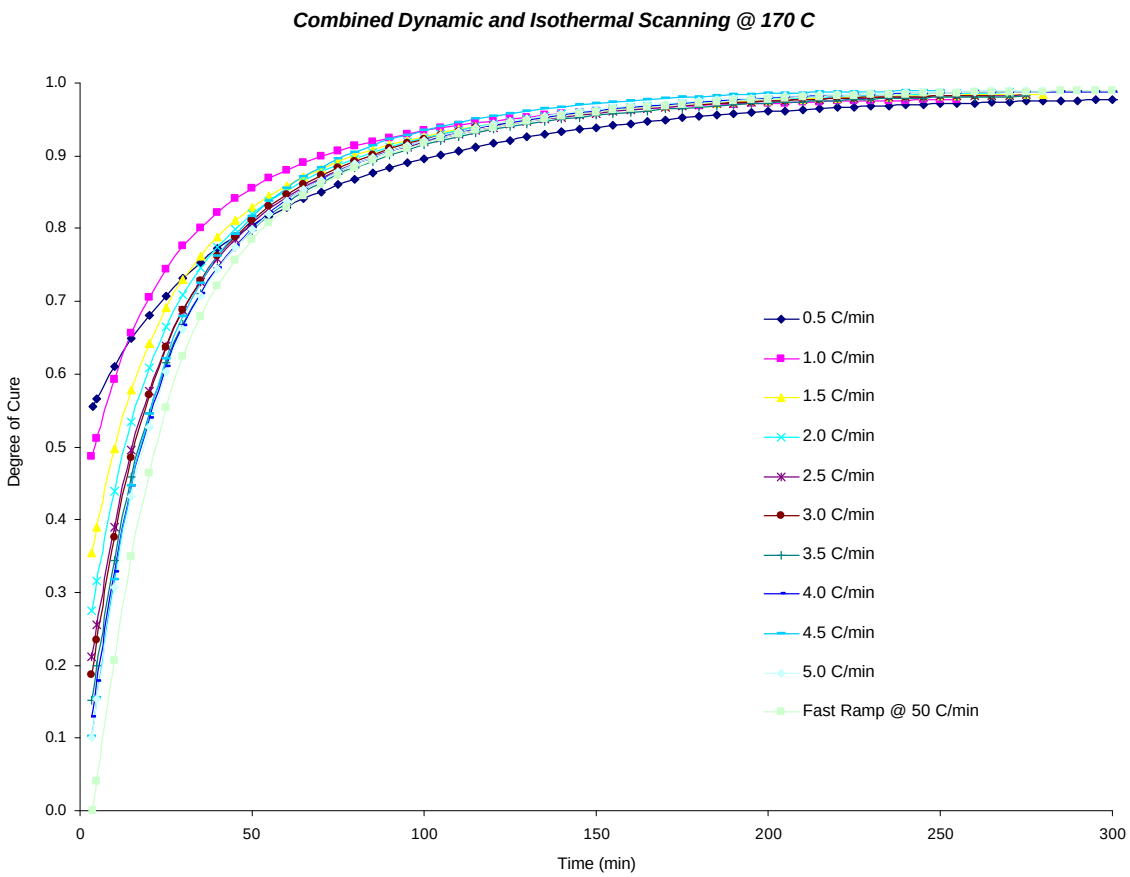

APPENDIX B *(continued)*

2D plot of the degree of cure (α) versus time for the film adhesive cured under isothermal conditions at 175 °C after a slow ramp to that temperature

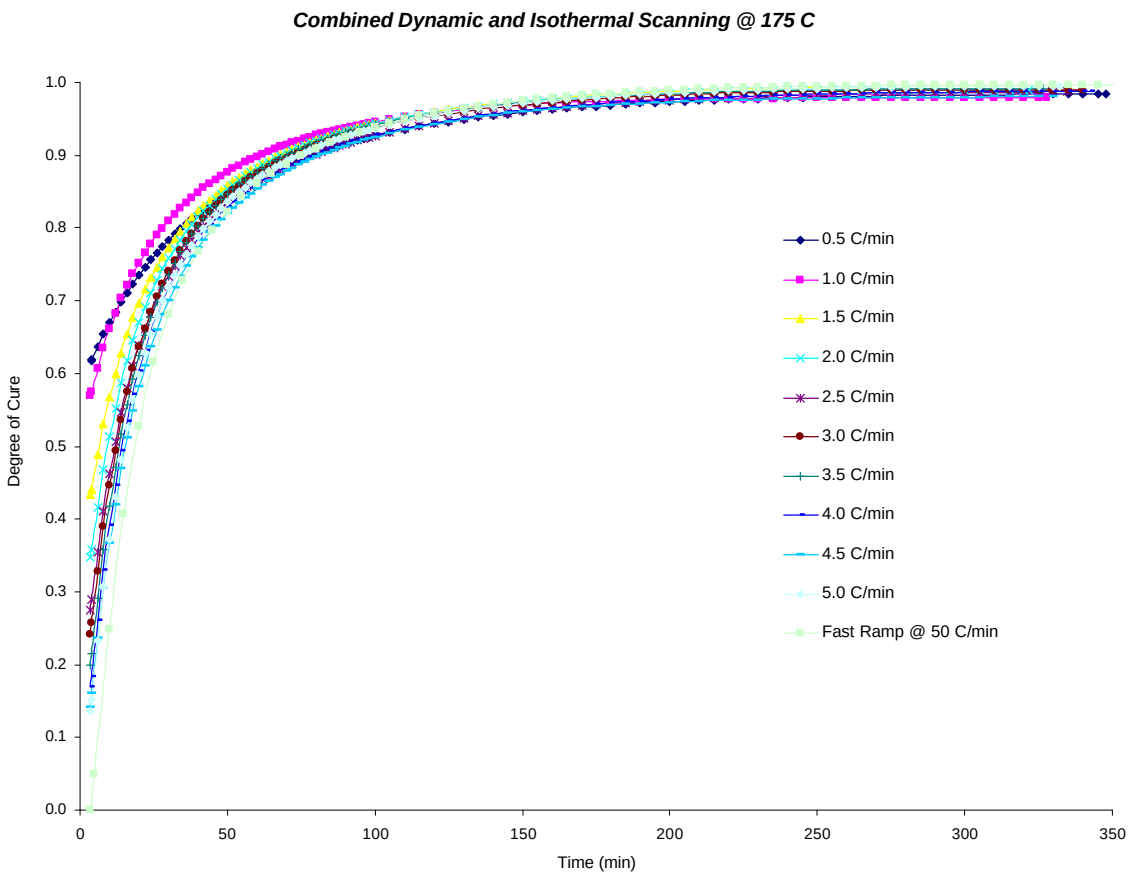

APPENDIX B *(continued)*

2D plot of the degree of cure (α) versus time for the film adhesive cured under isothermal conditions at 180 °C after a slow ramp to that temperature

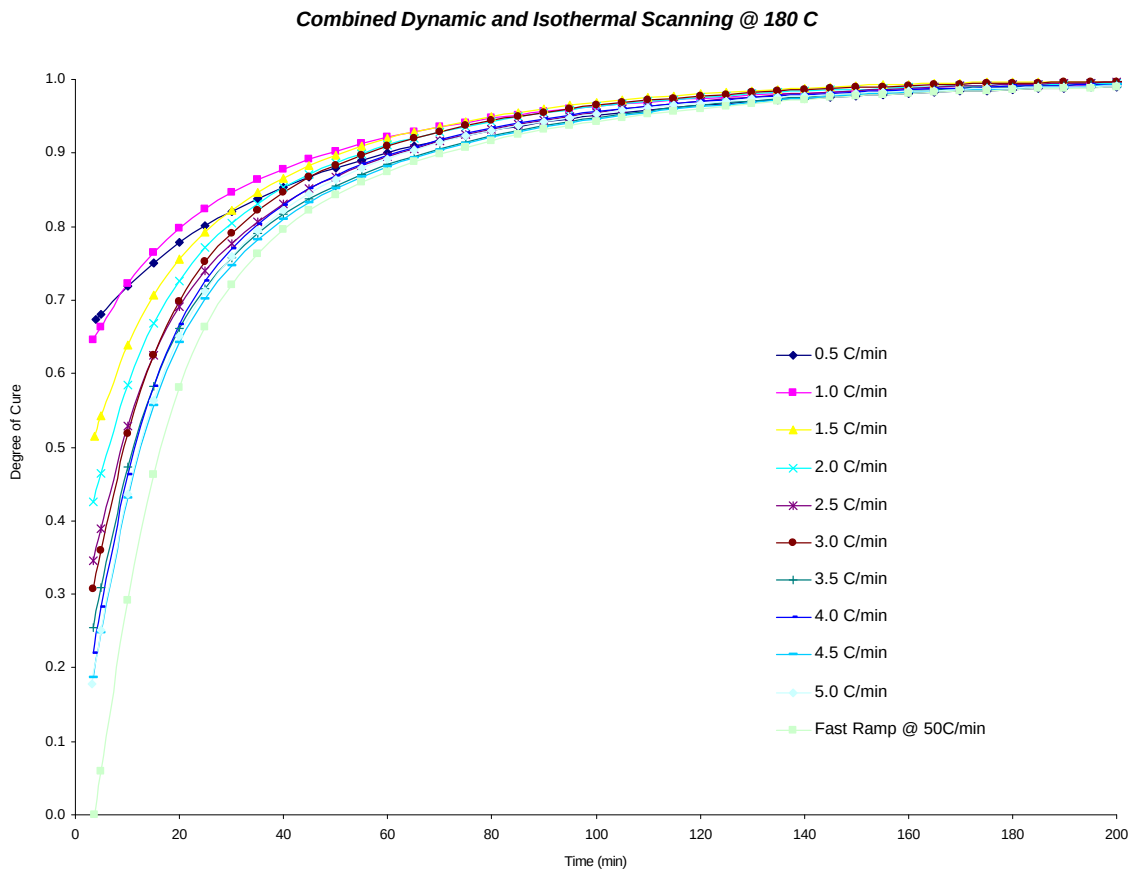

APPENDIX C

3D plot of the degree of cure (α) versus time and initial degree of cure for the film adhesive cured under isothermal conditions at 140 °C and 150 °C after a slow ramp to that temperature (*initial degree of cure from step 1 of the combined ramp and soak experiment)*

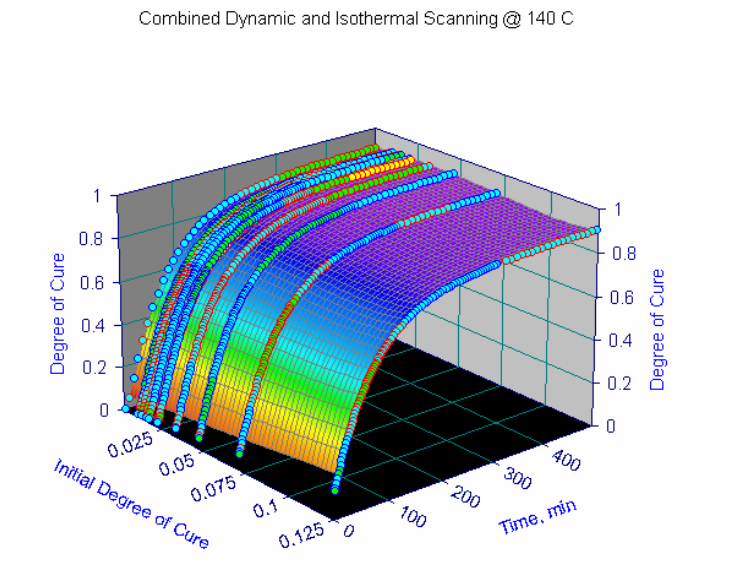

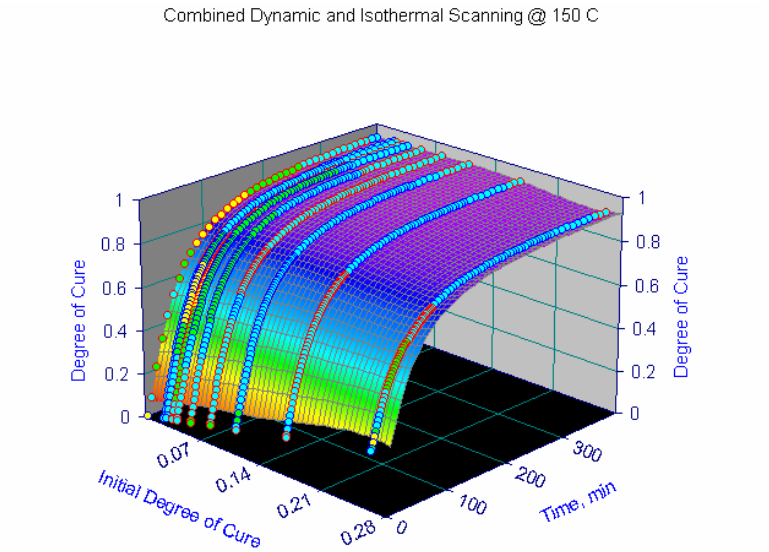

APPENDIX C *(continued)*

3D plot of the degree of cure (α) versus time and initial degree of cure for the film adhesive cured under isothermal conditions at 155 °C and 160 °C after a slow ramp to that temperature (*initial degree of cure from step 1 of the combined ramp and soak experiment)*

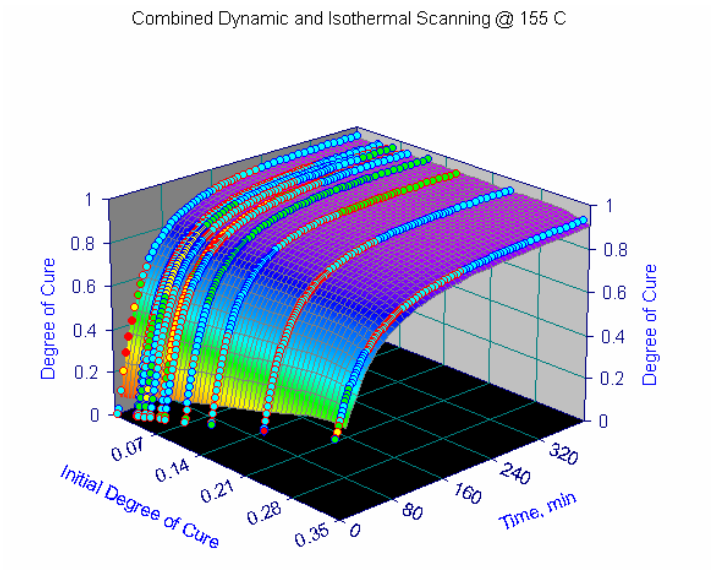

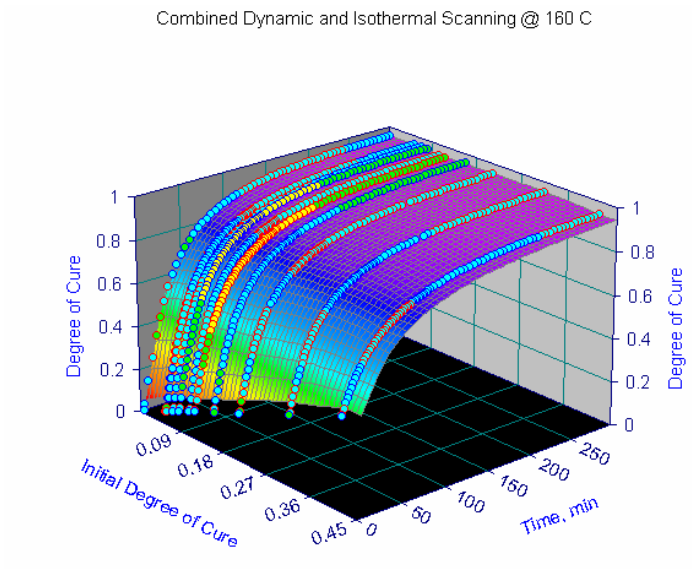

APPENDIX C *(continued)*

3D plot of the degree of cure (α) versus time and initial degree of cure for the film adhesive cured under isothermal conditions at 165 °C and 170 °C after a slow ramp to that temperature (*initial degree of cure from step 1 of the combined ramp and soak experiment)*

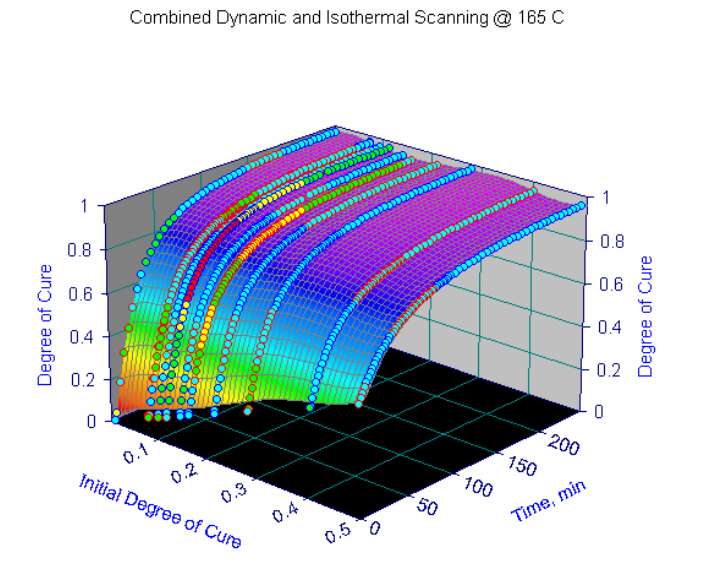

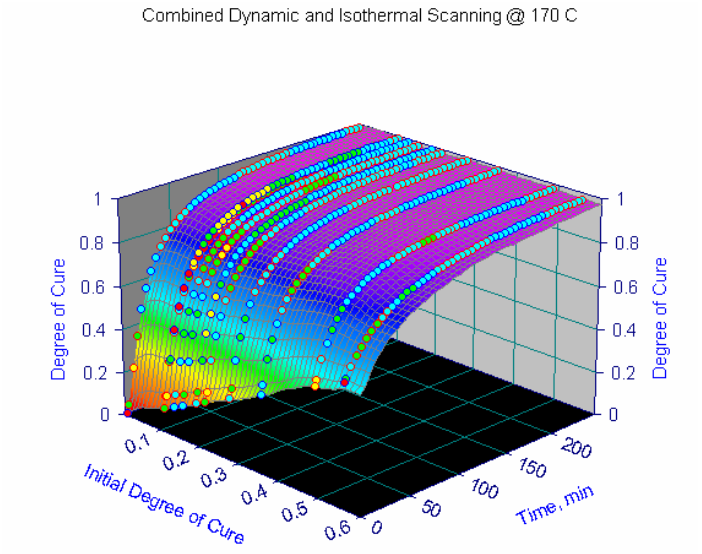

APPENDIX C *(continued)*

3D plot of the degree of cure (α) versus time and initial degree of cure for the film adhesive cured under isothermal conditions at 175 °C and 180 °C after a slow ramp to that temperature (*initial degree of cure from step 1 of the combined ramp and soak experiment)*

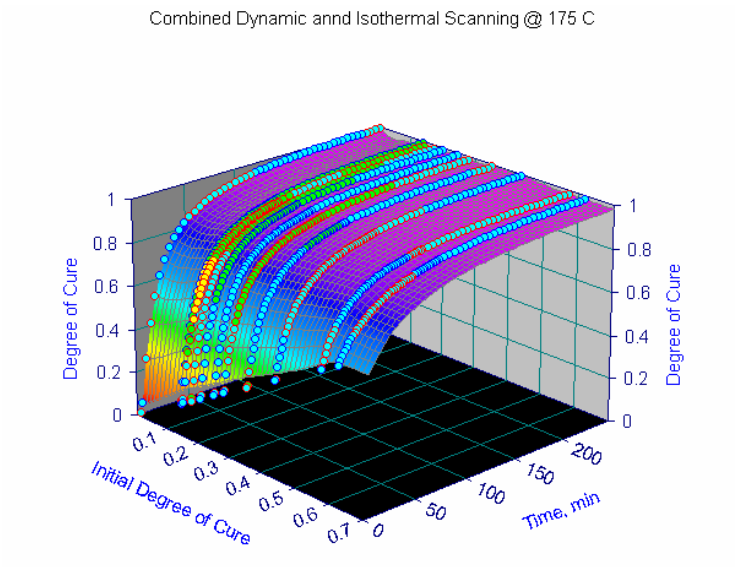

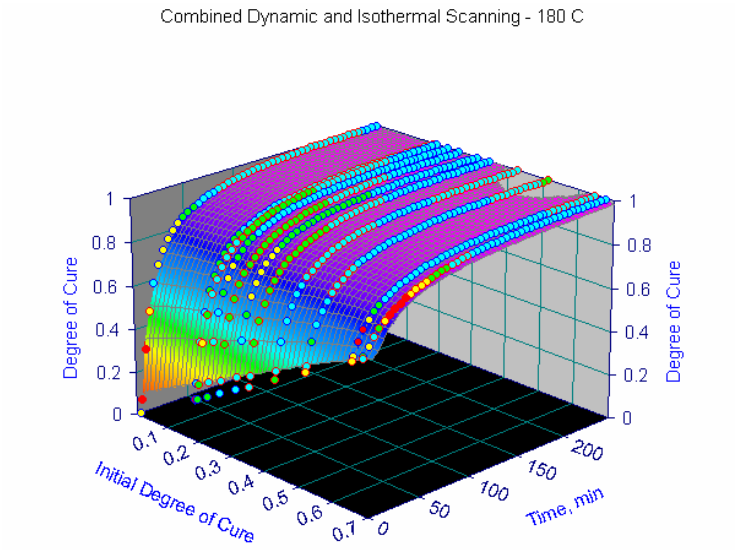

APPENDIX D

2D plot of the rate of cure versus time for the film adhesive cured under isothermal conditions at 140 °C after a slow ramp to that temperature

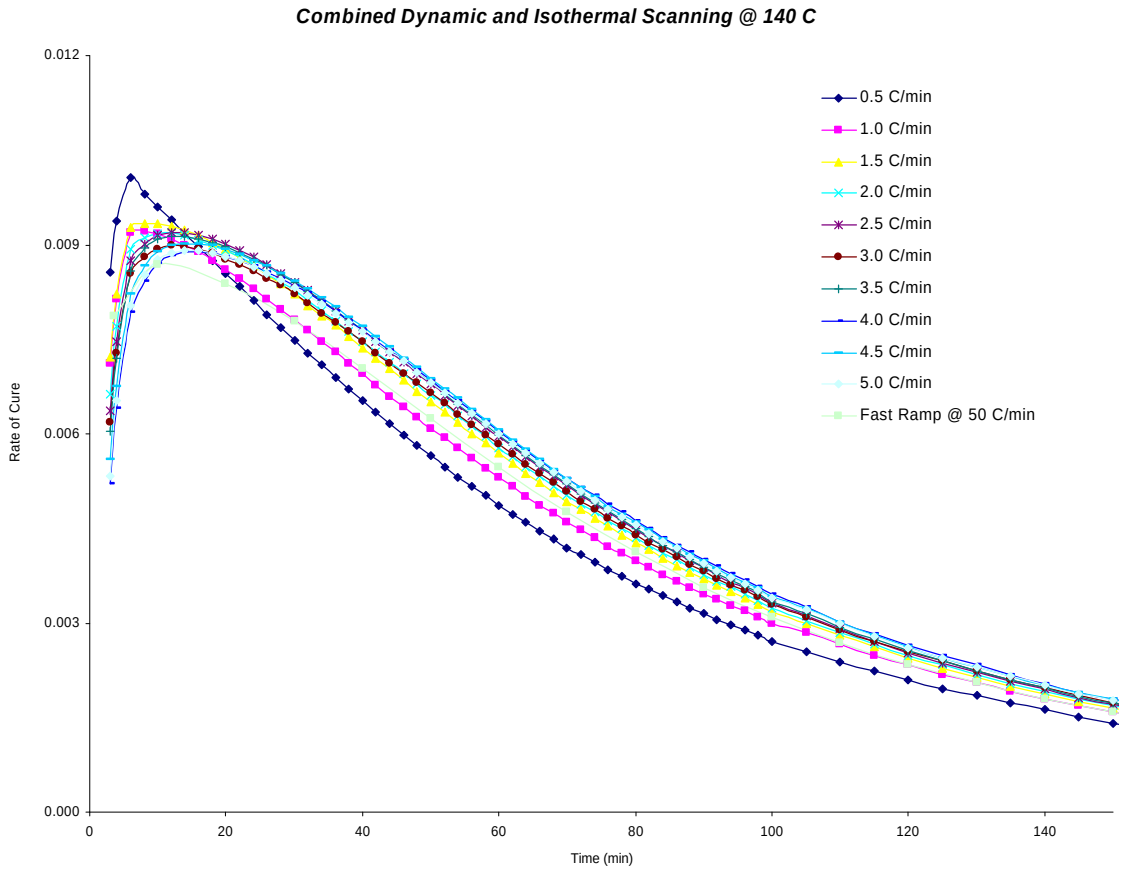

APPENDIX D *(continued)*

2D plot of the rate of cure versus time for the film adhesive cured under isothermal conditions at 150 °C after a slow ramp to that temperature

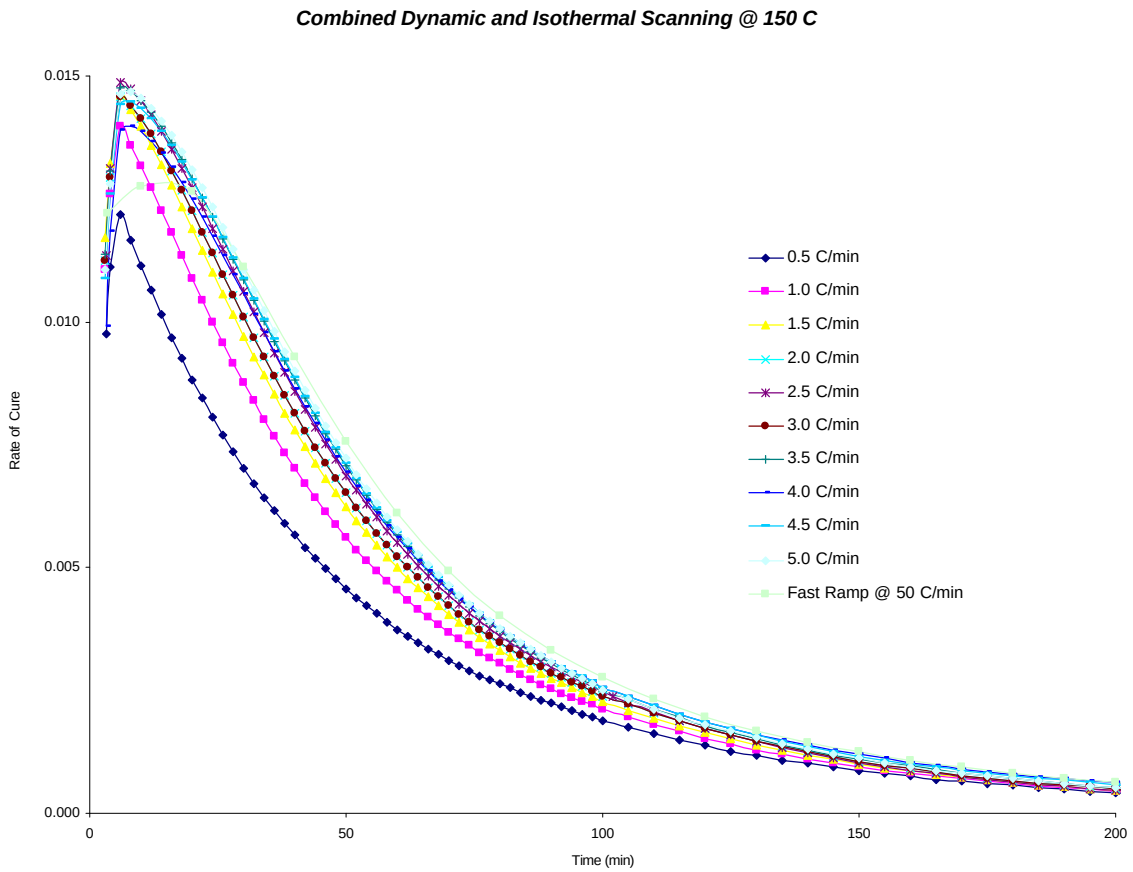

APPENDIX D *(continued)*

2D plot of the rate of cure versus time for the film adhesive cured under isothermal conditions at 155 °C after a slow ramp to that temperature

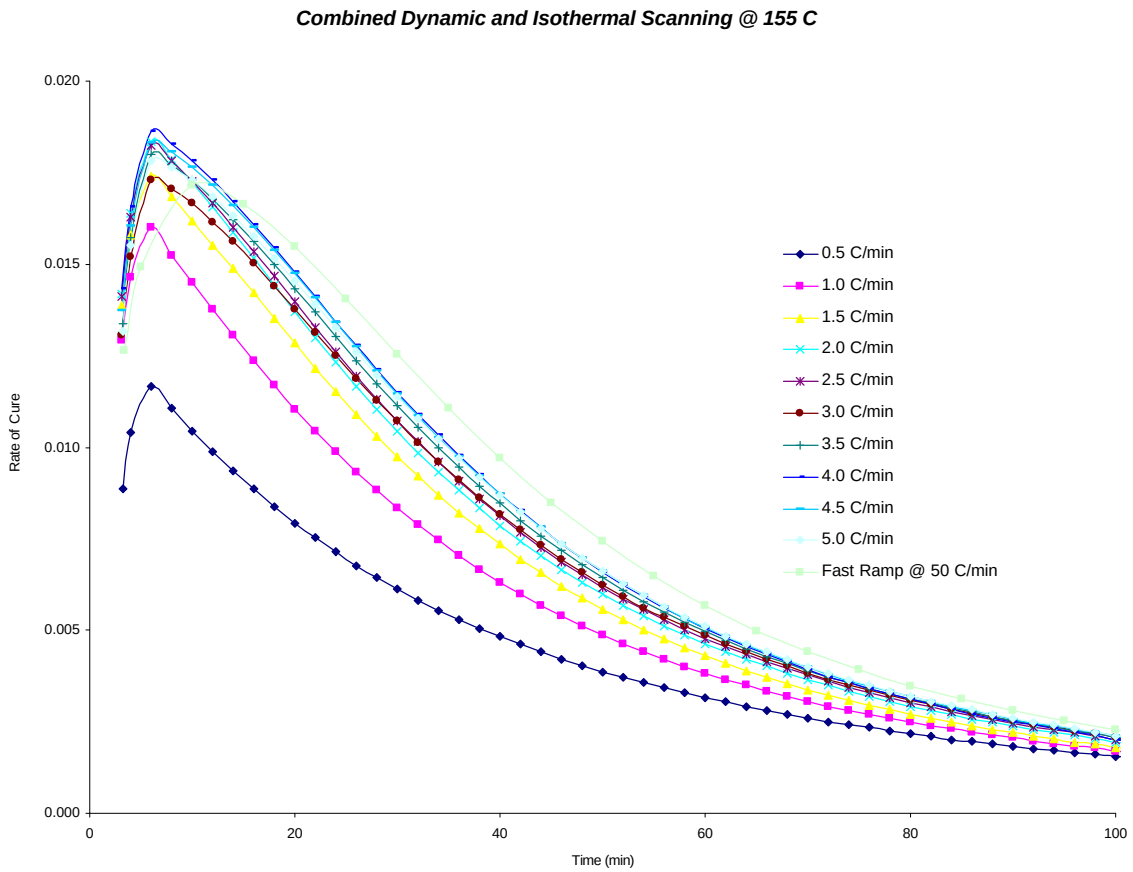

APPENDIX D *(continued)*

2D plot of the rate of cure versus time for the film adhesive cured under isothermal conditions at 160 °C after a slow ramp to that temperature

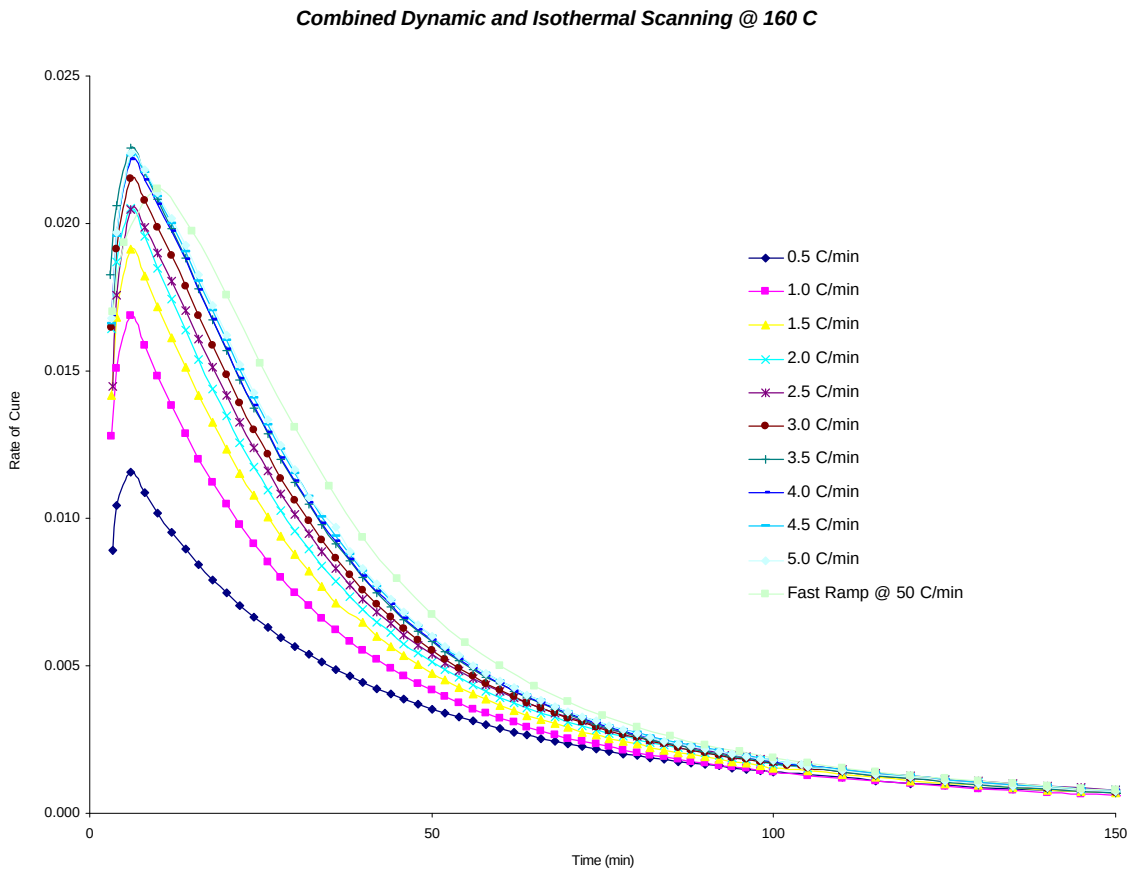

APPENDIX D *(continued)*

2D plot of the rate of cure versus time for the film adhesive cured under isothermal conditions at 165 °C after a slow ramp to that temperature

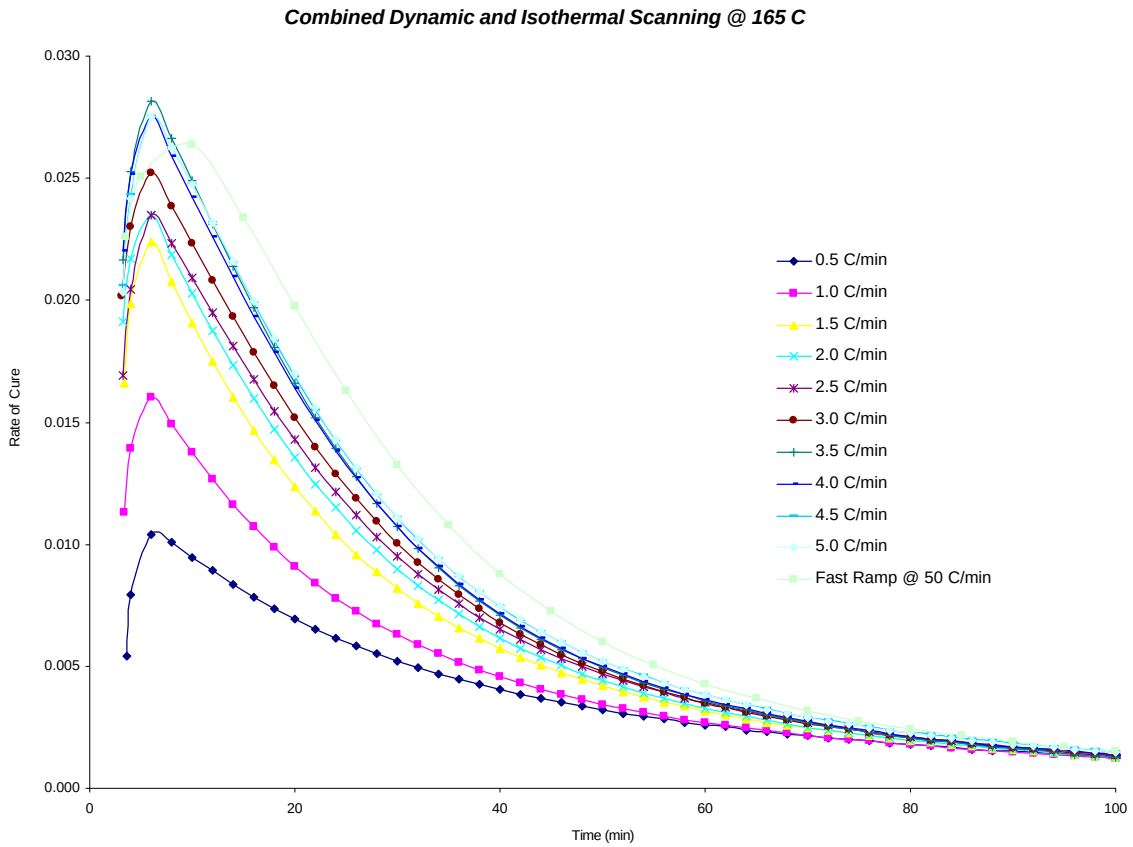

APPENDIX D *(continued)*

2D plot of the rate of cure versus time for the film adhesive cured under isothermal conditions at 170 °C after a slow ramp to that temperature

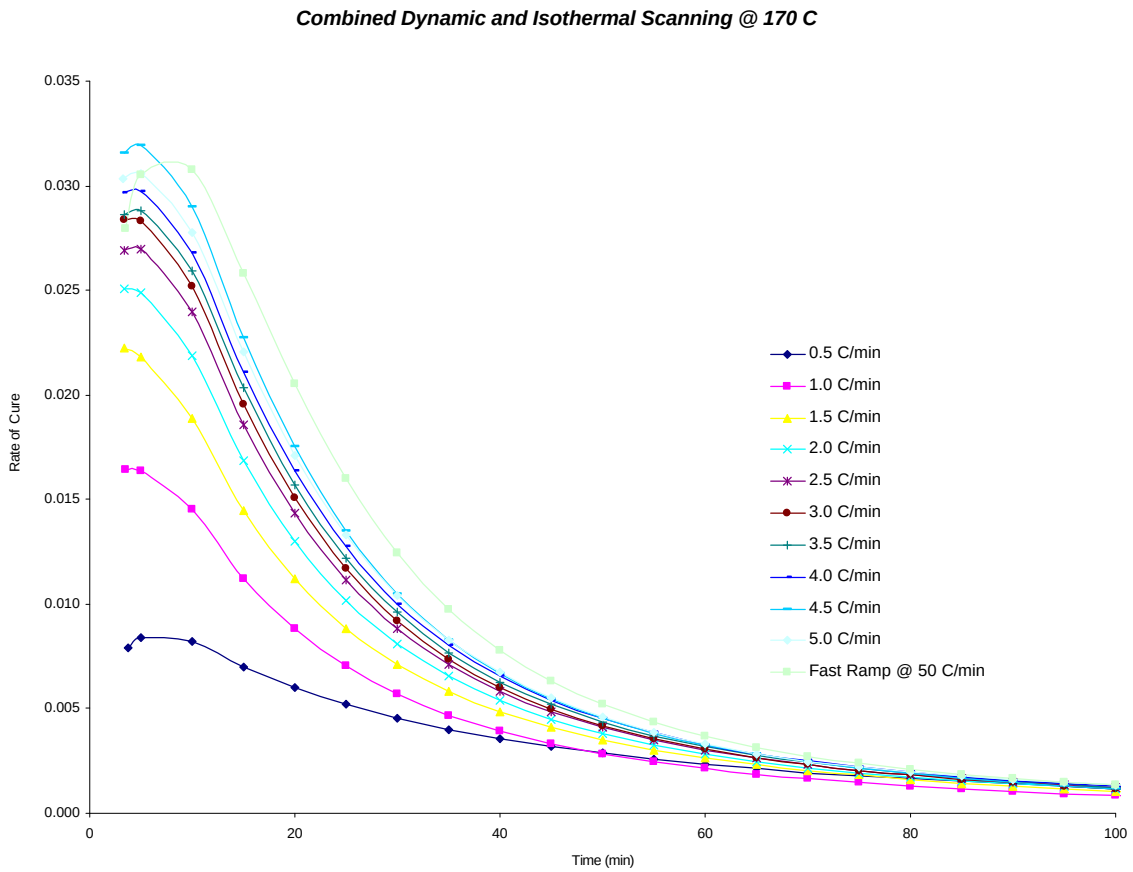

APPENDIX D *(continued)*

2D plot of the rate of cure versus time for the film adhesive cured under isothermal conditions at 175 °C after a slow ramp to that temperature

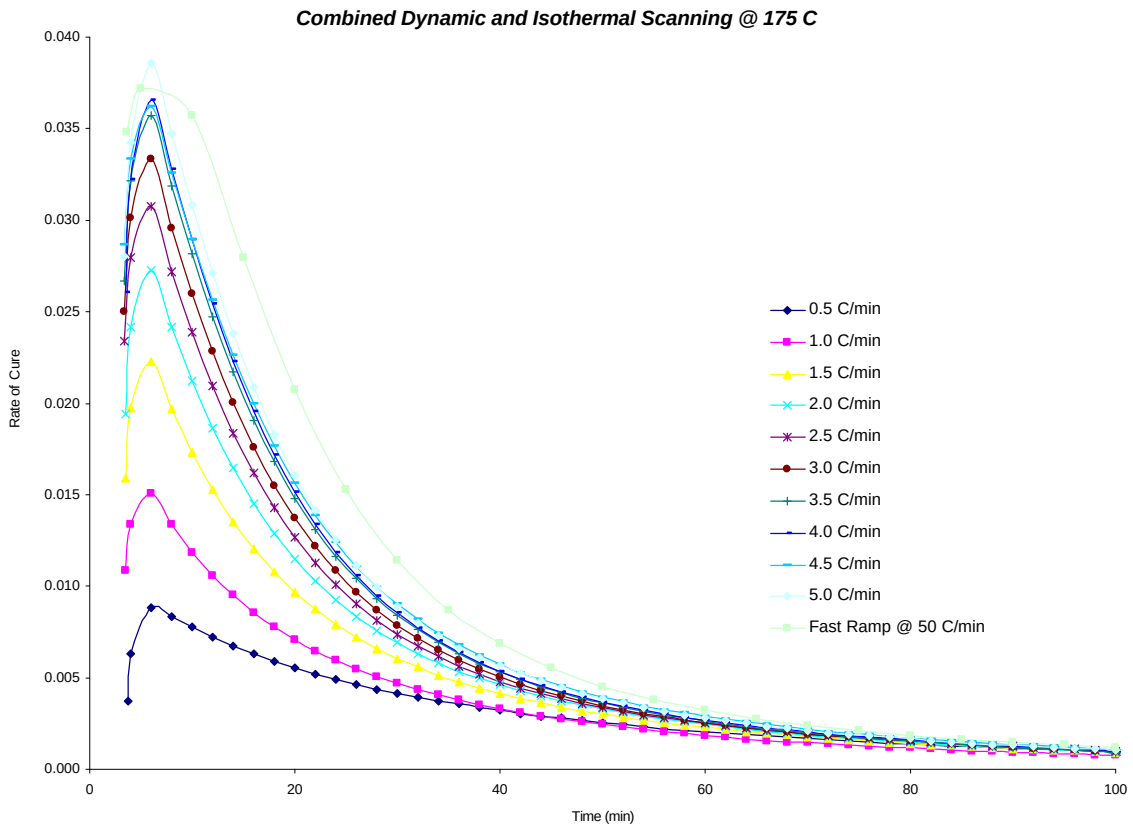

APPENDIX D *(continued)*

2D plot of the rate of cure versus time for the film adhesive cured under isothermal conditions at 180 °C after a slow ramp to that temperature

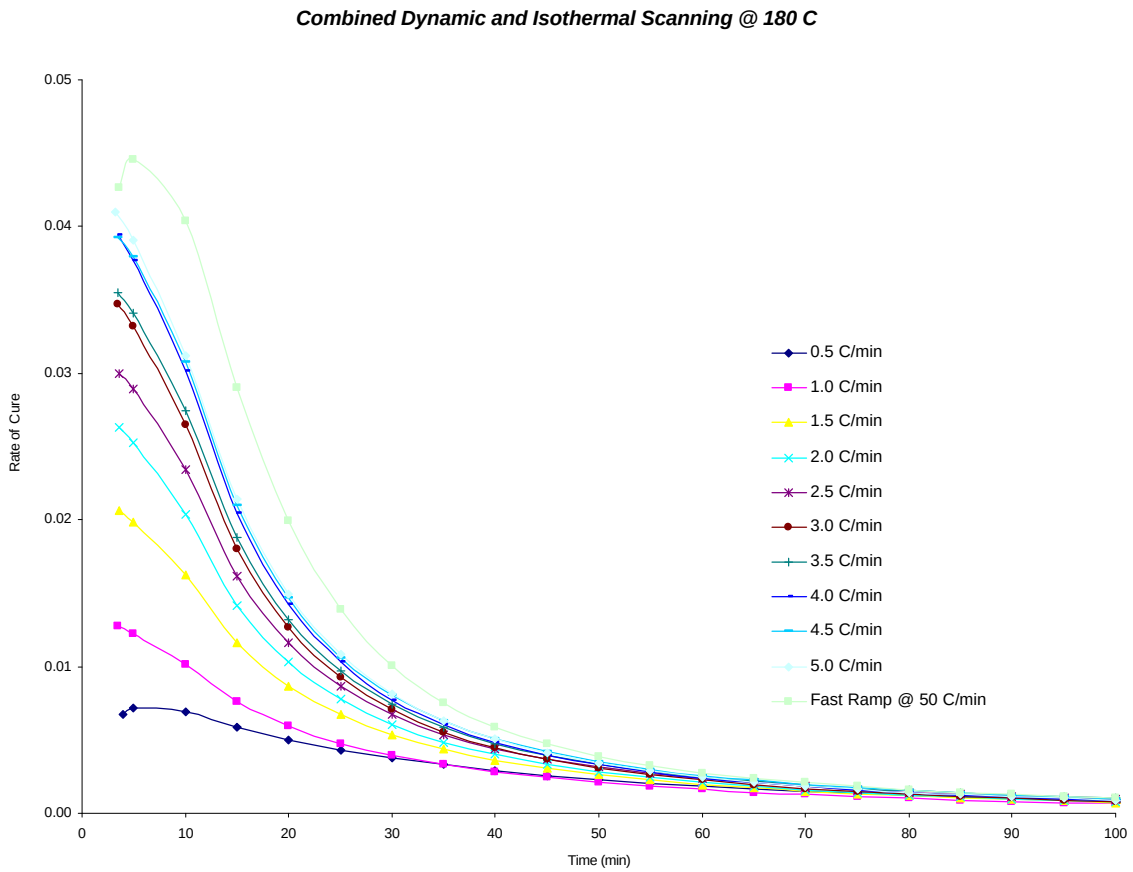

APPENDIX E

3D plot of the rate of cure versus time and initial degree of cure for the film adhesive cured under isothermal conditions at 140 °C and 150 °C after a slow ramp to that temperature (*initial degree of cure from step 1 of the combined ramp and soak experiment)*

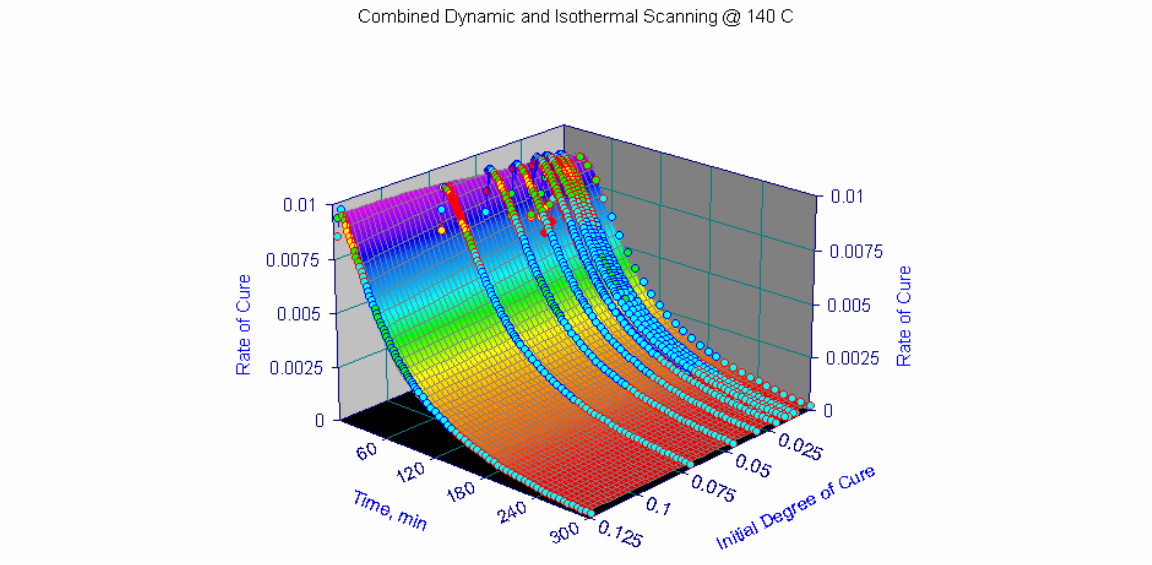

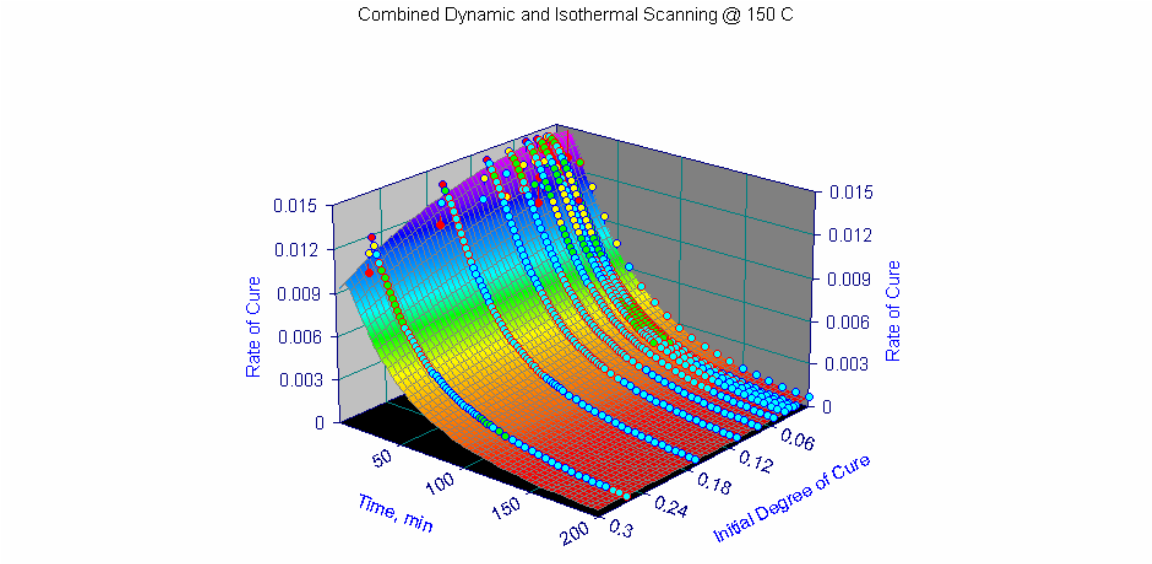

APPENDIX E *(continued)*

3D plot of the rate of cure versus time and initial degree of cure for the film adhesive cured under isothermal conditions at 155 °C and 160 °C after a slow ramp to that temperature (*initial degree of cure from step 1 of the combined ramp and soak experiment)*

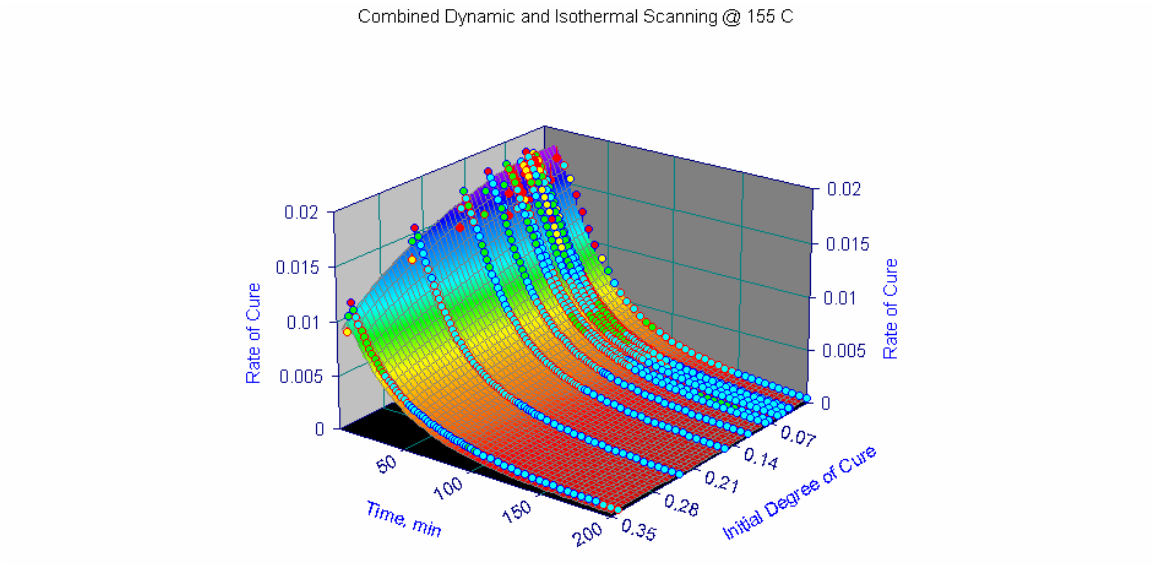

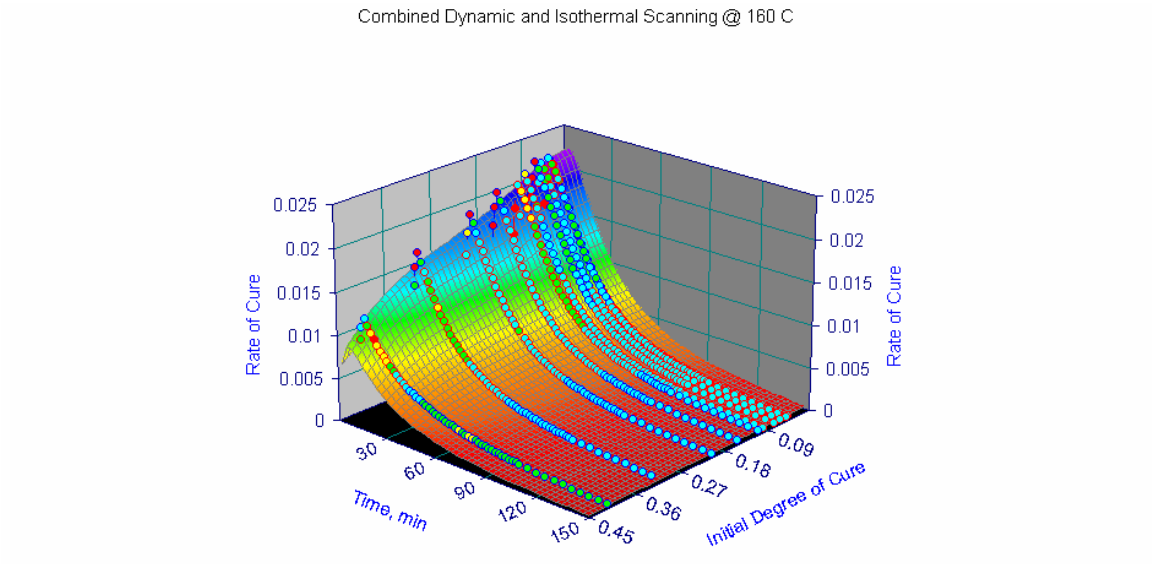

APPENDIX E *(continued)*

3D plot of the rate of cure versus time and initial degree of cure for the film adhesive cured under isothermal conditions at 165 °C and 170 °C after a slow ramp to that temperature (*initial degree of cure from step 1 of the combined ramp and soak experiment)*

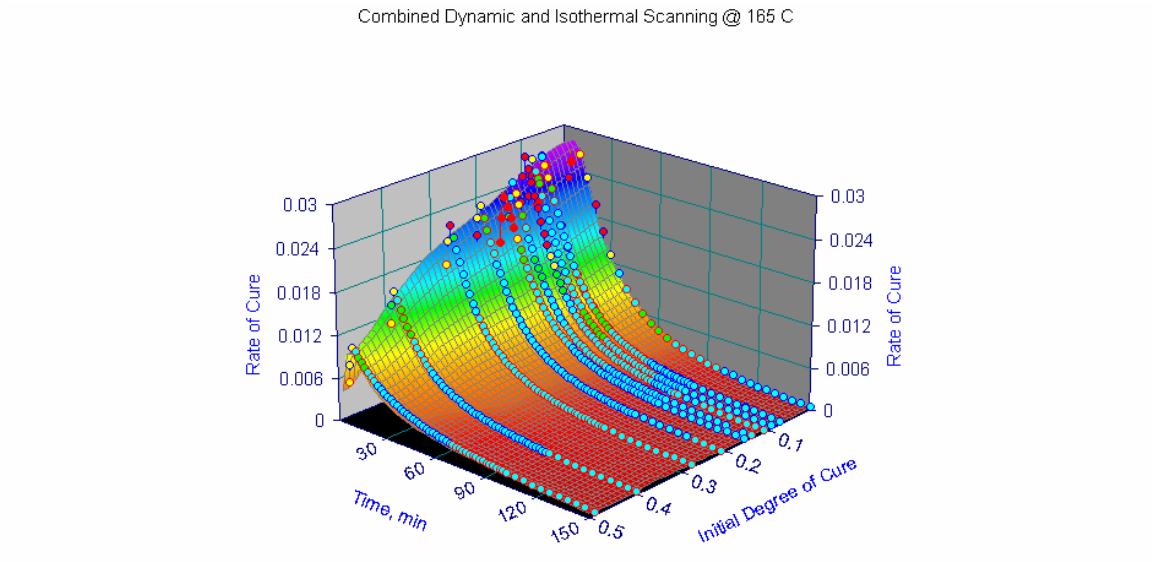

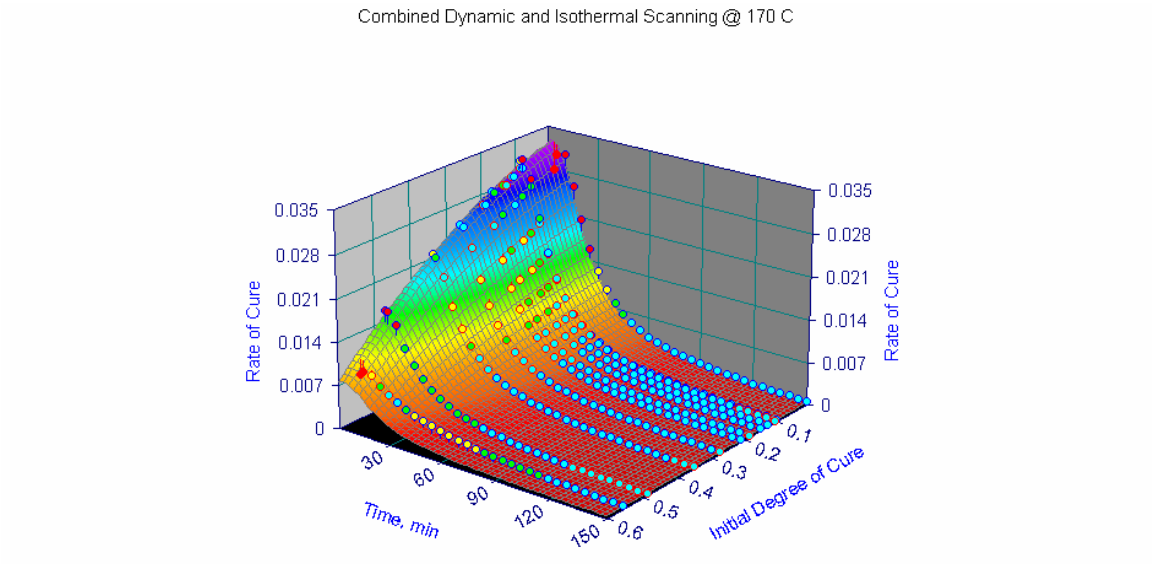

APPENDIX E *(continued)*

3D plot of the rate of cure versus time and initial degree of cure for the film adhesive cured under isothermal conditions at 175 °C and 180 °C after a slow ramp to that temperature (*initial degree of cure from step 1 of the combined ramp and soak experiment)*

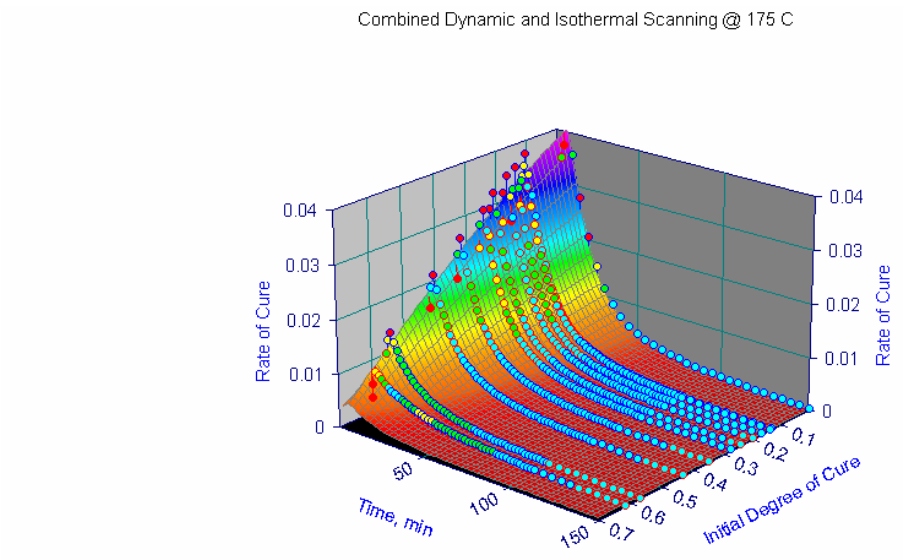

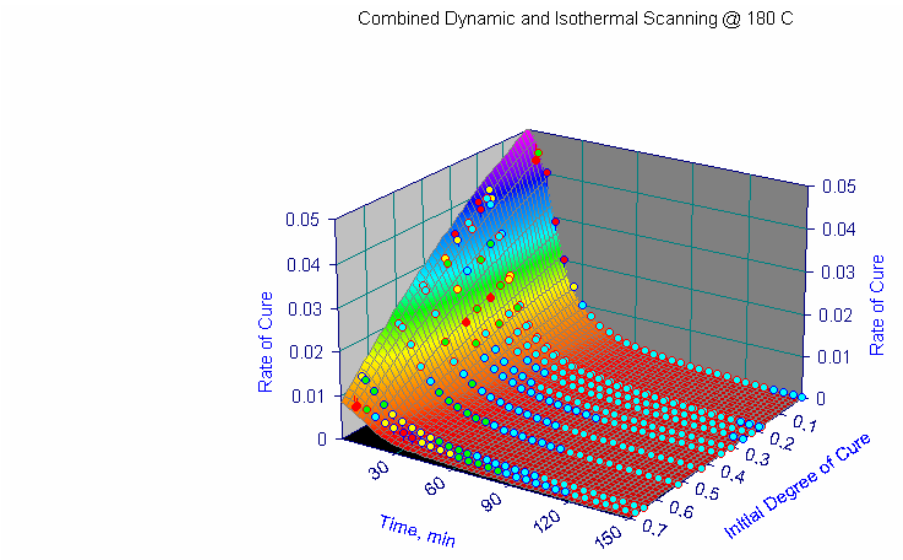

APPENDIX F

2D plots of the degree of cure (a) as a function of time for the combined ramp and soak experiments over a range of heating rates up to soak temperatures of 170 °C, 175 °C, and 180 °C, followed by isothermal scan at that temperature. Data to the right of the y-axis correspond to the soak segment (step 2) while those to the left correspond to the ramp 1 segment (step 1). The apparent gel point at $\alpha = 0.36$ is indicated by a horizontal line.

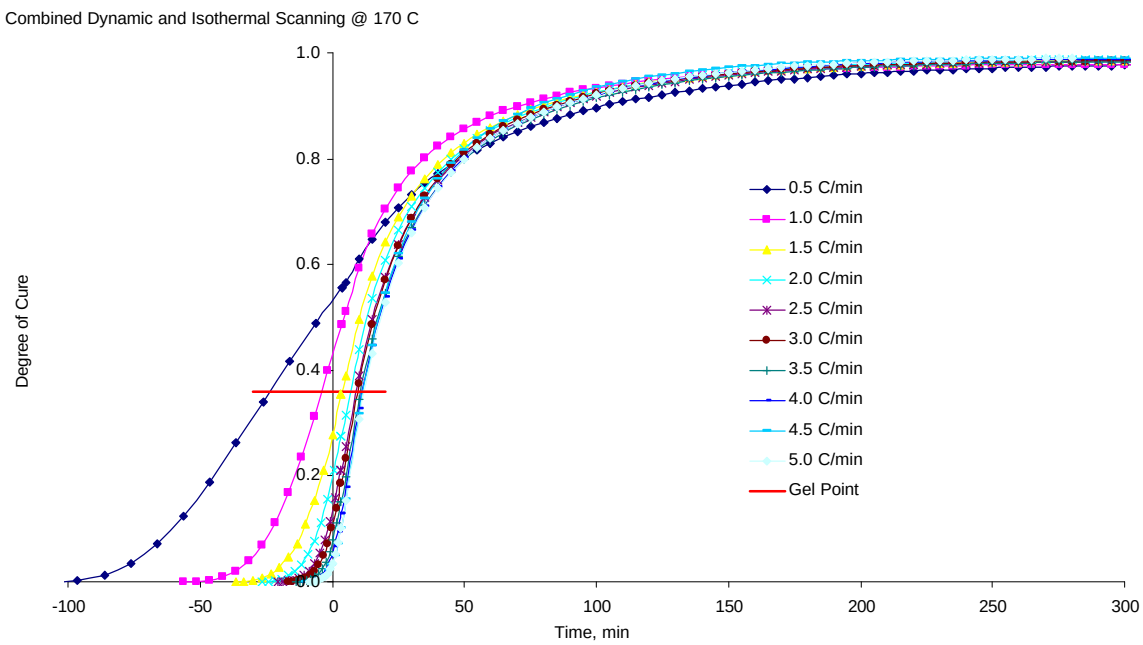

APPENDIX F *(continued)*

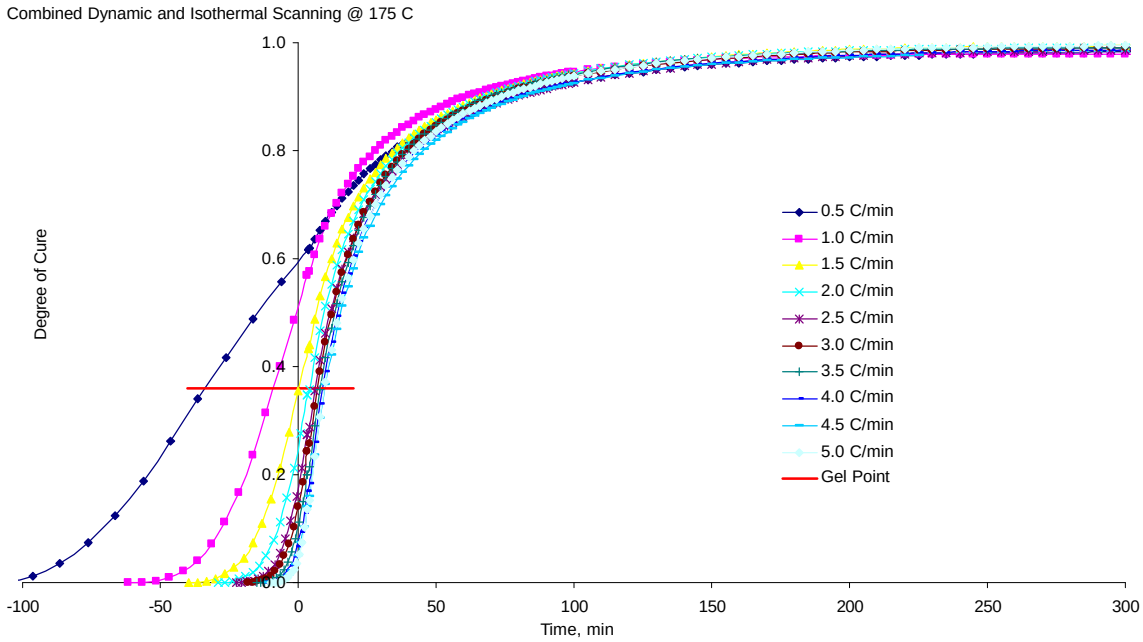

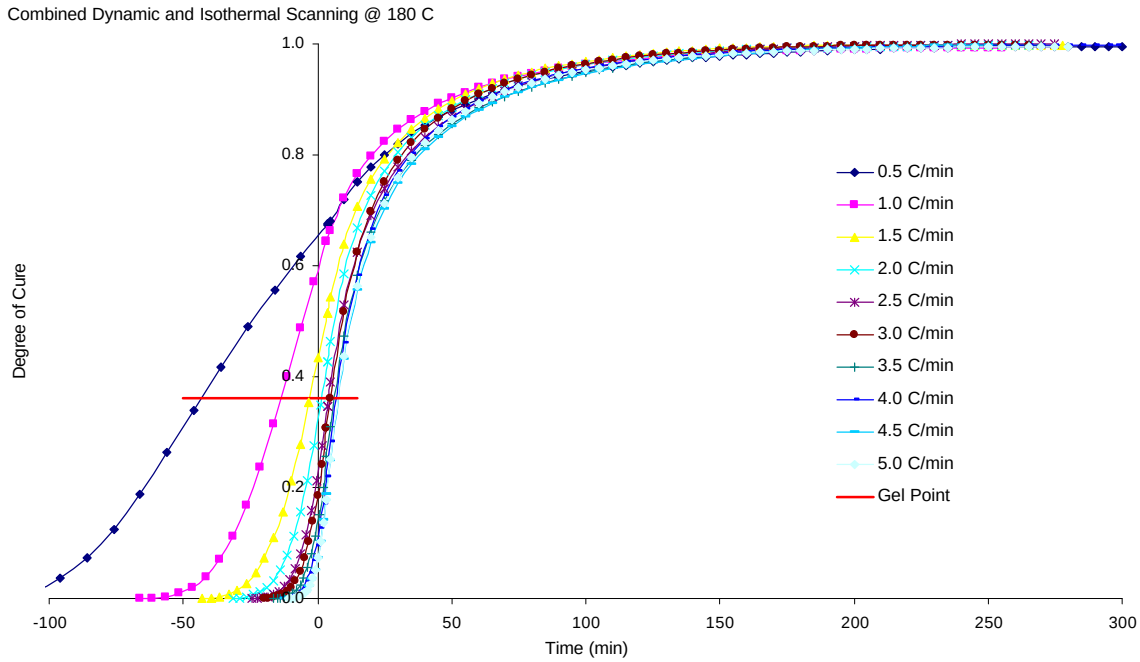

APPENDIX G

2D plots of the rate of cure as a function of time for the combined ramp and soak experiments over a range of heating rates up to soak temperatures of 170 °C, 175 °C, and 180 °C, followed by isothermal scanning at that temperature. Data to the right of the y-axis correspond to the soak segment (step 2) while those to the left correspond to the ramp 1 segment (step 1).

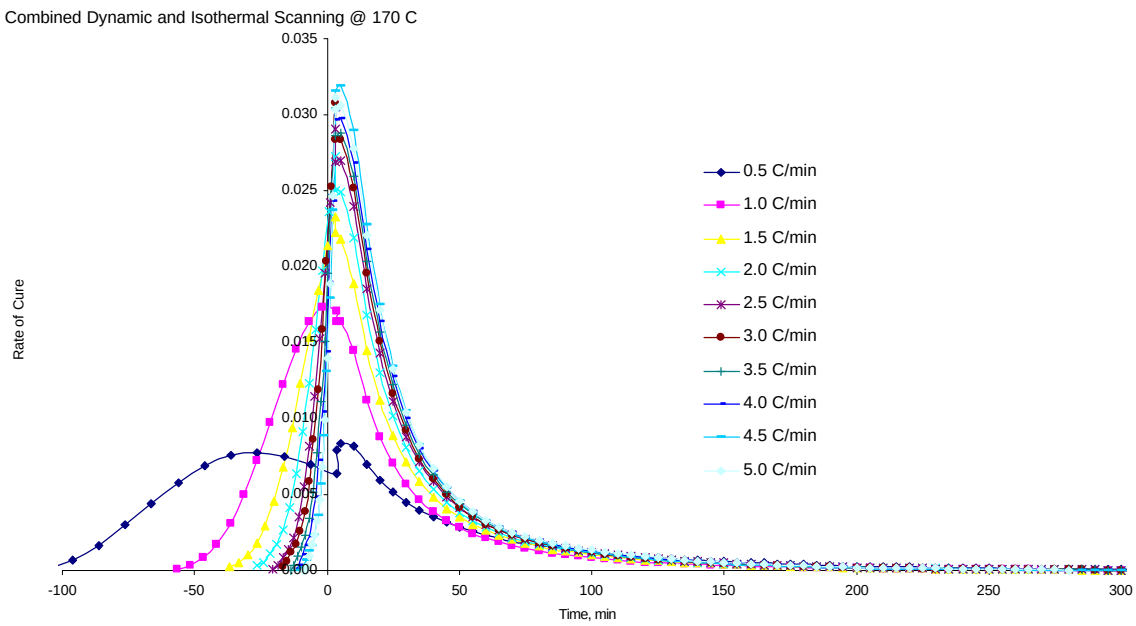

APPENDIX G *(continued)*

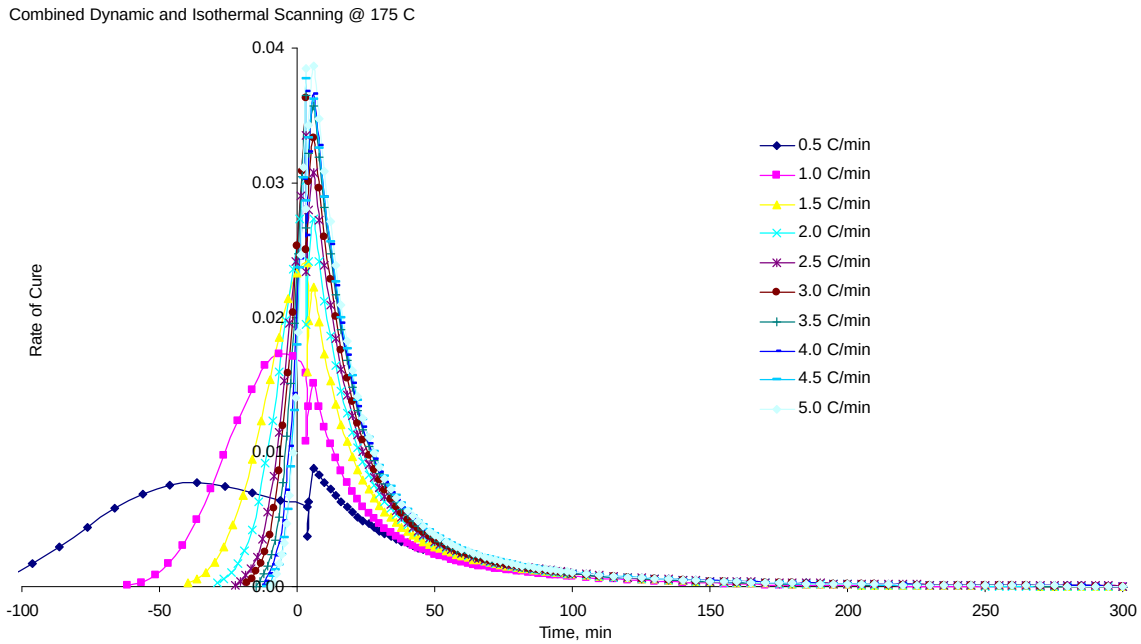

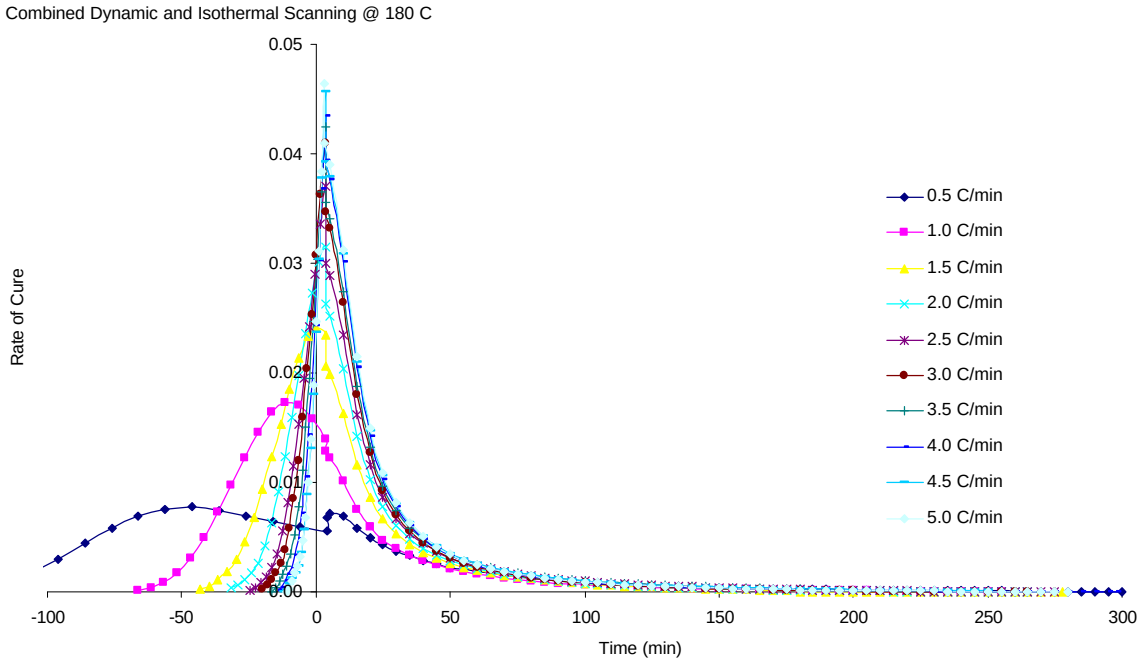

APPENDIX H

Plots of the development of storage modulus (G'), loss modulus (G") and complex modulus (G*) for the film adhesive as a function of time during isothermal cure at 130 °C, 135 °C, 140 °C, and 150 °C.

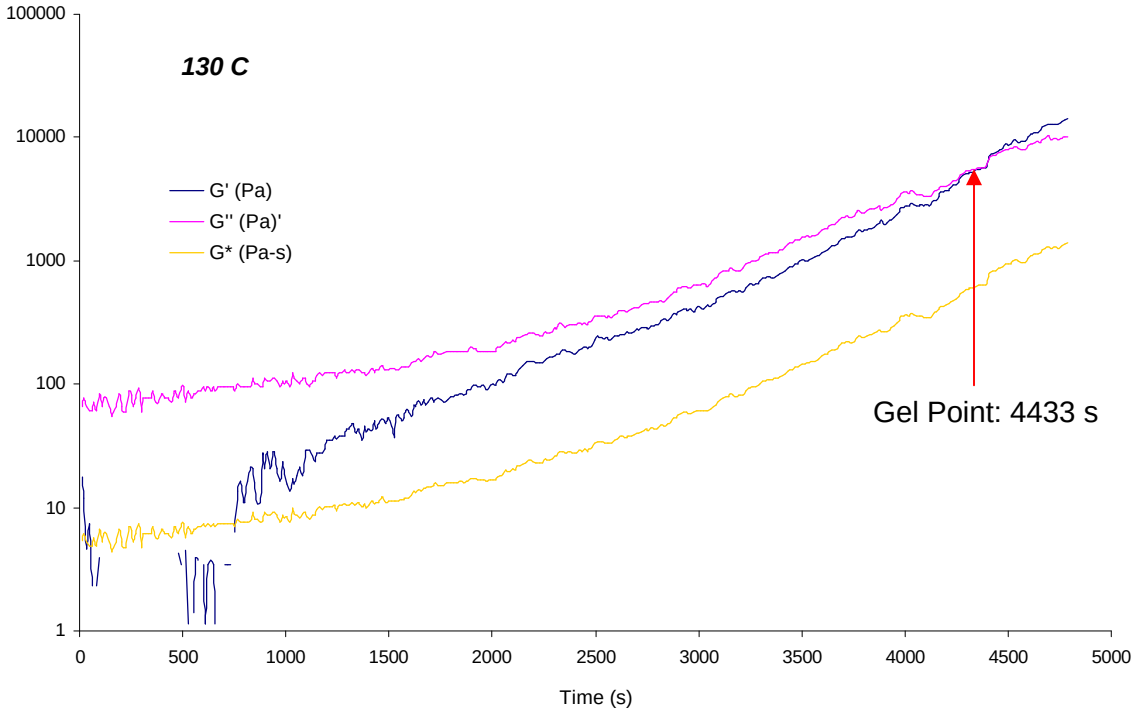

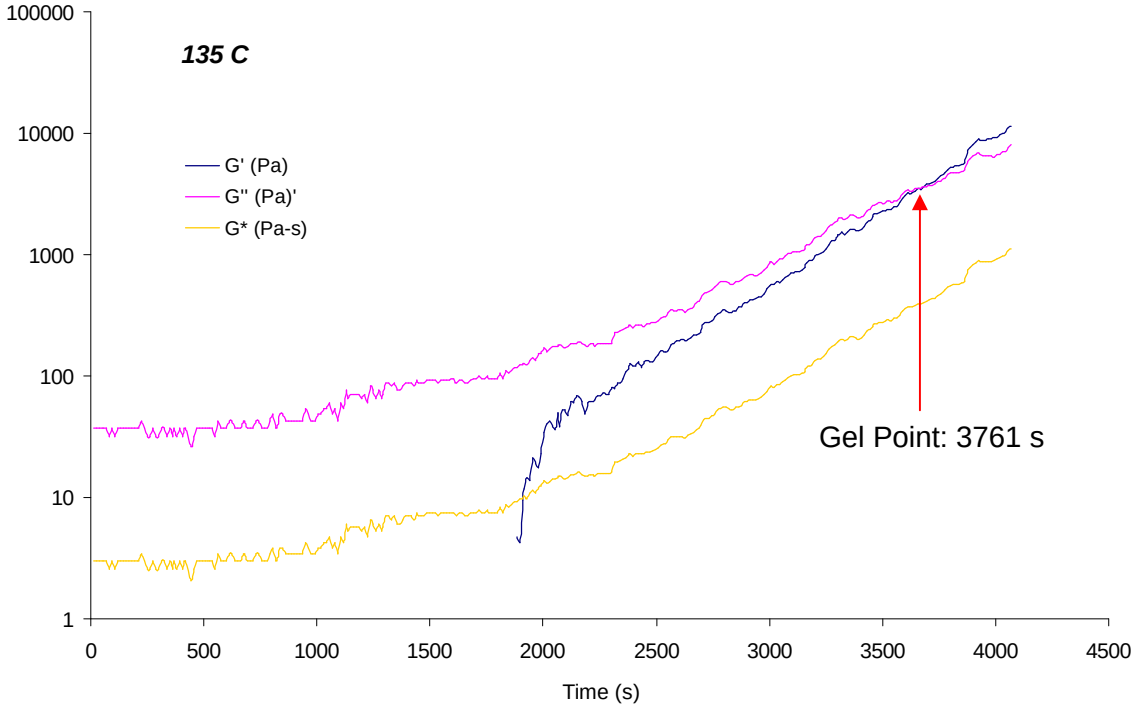

APPENDIX H *(continued)*